



REFERENCE ONLY

UNIVERSITY OF LONDON THESIS

Degree *PhD*

Year *2005*

Name of Author *Long, G. L.*

COPYRIGHT

This is a thesis accepted for a Higher Degree of the University of London. It is an unpublished typescript and the copyright is held by the author. All persons consulting the thesis must read and abide by the Copyright Declaration below.

COPYRIGHT DECLARATION

I recognise that the copyright of the above-described thesis rests with the author and that no quotation from it or information derived from it may be published without the prior written consent of the author.

LOANS

Theses may not be lent to individuals, but the Senate House Library may lend a copy to approved libraries within the United Kingdom, for consultation solely on the premises of those libraries. Application should be made to: Inter-Library Loans, Senate House Library, Senate House, Malet Street, London WC1E 7HU.

REPRODUCTION

University of London theses may not be reproduced without explicit written permission from the Senate House Library. Enquiries should be addressed to the Theses Section of the Library. Regulations concerning reproduction vary according to the date of acceptance of the thesis and are listed below as guidelines.

- A. Before 1962. Permission granted only upon the prior written consent of the author. (The Senate House Library will provide addresses where possible).
- B. 1962 - 1974. In many cases the author has agreed to permit copying upon completion of a Copyright Declaration.
- C. 1975 - 1988. Most theses may be copied upon completion of a Copyright Declaration.
- D. 1989 onwards. Most theses may be copied.

This thesis comes within category D.



This copy has been deposited in the Library of

UCL



This copy has been deposited in the Senate House Library, Senate House, Malet Street, London WC1E 7HU.

Wire Guided Endoscopy with a Finite Element Analysis of Planar Electrodes

PhD Thesis

Gary Long
University College London
Medical Physics and Bioengineering Department
June 2005

UMI Number: U592259

All rights reserved

INFORMATION TO ALL USERS

The quality of this reproduction is dependent upon the quality of the copy submitted.

In the unlikely event that the author did not send a complete manuscript and there are missing pages, these will be noted. Also, if material had to be removed, a note will indicate the deletion.



UMI U592259

Published by ProQuest LLC 2013. Copyright in the Dissertation held by the Author.
Microform Edition © ProQuest LLC.

All rights reserved. This work is protected against
unauthorized copying under Title 17, United States Code.



ProQuest LLC
789 East Eisenhower Parkway
P.O. Box 1346
Ann Arbor, MI 48106-1346

To my family: Lynn, Max, Karin and Ellie. This was an adventure and a journey I hope none of us will soon forget.

Abstract

As an alternative to conventional colonoscopy, which is time-consuming, requires considerable operator skill, and is often painful and hazardous to the patient, this thesis proposes a new method of examining the colon. It involves using a guide wire, which helps the endoscopist advance the colonoscope with a reduced risk of loop formation. It does this by ensuring that it follows a path along the lumen of the colon and by acting as an anchor against which a motor attached to the tip of the colonoscope pulls the colonoscope forward. Clinical measurements show that use of a conventional colonoscope exceeds the human pain threshold 17% of the time, whilst use of the guide wire assisted colonoscope exceeds the human pain threshold only 4% of the time. It is concluded that guide wire assisted colonoscopy is likely to reduce pain and make the procedure easier for both the patient and the endoscopist.

In addition to the guide wire assisted colonoscope, the thesis proposes and assesses the 'planar electrode', an instrument designed to treat colorectal cancer in a more precise and controlled manner than conventional, endoscopic, electrosurgical methods. The planar electrode is assessed using tissue studies and a finite element model. When optimally configured, the planar electrode is shown to coagulate only the tissue between the electrode pair, thereby allowing the endoscopist to oversee the coagulation process as it happens. The finite element model is shown to predict the depth of tissue coagulation within 15% of the depth of coagulation measured in the tissue studies. It is concluded that the planar electrode coagulates tissue in a predictable and controlled manner, and the finite element model is likely to be a useful tool when designing planar electrode configurations for specific tasks.

Table of Contents

1	Introduction	1-1
1.1	Objectives and Structure of the Thesis	1-2
1.2	Personal Statement.....	1-3
2	Clinical Background	2-1
2.1	Anatomy and Physiology of the Colon.....	2-1
2.1.1	Neural Control of the Digestive Tract	2-4
2.1.2	Blood Supply to the Digestive Tract.....	2-6
2.2	Colorectal Cancer.....	2-8
2.2.1	Colorectal Cancer Screening.....	2-10
2.2.1.1	Pros and Cons of each Screening Method	2-14
2.3	Diathermy for Therapeutic Colonoscopy.....	2-18
2.4	Conclusion and the Aim of this Research.....	2-19
3	Guidewire Endoscopy.....	3-1
3.1	Introduction.....	3-1
3.2	Background.....	3-1
3.3	The Colonoscope	3-5
3.3.1	Techniques in Colonoscopy.....	3-7
3.3.2	Delays in Colonoscopy	3-9
3.3.3	Measurements of Time Delays During Colonoscopy	3-11
3.4	The Guidewire	3-14
3.4.1	Background.....	3-15
3.4.2	Guidewire Assistance in the Colon.....	3-17
3.4.2.1	Reduced Insertion Force in a Tissue Model	3-19
3.4.2.1.1	Introduction.....	3-19
3.4.2.1.2	Methods.....	3-20
3.4.2.1.3	Results.....	3-21
3.4.2.1.4	Discussion	3-23
3.4.2.2	Pig Colonoscopy In-Vivo Experiments with Guidewire Assistance	3-24
3.4.2.2.1	Background.....	3-24
3.4.2.2.2	Methods.....	3-26
3.4.2.2.3	Results.....	3-30
3.4.2.2.4	Discussion and Analysis	3-33
3.4.2.2.5	Results from the Cathcam Clinical Trial	3-35
3.4.2.2.6	Conclusions.....	3-37
3.4.3	Motorized Guidewire Assistance in Colonoscopy.....	3-38
3.4.3.1	Background	3-38
3.4.3.2	Guidewire Force Measurements In-Vitro	3-40
3.4.3.2.1	Introduction and Aim.....	3-40
3.4.3.2.2	Methods.....	3-40
3.4.3.2.3	Results.....	3-43
3.4.3.2.4	Discussion and Conclusions	3-44

3.4.3.3	Pig Colonoscopy Expts with Motorized Guidewire Assistance	3-46
3.4.3.3.1	Introduction and Aim	3-46
3.4.3.3.2	Methods.....	3-46
3.4.3.3.3	Results.....	3-49
3.4.3.3.4	Discussion and Conclusion	3-54
3.4.4	Conclusion	3-54
4	Therapeutic Diathermy in Colonoscopy	4-1
4.1	Planar Electrodes for Thermal Denaturation and Tissue Haemostasis	4-1
4.1.1	Background	4-1
4.1.2	Methods.....	4-6
4.1.2.1	Experiments in Ex-Vivo Tissue.....	4-6
4.1.2.2	Experiments In-Vivo.....	4-9
4.1.2.3	Finite Element Model	4-12
4.1.3	Results and Discussion	4-19
4.1.3.1	Experimental Results	4-19
4.1.3.2	Experimental Results Discussion.....	4-22
4.1.3.3	In Vivo Results	4-23
4.1.3.4	Finite element results	4-23
4.1.3.5	Electrical model	4-24
4.1.3.6	Discussion of Electrical Modelling.....	4-29
4.1.3.7	Thermal model.....	4-31
4.1.3.8	Thermal Model Discussion	4-35
4.1.3.9	Comparison of In-vivo results with the model	4-36
4.1.3.10	Limitations of the finite element model.....	4-42
4.1.4	Conclusions.....	4-43
5	Conclusion	5-1
5.1	Guidewire Endoscopy	5-1
5.1.1	Cathcam	5-2
5.1.2	Colonicam	5-3
5.2	Planar Electrodes	5-3
5.3	Further Work.....	5-5
6	Acknowledgements	6-6
7	References	7-1
8	Glossary of Terms	8-1
9	Appendix I: Publications	9-1
10	Appendix II: Technical Specifications.....	10-1

List of Figures

Figure 2-1. Anatomy of the colon (reproduced from Netter (4)).	2-2
Figure 2-2. A typical cross section of the intestinal wall (reproduced from Guyton and Hall (6)).	2-3
Figure 2-3. A cross section view of the colon showing nerve plexuses and blood supply (reproduced from Netter (4)).	2-4
Figure 2-4. Anatomical drawing of the blood supply to the distal digestive tract including the large intestine (reproduced from Netter (4)).	2-7
Figure 2-5. Genetic changes in the tissue lead to the formation of a malignant polyp in the wall of the colon. An abnormal increase of cells can be seen at the hyperplastic stage which leads to adenomatous tissue and finally a malignant tumour (reproduced from Yamada (11)).	2-9
Figure 2-6. Two types of polyps form in the wall of the colon: pedunculated and sessile (reproduced from Yamada (11)).	2-9
Figure 2-7. Data demonstrating the benefit of the three modalities of colorectal cancer screening. The X-axis is each age group and the Y-axis is the increased in life expectancy due to screening. Patients had a colonoscopy performed once at age 50 and repeated every 5 years or every 3 years if a polyp was found (reproduced from Inadomi (23)).	2-15
Figure 2-8. Artistic rendering of a colonoscope forming a loop in the colon (reproduced from Wayne (22)).	2-16
Figure 3-1. Bozzini's light conductor (reproduced from Wayne (34)).	3-2
Figure 3-2. Wolf-Schindler endoscope. This instrument was designed to examine the upper gastrointestinal tract including the oesophagus and the stomach (reproduced from Edmonson(36)).	3-3

Figure 3-3. A standard colonoscope (Olympus Corp.). The insertion tube has length labels printed in white to determine the distance the tip has been advanced into the colon.	3-5
Figure 3-4. The tip of the colonoscope has had the outer layer removed to expose the contents.	3-6
Figure 3-5. Radiograph of a loop which has formed in a colon during a colonoscopy (reproduced from Mosse (43)).....	3-10
Figure 3-6. Recorded times to reach anatomical landmarks of the colon. These times were recorded with a stopwatch when the colonoscopists indicated that the landmark had been reached.	3-13
Figure 3-7. Early "wire guide" manufactured by Cook Inc., Bloomington, Indiana, USA, circa 1962 (reproduced from Sargent (51))......	3-16
Figure 3-8. The blue shaded region in this illustration represents the fixed retroperitoneal structures. The non-shaded regions are not fixed and tend to move and stretch when pushed by the colonoscope (modified reproduction from Netter (4)).	3-17
Figure 3-9. An anatomical drawing of the pig gut (reproduced (53))......	3-18
Figure 3-10. Experimental setup of insertion force measurements of a tube in a model of a colon. The force gage measured the force that the wheels applied to advance the tube.	3-20
Figure 3-11. Comparison of the insertion force of the tube with and without the assistance of the guidewire.....	3-22
Figure 3-12. Hinged guidewire. The thin section connecting the two "legs" allows the wire to be folded and placed in the working channel of the colonoscope...	3-25
Figure 3-13. Force handle. The load cell is connected to a linear slide which is aligned with the axis of the insertion tube. The top half of the handle squeezes on the insertion tube.	3-27

Figure 3-14. Insertion force measured during the first colonoscopy. This colonoscopy was performed with the Olympus colonoscope.	3-30
Figure 3-15. Insertion force measured during the third colonoscopy. The guidewire was used to assist the colonoscope.	3-31
Figure 3-16. Insertion force measured during the fourth colonoscopy. The Cathcam was used to perform this colonoscopy.....	3-31
Figure 3-17. Histogram of the time spent at each level of insertion force while performing a colonoscopy on a pig. 22% of the time was spent pushing with a force greater than 10 N.....	3-32
Figure 3-18. Histogram of the time spent at each level of insertion force while performing a colonoscopy with guidewire assistance on a pig. 11% of the time was spent pushing with a force greater than 10 N.....	3-32
Figure 3-19. Histogram of the time spent at each level of insertion force while performing a Cathcamoscopy on a pig. 0% time was spent pushing greater than 10 N (rounded to zero).....	3-33
Figure 3-20. Schematic of a motor mounted at the distal end of an experimental colonoscope. The motor turns a gear which pulls the colonoscope along a threaded guidewire. The smooth guidewire is contained within a separate channel of the scope (not shown). The tip can be steered like a standard colonoscope.....	3-39
Figure 3-22. Experimental setup to measure the force the looped guidewire applies to the colon (normal force).....	3-41
Figure 3-23. Schematic drawing of the porcine colon laying flat on a table top. It is wrapped around a large post to form a smooth turn. The guidewire has been advanced into the colon. The inset is an enlarged view of the guidewire.	3-42

Figure 3-24. Coefficients of static friction for GW06 and GW06T on excised porcine colon. These values were calculated using experimental values of the normal force to form a loop and the pull force in tissue.	3-44
Figure 3-25. Comparison of the pull force of various guidewires. GW03, GW05 and GW06 have the same core diameter. GW09 has approximately half the core diameter of the other three, but like GW03, has threads.	3-45
Figure 3-26. Line drawing of the Colonicam in a human rectum. The guidewire is in the tucked position and cannot be seen in the endoscopic view.....	3-47
Figure 3-27. The guidewire has been advanced approximately 20 cm. The threaded leg of the guidewire has formed the loop and is now providing an anchor.	3-48
Figure 3-28. Insertion force vs. time of the colonoscope.	3-50
Figure 3-29. Insertion force vs. time of the Colonicam with the aid of the guidewire.	3-50
Figure 3-30. Pig Colonoscopy histogram. 56% of the time was spent pushing with an insertion force exceeding 10 N.....	3-51
Figure 3-31. Pig Colonicam histogram. 5% of the time was spent pushing with an insertion force exceeding 10 N.	3-51
Figure 3-32. A comparison of the means of the percentage of time spent pushing with an insertion force exceeding 10 N. The difference between the colonoscope and the Colonicam is 17% vs. 4% ($p=0.034$). The difference between the Colonicam with and without the guidewire is 4% vs. 32% ($p=0.26$).	3-52
Figure 3-33. Fluoroscopic image of the colonoscope at the furthest point (70 cm) the tip could be advanced in the pig colon.	3-52
Figure 3-34. Fluoroscopic image of the Colonicam at about the same depth (70 cm) as the colonoscope in Figure 3-33.	3-53

Figure 3-35. Fluoroscopic image of the Colonicam advanced 50 cm further than in Figure 3-34. The tip is entering the spiral colon.	3-53
Figure 3-36. Fluoroscopic image of the Colonicam advanced 145 cm in the pig colon.	3-53
Figure 4-1. Diagram of the planar electrode configuration. The electrodes are in contact with the colon and are shown in both plan and elevation (original design, <i>patent pending</i>).	4-5
Figure 4-2. Schematic of experiment to test the relationship of electrode geometry to coagulation zone on the tissue.	4-7
Figure 4-3. Experimental device for in vivo testing.	4-10
Figure 4-4. Measured power curve of bipolar generator. The load was a non-inductive power resistor.	4-11
Figure 4-5. Endoscopic view of the electrodes supported by a clear plastic tube in a canine oesophagus. The white stripe is the coagulated tissue between the electrodes.	4-12
Figure 4-6. Electrodes on a tissue slab, showing width (W) , length (L) and separation (S) of the electrodes. The finite element mesh is shown.	4-13
Figure 4-7. Model of 1/4 of the slab of tissue and the electrode. The number of mesh elements is 8,191.	4-14
Figure 4-8. Electrical conductivity as a function of temperature, experimental vs. modelled curve.	4-18
Figure 4-9. Simple curve fit of the subjective rating versus the index for the experimental data. The red line indicates the value at which the two lines converge. Above this value ($I=20$), the rating remains between 8 and 10.	4-21
Figure 4-10. Canine oesophagus cross-section at 14 days.	4-23

Figure 4-11. Graphical representation of the voltage profile on a half symmetry model. The model has been sliced in half across the electrodes. Figure 4-12 is a quarter symmetry slab.	4-24
Figure 4-12. Steady state surface voltage plot for the quarter symmetry planar electrode. The left surface is set to 25 V.	4-25
Figure 4-13. The electric field along the tissue surface (red bars represent the electrodes). The inset shows the full width plot of the electric field, illustrating the symmetry.	4-25
Figure 4-14. Location of plot line (red broken line) for cross section in Figures 15 through 18.	4-26
Figure 4-15. Cross section plot of small separation and large width (red bar represents the electrode).	4-27
Figure 4-16. Cross section plot of small separation and small width (red bar represents the electrode).	4-27
Figure 4-17. Cross section plot of large separation and large width (red bar represents the electrode).	4-28
Figure 4-18. Cross section plot of large separation and small width (red bar represents the electrode).	4-28
Figure 4-19. Graphical representation of the solution for temperature. The scale to the right is in Kelvins	4-31
Figure 4-20. Cross section of temperature along the tissue/electrode interface, for time = 0 seconds to 1.2 seconds in 0.2 second steps.	4-32
Figure 4-21. Cross section of conductivity at the tissue/electrode interface at time = 0 seconds to 1.2 seconds, in 0.2 second steps. These values are calculated with equation 4-10, therefore $\sigma=0.60$ S/M at time=0 sec.	4-33
Figure 4-22. Cross section of current density at the tissue/electrode interface at time = 0 seconds to 1.2 seconds, in 0.2 second steps.	4-34

Figure 4-23. The temperature rise between the electrodes at a distance 1.5 mm into the tissue.....	4-35
Figure 4-24. Temperature of the modelled tissue from time = 0 seconds to 1.2 seconds. This plot begins at the midpoint between the electrodes and ends 3 mm directly into the tissue (inset figure). The maximum temperature reached for the depths of coagulation determined by a pathologist are labelled.....	4-36
Figure 4-25. Multiple plots of the tissue cooling after the heat source has been removed. This is the temperature of the tissue, midway between the electrodes, from the surface to 3.0 mm into the tissue.	4-38
Figure 4-26. Temperature history at a point midway between the electrodes and at depths of 1.5 through 2.0mm The tissue is heating up to 1.2 seconds, while the heat is dissapating beyond 1.2 seconds. The crtitical temperatur (Tcrit=64 C) has been labeled).....	4-41
Figure 4-27. Total accumulated injury for tissue midway between the electrodes and at depths of 1.5mm through 2.0mm. The horizontal, dotted, red lines indicate values at which the chance of cell death is between 63% and 99%.	4-41
Figure 10-1. Schematic drawing of guidewire GW03.....	10-1
Figure 10-2. Schematic drawing of guidewire GW05.....	10-2
Figure 10-3. Schematic drawing of guidewire GW06.....	10-3
Figure 10-4. Schematic drawing of guidewire GW06T.	10-4
Figure 10-5. Schematic drawing of guidewire GW08.....	10-5
Figure 10-6. Schematic drawing of guidewire GW09.....	10-6
Figure 10-7. Photograph and drawing of the Cathcam. See Table 10-1 for details.	10-7
Figure 10-8. Schematic drawing of the Lumenguidew guidewire.	10-9
Figure 10-9. End view of the FH-06 force handle.....	10-10

Figure 10-10. Cross section view of the force handle. When the insertion tube is advanced along the colon, the slider transmits axial force to the load cell. 10-11

List of Tables

Table 2-1. Levels of sedation as defined by the American Society of Anesthesiologists (Waye).....	2-13
Table 3-1. Rex data on techniques to complete failed colonoscopies. (1) Paediatric colonoscope or upper endoscope. (2) External straightener.....	3-8
Table 3-2. Caecal intubation time for 12 colonoscopies. The forward time denotes the time that the tip of the colonoscope was moving forward. The data are in decimal format.....	3-12
Table 3-3. Mean values of times to reach the anatomical landmarks of the colon. See Table 2-2.....	3-14
Table 3-4. Insertion force to advance the tube from B to C in Figure 3-10, with and without the guidewire. The force required to advance the wheels without the tube was subtracted from the values recorded with the tube to yield the total insertion force.	3-22
Table 3-5. A comparison of two properties of colon and porous PTFE. * A value for Young's modulus of human colon could not be located in the literature; a value for human aorta was used as a comparison.	3-24
Table 3-6. Colonoscopies performed on the pig. The custom guidewire was used during the 2 nd , 3 rd , and 4 th colonoscopies. *Approximate distances-loops may have formed.	3-27
Table 3-7. Summary of the 15 patients treated with the Cathcam.	3-37
Table 3-8. Construction of the guidewires used for testing and comparison. The core diameter was tapered at the midpoint of the wire for GW05 and GW08. NOTES 1-Half of this length had a Teflon [™] coating only on the core (no winding). 2- Wire had an additional tight winding between the core and the	

outer winding. 3- Wire had a Teflon™ coating. * Inches is standard denomination for guidewires.....	3-43
Table 4-1. Length, width and separation distance of multiple experimental pairs of planar electrodes.....	4-8
Table 4-2. Subjective scale used to describe the coagulation zone for each pair of planar electrodes.	4-9
Table 4-3. Electrical and thermal properties used for finite element model.	4-15
Table 4-4. Arrhenius parameters for various tissues.	4-39
Table 10-1. Details of Cathcam drawing.....	10-8

1 Introduction

I often say that when you can measure what you are speaking about, and express it in numbers, you know something about it; but when you cannot express it in numbers, your knowledge is of a meagre and unsatisfactory kind; it may be the beginning of knowledge, but you are scarcely, in your thoughts, advanced to the stage of science, whatever the matter may be.

Lord Kelvin (1824-1907)

The medical term endoscopy means to look into the body. A complete examination of the colon (colonoscopy) can reduce the risk of colorectal cancer (CRC), locate unknown sources of bleeding or diagnose other lower abdominal ailments. Whereas it is relatively simple to examine a natural orifice such as the mouth, it is difficult for a physician to examine the colon and can be quite painful for the patient to endure the examination.

In the United States alone, 65,000 people die from colorectal cancer annually, yet it was only recently recommended that average risk patients over 50 years of age receive a colonoscopy every 10 years to reduce the risk of colorectal cancer (1).

Instruments similar to modern anosopes and colposcopes (instruments to view the anal canal and the vagina) were discovered in the ruins of Pompeii, indicating that examinations of the human body through natural orifices were carried out as early as the first century A.D. For the past 200 years physicians have explored the digestive tract with endoscopes that give them a direct view of the diseased tissue.

Having access to the digestive tract can benefit both the physician and the patient. The digestive tract is a tube with multiple layers. Diseases of the digestive tract generally begin at the mucosa or endothelium and may progress into the underlying layers. Through the use of flexible endoscopy, this diseased tissue can be removed (to make a histological confirmation of the pathology) or destroyed (to reduce the risk of further advancement of the disease).

The flexible endoscope provides two main functions: to examine the tissue visually and to visualize and control treatment of the tissue in some way. Modern colonoscopes contain a miniature camera to view the tissue. As technology advances, these cameras are likely to become even smaller while the quality of the images improves. To treat the tissue, instruments are introduced through an access channel in the endoscope. These are relatively simple instruments to grasp and remove the tissue.

1.1 Objectives and Structure of the Thesis

The goals of this thesis are:

- Reduce the insertion force of a colonoscope. This will reduce the pain felt by the patient.
- Reduce the amount of skill required to perform a screening colonoscopy. This will enable less skilled practitioners to perform the procedure and increase the number of patients screened for CRC.
- Develop a finite element model of the planar electrodes. Thermal profiles from the model will be used to calculate depth of tissue damage using the

Arrhenius integral. The results will be compared to in-vivo measurements to validate the model.

The three chapters that follow are: clinical background, guidewire endoscopy and therapeutic endoscopy. The clinical background chapter will discuss the anatomy of the colon and will provide background material on how patients have been historically screened for CRC. The guidewire chapter will discuss the original work done to develop a new device to help provide CRC screening to more patients. The third chapter, therapeutic endoscopy, will introduce a new way to use diathermy in the colon. This new method will be shown to be more predictable when applying the electrical current to coagulate the target tissue.

1.2 Personal Statement

The work that I performed for this thesis was part of a project sponsored by Ethicon Endo-Surgery (EES), a company with whom I am employed full time. My goal was to develop a product for the company in an academic environment. This would allow me to draw from resources within the University and also apply more scientific rigor to the project than is typically afforded in the very early stages of development at a commercial institution. With this approach, resources were available from EES to build and test these devices for a clinical trial. My task was to take an original idea and do the experimentation that would lead to a basic design. Prototype devices would then be built, based on the original design, to be used to gather clinical data. These data would then help the company decide whether to continue with the device as a product or to discontinue the work. Gathering clinical data for a device, which is used to

screen patients for CRC, is of particular importance. It is difficult to model the human colon in a way that can ascertain whether or not the device would provide improved utility over existing devices, such as a colonoscope. Therefore the device must be tested in a human colon. This incurs risk, which can be reduced by taking the proper regulatory and engineering design steps.

Some of the initial work on the planar electrodes was done before I was accepted as a PhD student. Specifically, the experimental device (Figure 4-3) was developed and tested in a canine model before my arrival at University. The prototype was built from my design. The clinical trials were conducted while I was at University as well as all of the statistical and finite element analysis described in Chapter 4.

2 Clinical Background

2.1 Anatomy and Physiology of the Colon

This section will discuss the anatomy of the colon, particularly the structure, innervation and blood supply. This will provide background on how to reduce pain and risk to the patient. The large intestine (colon) is the last section of the digestive tract, consisting of a tube approximately 1 to 1.5 meters in length beginning with the caecum (the end of the small intestine) and ending with the rectum (Figure 2-1). The colon varies in diameter and fixation, is very elastic, and is poorly supported over much of its length.

The main function of the colon is to receive contents from the small intestine. The contents are passed from the end of the small intestine (ileum) into the beginning of the colon (caecum) through the illeocaecal orifice (valve). The colon then removes fluids and stores the waste products from digestion.

The ascending colon, descending colon, rectum and posterior surface of the hepatic and splenic flexures are fixed retroperitoneal structures. The caecum, transverse colon and sigmoid colon are intraperitoneal and have a relative lack of fixation (2). The sigmoid colon is attached to the posterior parietal peritoneum by mesenteric tissue (3).

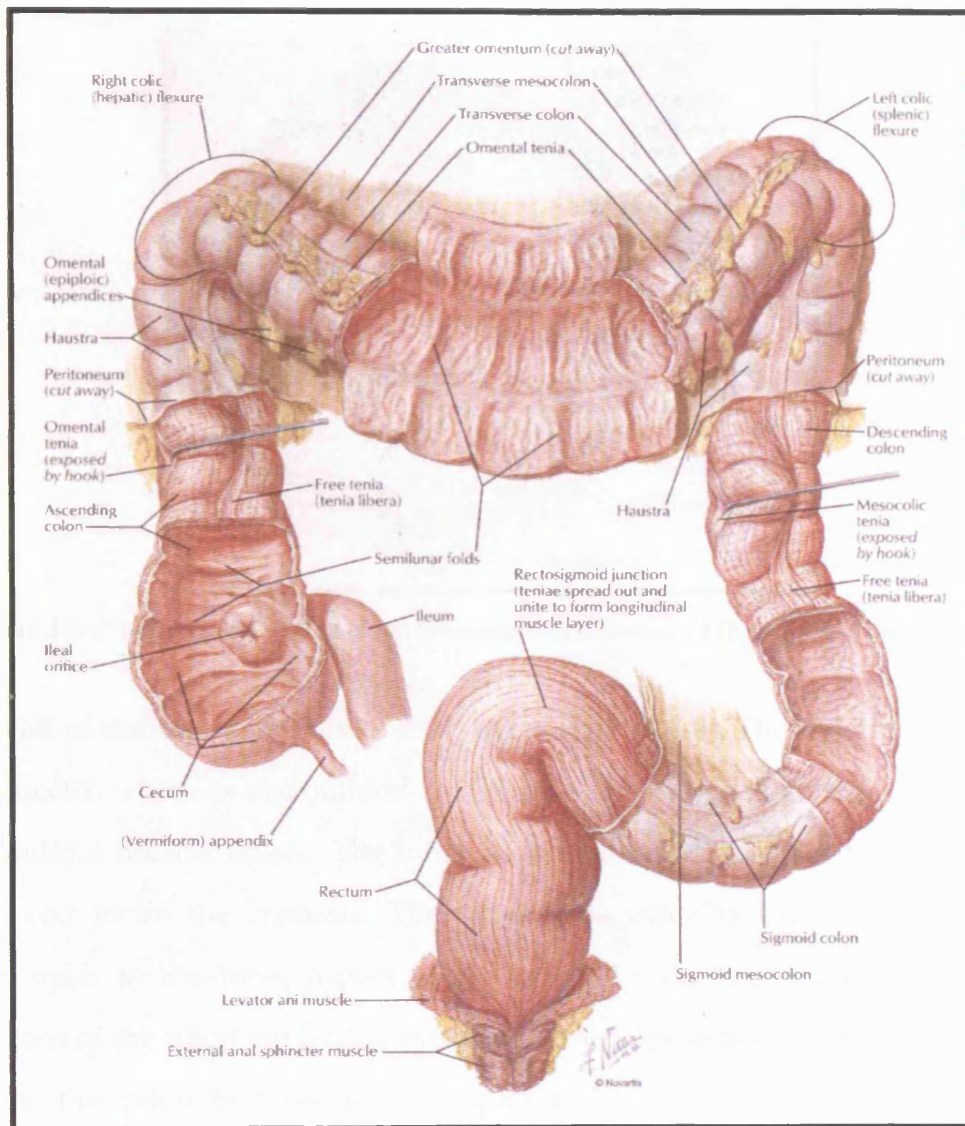


Figure 2-1. Anatomy of the colon (reproduced from Netter (4)).

The colon is divided into proximal and distal sections. The proximal section allows water and electrolytes to be absorbed by the body while the distal colon stores the faeces (5). Once the contents enter the caecum, they are moved back and forth in a mixing motion to facilitate the removal of the excessive fluid and electrolytes.

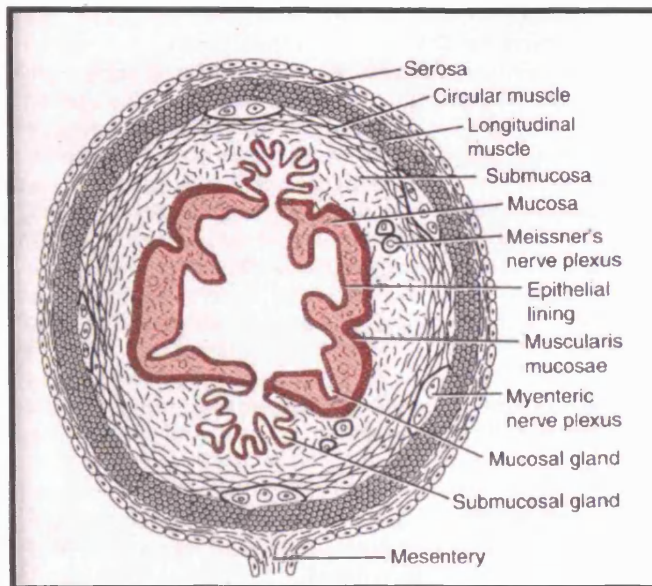


Figure 2-2. A typical cross section of the intestinal wall (reproduced from Guyton and Hall (6)).

The wall of the colon consists of four layers (Figure 2-2). The innermost layer is the mucosa, which is surrounded by the submucosa and then the circular and longitudinal muscle layers. The outer muscular layers contract to squeeze the colon and move the contents. The submucosa contains the secretion glands which open to the inner aspect of the colon. Unlike the small intestine, the secretions of the colon are largely mucus (6). The large amount of secreted mucus protects the colon in three ways: it protects the wall against excoriation or damage due to scraping by the contents within the colon; it provides a medium to hold the faecal material together; and it protects the wall from the large amount of bacteria present in the faeces. In the event that the wall becomes intensely irritated, the mucosa secretes large amounts of water and electrolytes to dilute the irritating factors and cause rapid movement of the faeces or diarrhoea (6).

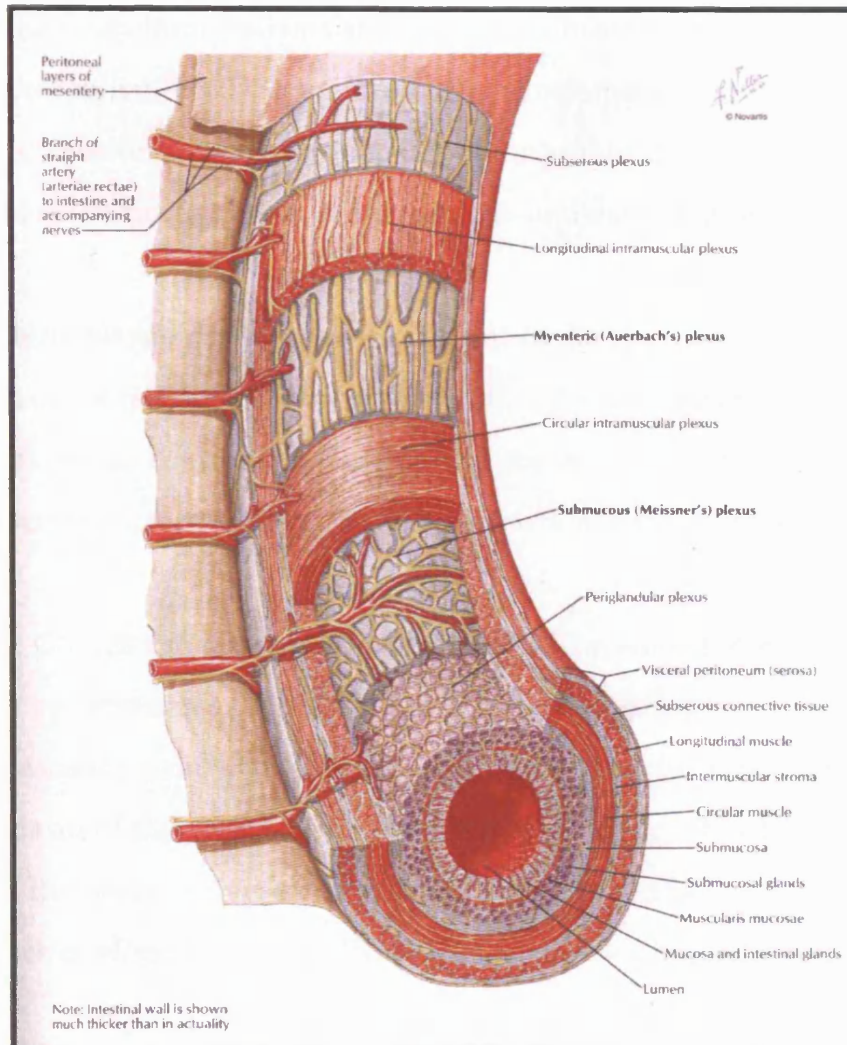


Figure 2-3. A cross section view of the colon showing nerve plexuses and blood supply (reproduced from Netter (4)).

2.1.1 Neural Control of the Digestive Tract

The enteric nervous system (part of the autonomic nervous system) supplies the nerves to the gastrointestinal (GI) tract from the oesophagus to the anus. It controls the movements and secretions of the GI tract through the myenteric and the submucosal plexuses (Figure 2-3). Extrinsic control of the plexuses is achieved through sympathetic and parasympathetic nervous systems. In

addition, the epithelium contains afferent nerve fibres which connect to the brain through the spinal cord along both the sympathetic and parasympathetic pathways (7). Sensory nerve endings originate within the epithelium and send the afferent nerve fibres to both of the plexuses and the spinal cord (8).

The myenteric plexus controls the movement of the gut by controlling the tone, or contraction, of the muscle fibre in the wall of the gut (the entire GI tract). The submucosal plexus controls the functions of the inner wall of the gut, including intestinal secretion, local absorption and contraction of the submucosal muscles.

Pain in the GI area can be due to several causes. The afferent nerve fibres can be stimulated by irritation of the gut mucosa as well as excessive distension of the gut wall, causing pain. Pain can also be caused by chemical damage to the mucosa, spasm of the muscle and stretching of the ligaments which support the gut. When the tissue is over-stretched, the blood vessels will collapse. This may lead to a lack of blood flow to the tissue (ischaemia) causing ischaemic pain (9).

Under other circumstances, sensory receptors in the epithelium can respond to stimuli without being perceived as a conscious sensation (7). However, sensory receptors have been reported in the literature as sources of pain in the colon (7). The "intensity" encoding receptor of the cat responds to low intensity colonic distension and responds more frequently as the level of distension increases. These receptors have also been shown to respond to ischaemia. Mesenteric receptors respond to stretching forces and can cause severe pain. In addition to the sensation of pain, these receptors can cause pseudoaffective cardiovascular reflexes, including increases of blood pressure and heart rate (7). Mesenteric forces as low as 10 mN have been shown to elicit a response.

2.1.2 Blood Supply to the Digestive Tract

The small and large intestines are supplied by the superior mesenteric and inferior mesenteric arteries (Figure 2-4). The branches from these arteries continue to branch and eventually form straight arteries (arteriae rectae) which supply the colon wall (Figures 2-3 and 2-4). These arteries spread into the submucosa and muscular layers and serve the absorptive and secretory functions of the small and large intestines (5).

The function of the small intestine is to absorb nutrients from the bolus which passes through. The mucosal surface of the small intestine contains villi which are rich in arterioles and venules that interconnect with capillaries. The function of these tubular villi is to absorb the nutrients. By contrast, the large intestine contains no villi and instead is lined with mucus cells whose purpose is to secrete mucus to protect the wall from damage and bind the contents.

When performing a diagnostic colonoscopy, care must be taken to avoid damage to the mucosa and thus cause bleeding. Furthermore, when performing diathermy during a therapeutic colonoscopy, the tissue will be coagulated when the electrical current is passed through the tissue. The amount of blood supply to the tissue will affect the coagulation when the current flows through the tissue. This subject will be discussed in further detail in Chapter 4.

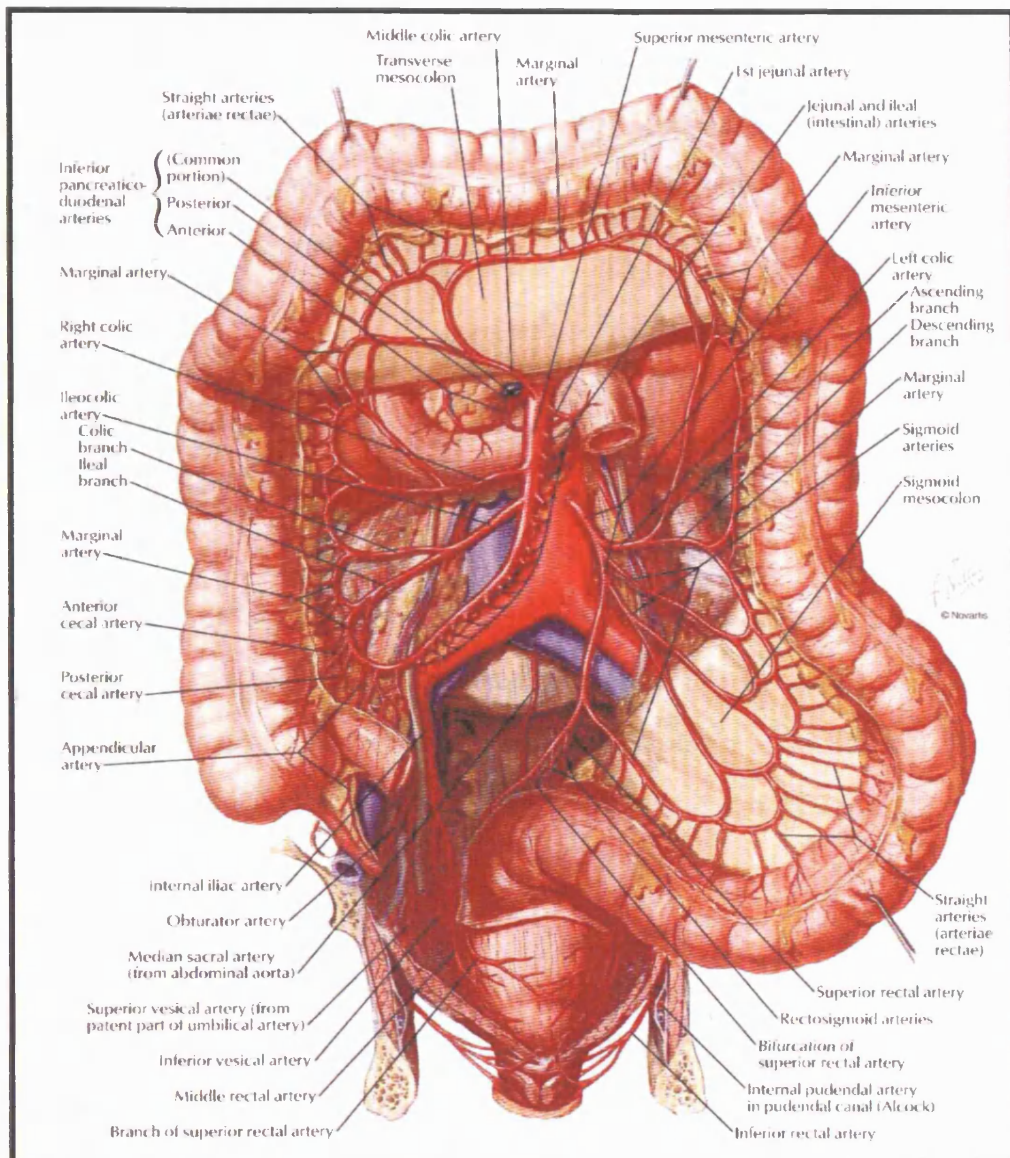


Figure 2-4. Anatomical drawing of the blood supply to the distal digestive tract including the large intestine (reproduced from Netter (4)).

2.2 Colorectal Cancer

Colorectal cancer begins as a small polyp in the mucosal layer of the wall of the colon. According to Ransohoff (10), 30%-50% of persons over the age of 50 in the United States have colorectal polyps.

Figure 2-5 is an illustration of the progression from normal tissue to a malignant polyp in the wall of the colon. The top part of the figure shows a normal epithelium.

A polyp is generally defined as a projecting mass of swollen and hypertrophied or tumourous membrane and can have a diameter of the order of 1cm. Colorectal polyps can be classified into two types: neoplastic and non-neoplastic. Neoplastic polyps are more clinically significant because of their risk of becoming adenomas and malignant lesions.

Polyps can protrude from the wall of the colon or lie flat (Figure 2-6). Adenomas are the most clinically significant colorectal polyps. They begin with an altered and disordered cell proliferation in the epithelium (2). This is illustrated as a darkened epithelium in Figure 2-5. There is typically a homeostasis between cell production, cell maturation and death. This homeostasis helps to maintain a constant epithelial thickness. When an adenoma begins to form, cell mitosis continues while cell maturation is delayed (11).

This disorderly cell production leads to an increase of epithelium cells (Hyperplastic in Figure 2-5) and the growth of the polyp (bottom drawing in Figure 2-5).

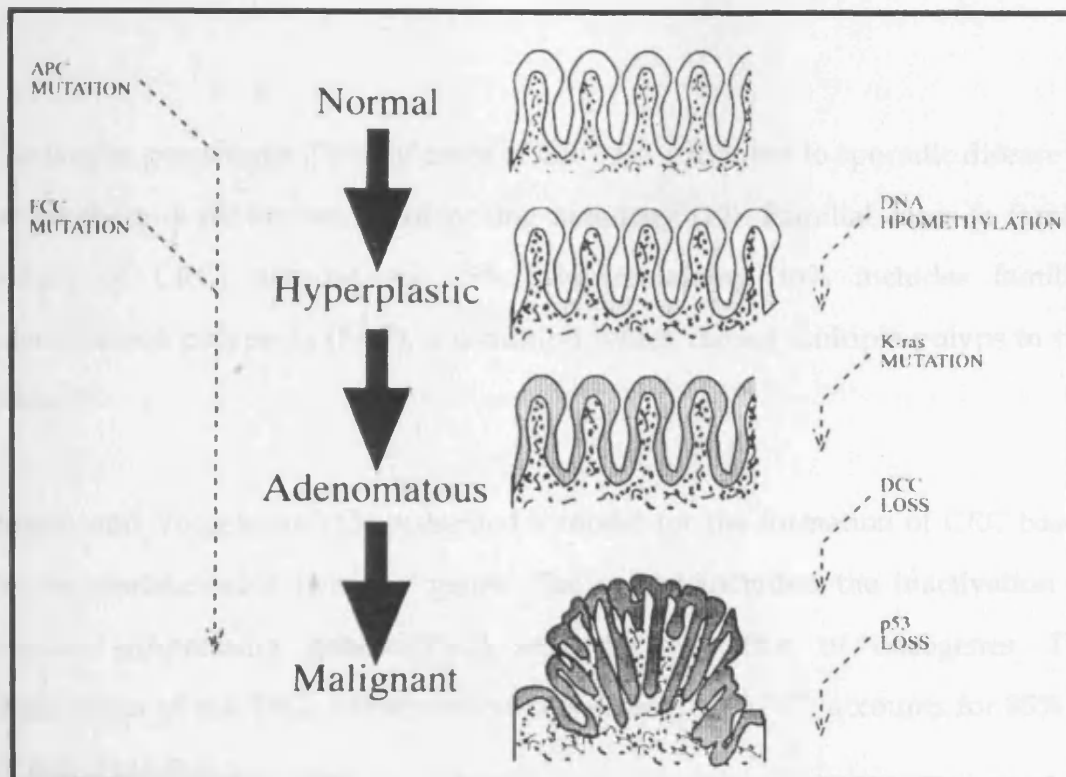


Figure 2-5. Genetic changes in the tissue lead to the formation of a malignant polyp in the wall of the colon. An abnormal increase of cells can be seen at the hyperplastic stage which leads to adenomatous tissue and finally a malignant tumour (reproduced from Yamada (11)).

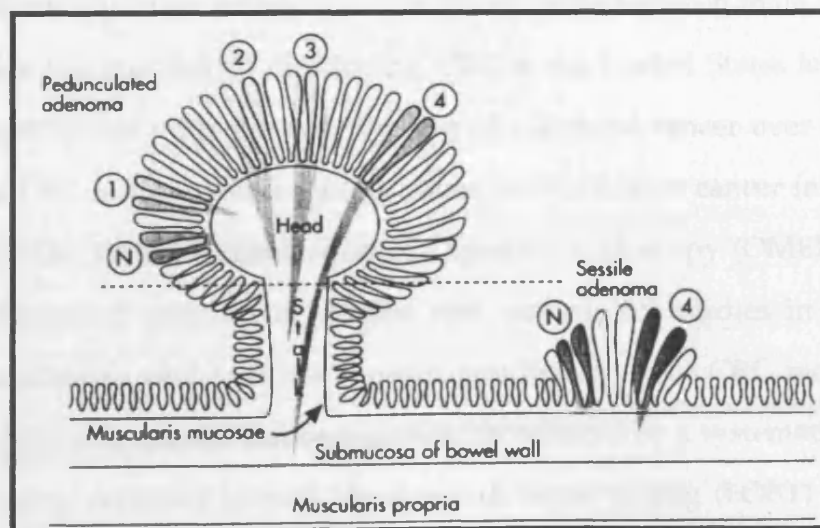


Figure 2-6. Two types of polyps form in the wall of the colon: pedunculated and sessile (reproduced from Yamada (11)).

The largest percentage (75%) of cases of CRC are attributed to sporadic disease in which there is no known predisposing aetiology (12). Familial cases (a family history of CRC) account for 15%. The remaining 10% includes familial adenomatous polyposis (FAP), a condition which causes multiple polyps in the colon.

Fearon and Vogelstein (13) presented a model for the formation of CRC based on the mutations of two key genes. The model included the inactivation of tumour suppressing genes (TSG) and the activation of oncogenes. The inactivation of the TSG, adenomatous polyposis coli (APC), accounts for 85% of all CRC (14;15).

2.2.1 Colorectal Cancer Screening

CRC is a form of cancer which does not discriminate between male and female. The average lifetime risk of developing CRC in the United States is 6% (16). A person aged 50 has a 2% chance of dying of colorectal cancer over the next 30 years (17). CRC is the second leading cause of death from cancer in the United States (18). The World Organization of Digestive Endoscopy (OMED) reported (19), "Randomized population studies and case-control studies in the United States, Scandinavia and U.K. all showed conclusively that CRC incidence and mortality from this disease can be significantly reduced by a systematic screening program using repeated annual faecal occult blood testing (FOBT) or periodic supplemental endoscopic examination of the large bowel".

There are three CRC screening methods: stool tests, barium enema and flexible endoscopy. Stool tests are the least invasive of the three. The first of the two stool tests is the faecal occult blood test (FOBT). The FOBT can be performed at home and involves placing a sample of stool on a chemically treated card. A solution is added to the card, which changes colour if there is blood in the stool. The second is the stool DNA test. Since tumour formation is associated with genetic changes (Figure 2.5), these assays detect the presence of DNA mutations in the stool. Specifically, the APC gene and its mutations have been targeted by these assays.

The second method for cancer screening, the barium enema, has been used for over 80 years as the primary non-surgical way to examine the colon (20). Radiological examination of the colon can be performed with the single contrast or double contrast technique. When performing a double contrast barium enema (DCBE), the colon is filled with a small amount of high-density barium (a contrast agent) and air. A radiologist then performs a fluoroscopic examination of the entire colon. The patient is moved into different positions on the table to assure that the entire colon is examined. A still radiograph (X-ray) can be obtained for a more detailed examination. A new technique called “virtual” colonoscopy is a natural complement to barium enema. To obtain images, air is introduced into the colon through the anus, just as it is for a barium enema. The patient is then guided through a rotating X-ray CT scanner to obtain cross section images of the abdomen and colon. The images are then reconstructed to form a “virtual” colon (computer tomography). Unlike a traditional barium enema where a “flat” image of the colon is observed, the reconstruction of the cross sections creates a 3 dimensional image of the colon. The radiologist can then examine the inside of the colon by “flying” through the virtual colon.

Flexible endoscopy refers to the use of a flexible tube with a camera on the end to examine the body through the natural orifices. Sigmoidoscopy and colonoscopy are two categories of flexible endoscopy and are outpatient procedures. Sigmoidoscopy is the examination of the colon from the rectum through the sigmoid colon. In colonoscopy, the entire colon is examined from the rectum to the caecum. Both procedures are performed transanally while the patient lies on his side.

During barium enema and colonoscopy the clinician is looking for abnormal growths in the tissue (polyps), so preparation (cleanliness) of the bowel is important. Total colonoscopy is rarely possible in an unprepared colon (21). The patient must prepare for the examination by taking laxatives the evening before to the exam. An enema may be required just prior the exam.

The patient may be given a sedative and analgesic to put them in a relaxed state. These agents will be administered throughout the procedure in response to pain and discomfort felt by the patient. The use of sedation and analgesia also helps the physician by keeping the patient calm and preventing them from moving during the procedure. Table 2-1 lists the states of sedation as defined by the American Society of Anesthesiologists (22). The target for colonoscopy is moderate sedation.

Table 2-1. Levels of sedation as defined by the American Society of Anesthesiologists (Waye).

Minimal sedation

Normal response to verbal stimulation.

Airway, ventilation, cardiovascular unaffected.

Moderate sedation

Purposeful response to nonpainful stimulation.

Airway, ventilation, cardiovascular adequate.

Deep sedation

Response only after repeated or painful stimulation.

May require airway/ventilatory intervention.

General anaesthesia

Unrousable.

May require airway/ventilatory/cardiovascular support.

According to Zuccaro Jr. (22), the most common sedative/analgesia medication for colonoscopy is a combination of parenteral narcotic and benzodiazepine. The narcotic relieves the pain while the benzodiazepine decreases anxiety and provides amnesia. A combination of meperidine/midazolam is commonly used for colonoscopy.

A colonoscopy is performed in two steps. The goal of the first step, caecal intubation, is to advance the tip of the colonoscope to the caecum. The physician will examine the colon as the colonoscope is advanced to the caecum but will likely advance the scope as quickly as possible. The second step involves a slow withdrawal of the colonoscope in order to examine the entire colon for polyps and any other pathology. If a polyp is found, the physician may choose to remove the polyp for histological examination. If the polyp is removed, the

procedure is no longer classified as a screening colonoscopy, but rather as a therapeutic colonoscopy.

2.2.1.1 Pros and Cons of each Screening Method

All three of the screening modalities discussed are currently being used throughout the world. Each has advantages and disadvantages for both the patient and the physician.

Inadomi (23) calculated the increase in life expectancy for FOBT, sigmoidoscopy and colonoscopy. The calculations were performed on a model which was based on the declining exponential approximation of life expectancy (DEALE) equation. DEALE assumes that with the advancement of time, the survival of a population cohort will decline exponentially. Using the DEALE equation, the life expectancy of a group of 50 to 54 year old residents in the US was decreased (due to colorectal cancer) by 292 days. For this group, screening with FOBT increased the life expectancy by 51 days, screening with sigmoidoscopy increased the life expectancy by 86 days and colonoscopy increased the life expectancy by 170 days (Figure 2-7). There were no data for barium enema in the report. All three modalities can have a positive impact on life expectancy.

FOBT is safe for both the patient and the physician. It is also easy to administer, aside from the unpleasantness of obtaining the sample. A disadvantage of FOBT is that it cannot ascertain the location or pathology of the location of the blood which has been detected. Another disadvantage of FOBT is that the physician cannot remove the polyp or tissue for a histological confirmation. While a

colonoscopy has the greatest impact on life expectancy, the FOBT could be given to a large number of patients as a way to screen patients for a colonoscopy.

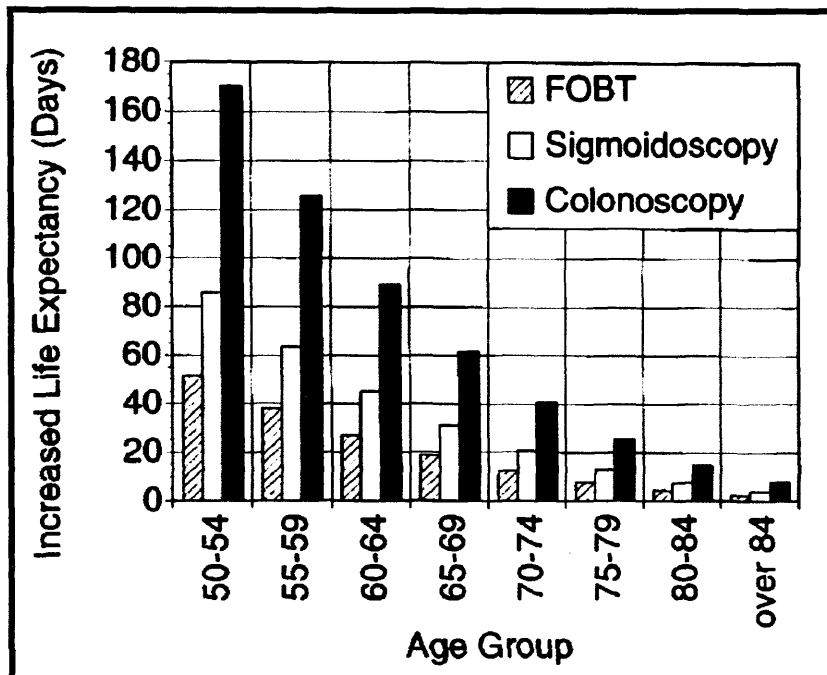


Figure 2-7. Data demonstrating the benefit of the three modalities of colorectal cancer screening. The X-axis is each age group and the Y-axis is the increased in life expectancy due to screening. Patients had a colonoscopy performed once at age 50 and repeated every 5 years or every 3 years if a polyp was found (reproduced from Inadomi (23)).

Barium enema has an advantage over FOBT in that it can locate polyps and other pathology in the entire colon. Barium enema is less sensitive than colonoscopy. Winawer et al (24) reported that the size of the polyp affected the detection rate during double contrast barium enema. In an editorial Rex (25) stated that "*The use of DCBE will continue to decline*".

Sigmoidoscopy overcomes the disadvantages of FOBT and barium enema by providing a direct view of the tissue. A sample can be obtained and removed through an access channel in the sigmoidoscope. In an overview of screening colonoscopy, Ransohoff (10) reported on the first studies on screening average

risk patients with colonoscopy and sigmoidoscopy. The two reports (12;26) concluded that if screening were limited to the distal part of the colon (sigmoidoscopy), many proximal lesions would be missed.

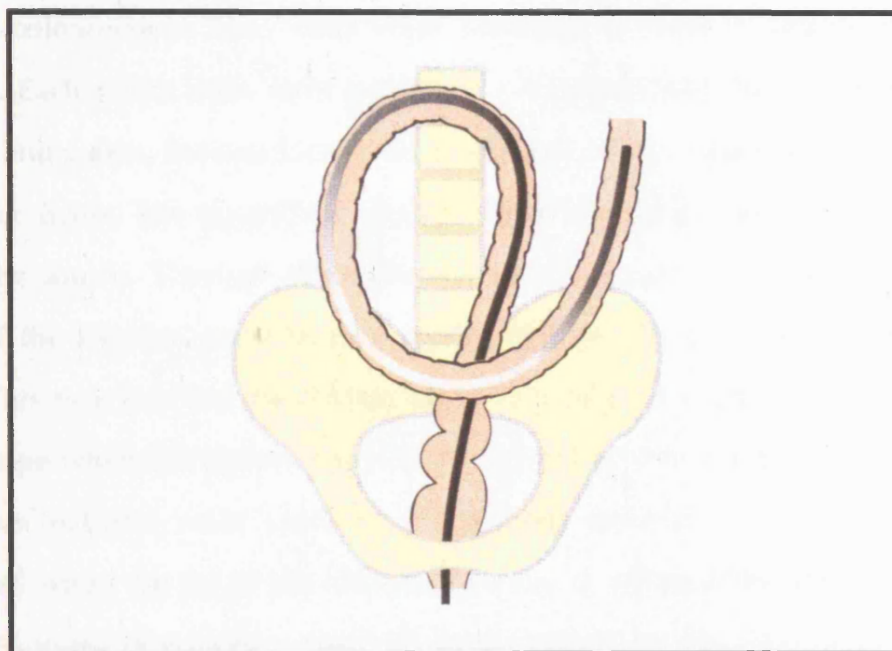


Figure 2-8. Artistic rendering of a colonoscope forming a loop in the colon (reproduced from Wayne (22)).

While colonoscopy has the potential to view the entire colon, it takes considerable skill to complete. Large studies have shown that the completion rate can be as low as 75% (27). The major difficulty encountered by colonoscopists is loop formation. This occurs when the flexible colonoscope is pushed through an even more flexible colon (Figure 2-8). The colonoscope stretches the colon and the mesenteric tissues connecting the colon. Loop formation makes it difficult for the colonoscopist to advance the colonoscope further. As the colon is stretched by the colonoscope, it can be extremely painful to the patient. If the colonoscope is pushed with greater force, a perforation can occur. It has been shown that a

force of 53 N (measured at the end of the colonoscope) can perforate a post mortem human colon (28).

Shah (29) reported on the use of real-time magnetic imaging of the colonoscope during colonoscopy. Nine coils were mounted in three locations under the patient. Each of the three coils generated a magnetic field that corresponded to the x,y and z axes. Sensors located along the axis of the colonoscope detected the magnetic fields. The magnitude of each signal was proportional to the distance from the source. Through the technique of triangulation, a three dimensional map of the location and direction of the colonoscope was constructed in real time. This map enabled the colonoscopist to record the location of the tip of the endoscope when the patient requested more medication for pain. One hundred and two patients were studied. The patient demand for more medication occurred when the tip of the colonoscope was in the sigmoid colon 77% of the time, 7% in the descending colon, 6% at the splenic flexure, 5% in the transverse colon, and 4% in the proximal colon. Since the afferent fibres can be stimulated by excessive distension of the gut wall, it is likely that the stretching of the sigmoid colon by the tip of the colonoscope caused the pain felt by the patient. Furthermore, when the tip of the scope presses against the wall of the colon the excessive pressure will compress the wall and likely to cause to ischaemic pain.

The Flexible Sigmoidoscopy Subcommittee of OMED recommended (30) that a low-cost reliable instrument be made available for an efficient mass screening population program. They made this recommendation in light of the fact that, in some parts of the world, non-physician personnel may perform the screening procedure. They further recommended that the instrument should be thin, flexible and have biopsy capabilities. The flexibility of the scope will have an

effect on the forces the scope applies to the tissue. Biopsy capability will enable the colonoscopist to perform a therapeutic procedure.

2.3 Diathermy for Therapeutic Colonoscopy

The main advantages of colonoscopy over the other modalities are that it provides the physician with the capability to see the entire colon and remove the diseased tissue. If a patient has polyps, the physician can remove them and can reduce the risk of the patient developing cancer (1). However, when large pedunculated polyps (see Figure 2-6) are removed endoscopically, there is a risk of significant bleeding. But if they are not removed endoscopically, the patient will be referred for surgical intervention to remove the polyp.

There are two methods for preventing or managing bleeding when a polyp is removed. The first method is to apply mechanical clips to the base of the polyp. The clip is delivered to the polyp through the access channel in the colonoscope. The clip is attached to a long cable and can be opened and closed by the physician. Once the polyp has been located, the clip can be opened, placed on the stalk of the polyp, and then closed. The polyp can then be resected either by a snare device or by a small needle knife (31).

The second method is more commonly used. A wire loop, or snare, is placed around the polyp. The loop is decreased in diameter, tightening around the polyp. The increase in mechanical pressure shears the polyp away from the mucosa. This method can be used for polyps less than 4 mm without the aid of a haemostatic technique (32). For polyps larger than 4 mm, the base of the polyp is heated to cause haemostasis of the severed tissue with diathermy. The snare

delivers high frequency (0.5 MHz) electrical current through the tissue. A conductive pad is placed on the leg or the back of the patient to complete the electrical circuit. The high current density close to the surface of the snare heats the tissue (ohmic heating) to a temperature sufficiently high enough to cause tissue coagulation. The frequency is much higher than the frequency which can stimulate the muscle tissue to contract.

2.4 Conclusion and the Aim of this Research

Colorectal cancer is a disease which can be fatal if left undetected and untreated. Screening colonoscopy is the best way to reduce death worldwide due to colorectal cancer, yet the procedure is painful and unpleasant for the patient and requires great skill and experience for the clinician. Furthermore, it has been recommended that a low cost instrument would enable a mass screening population program. This instrument must be reliable enough to be operated by non-physician personnel. It is the aim of this research to address these challenges of colonoscopy and propose solutions.

A new colonoscope will be designed and tested. This system will use a guidewire to help overcome the problems laid out in this chapter. In-vitro and in-vivo experimentation will be performed. The data from these experiments will be used to help design a system for clinical use.

New therapeutic methods of using electrodes to deliver radio frequency electrical energy will be proposed as a way to make polypectomy a safer procedure. A finite element analysis of how the tissue is heated by current flow from the electrodes will be performed and analysed.

In spite of the complex socio-economical issues that are associated with medical care, technological advances in instrumentation can have a positive impact on patient care. It is the aim of this research to develop tools to provide screening colonoscopy and therapy to patients around the world regardless of their socio-economical status.

3 Guidewire Endoscopy

3.1 Introduction

Chapter 2 discussed the anatomy of the colon and how it can be examined with a colonoscope. This chapter will discuss in more detail how the flexible endoscope has changed from a simple tube and candle light source to a more complex instrument containing several mechanical systems. The colonoscopy procedure will also be examined and analyzed, and methods to improve colonoscopy will be proposed and assessed.

3.2 Background

Endoscopy has been described as passing through three principle phases: “rigid endoscope (1805 to 1932); “semi-flexible endoscope” (1932 to 1957); and “fiberoptic era” (1957 to present) (33). Bozzini (1773 to 1809) invented the first endoscope in 1805, known as the “Lichtleiter” or the light conductor. It was rigid and used a candle as a light source (Figure 3-1). The light source was, for the next 80 years, to have the biggest impact on the endoscope in terms of ease of use and acceptance. It wasn’t until 1887 that Leiter introduced a panelectroscope which featured Edison’s electric light.

In 1932 Rudolf Schindler introduced the flexible gastroscope (Figure 3-2), a collaborative effort with George Wolf. This instrument was superior to those of the past primarily because of the view it could provide in many directions. Schindler proposed that the end, rather than the entire endoscope, could be flexible and articulated. He and Wolf developed an optical system that could accomplish this.

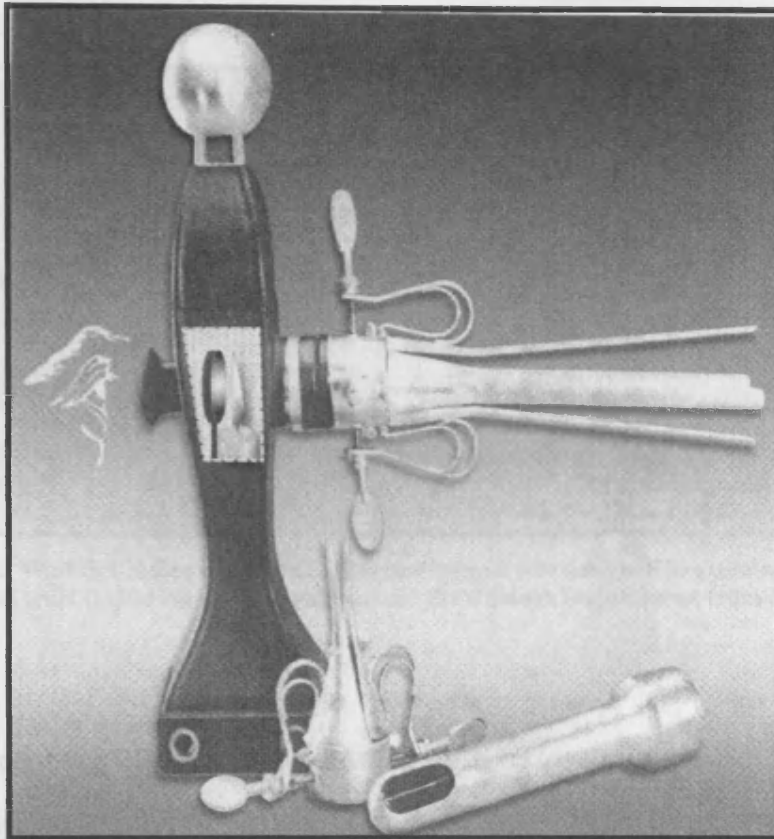


Figure 3-1. Bozzini's light conductor (reproduced from Wayne (34)).

Phase three began in 1963 (35) when Basil Hirschowitz announced that "the conventional gastroscope has become obsolete on all accounts" and introduced the first fiberscope. The fiberscope contained flexible optical fibres which were arranged in a way to transmit an image to the proximal end of the scope. This type of fibre bundle is known as a coherent bundle. This meant that the image could be transmitted through a flexible shaft. Hirschowitz went beyond the stomach and began to explore the duodenum. Although at the time the quality of the image produced by a fibre bundle was poorer than that of earlier scopes, it was obvious that the flexibility of the fiberscope would make it the scope of the future.

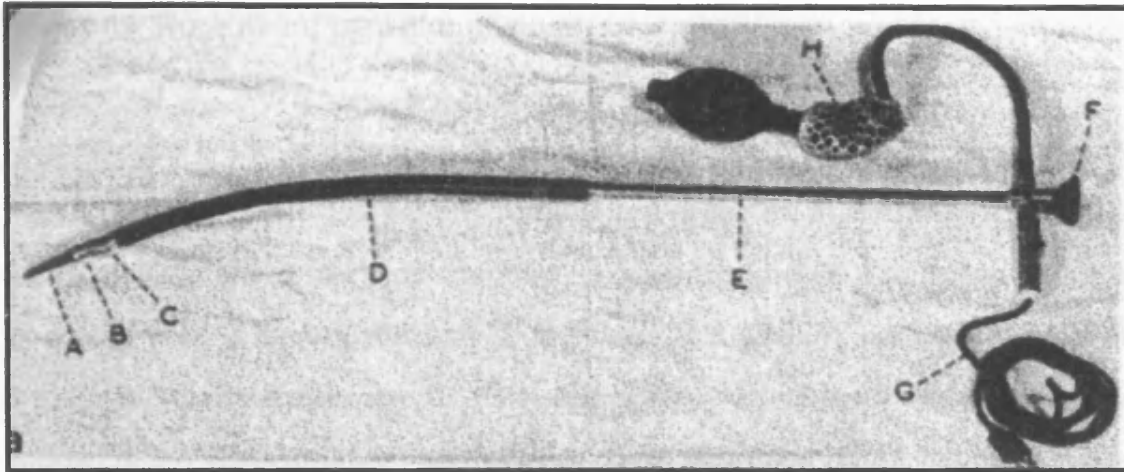


Figure 3-2. Wolf-Schindler endoscope. This instrument was designed to examine the upper gastrointestinal tract including the oesophagus and the stomach (reproduced from Edmonson(36)).

The most recent significant advance in flexible endoscopy is the incorporation of miniature video cameras. These cameras were first incorporated into an endoscope by Welch Allyn (Skaneateles, NY) in 1983, and are now the most commonly used endoscopes. The use of videoendoscopy has many advantages, including the ability to collect and analyze the video signal to detect diseased tissues.

The examination of the entire colon was preceded for years by the examination of the rectum and the sigmoid colon (34) using various proctosigmoidsopes. These began as rigid instruments and with time became more flexible. Whereas the rectum could be examined with moderate levels of light and a rigid instrument, the sigmoid colon was more difficult since more illumination was needed. In 1899, Pennington sealed the eyepiece and inflated the sigmoid with a rubber bulb (34). The air distended the sigmoid and exposed tissue which

previously had been difficult to see. He also placed an incandescent lamp at the end of the scope to improve illumination.

Colonoscopy is the examination of the colon from the anus to the caecum. With modern colonoscopes a complete examination of the colon is highly achievable. Most colonic disease starts on the mucosa or epithelium (21), so early diagnosis and treatment is therefore feasible. Overholt and Collard performed the first successful total colonoscopy in 1966. Many more advances were made in the following ten years at which point Novis concluded that *"the colonoscope provides a valuable and effective means of diagnosis and therapy of lesions in the large bowel"* (37).

In the United States, patients are given intravenous sedation before the procedure. This helps to reduce the pain felt by the patient when the colonoscope is pushed through the colon. This pain is mainly due to stretching of the mesentery. When performing a colonoscopy, it is possible to form "loops" in the colon. These loops can increase the force required to push the colonoscope further. When greater force is applied to overcome the effects of these loops, the mesentery is stretched and the patient can feel quite significant pain, often requiring more sedation.

Sigmoidoscopy is the examination of only the distal portion of the colon from the anus through the sigmoid colon. Recent literature has suggested that a colonoscopy is superior to a sigmoidoscopy to detect colon cancer (38).

3.3 *The Colonoscope*

A colonoscope is shown in Figure 3-3. The length of the main body is 1.6 metres in the UK, 1.35 metres in the United States and Europe. The most distal 10 cm of the main body can be articulated by turning two control knobs in the handle. The articulation provides steering as the main body is pushed into the colon. The articulation of the tip must be great enough to provide a retroflex view or a so-called "J" configuration to view the complete surface of the rectum. Instruments are introduced into the colonoscope through an access channel. This access channel is also used to vacuum fluids from the colon. These fluids pass through an umbilicus connected to the handle then through a fluid trap. The umbilicus also contains the cables to connect the camera to the video processor and the optical fibres used to transmit illumination light to the distal end of the colonoscope.

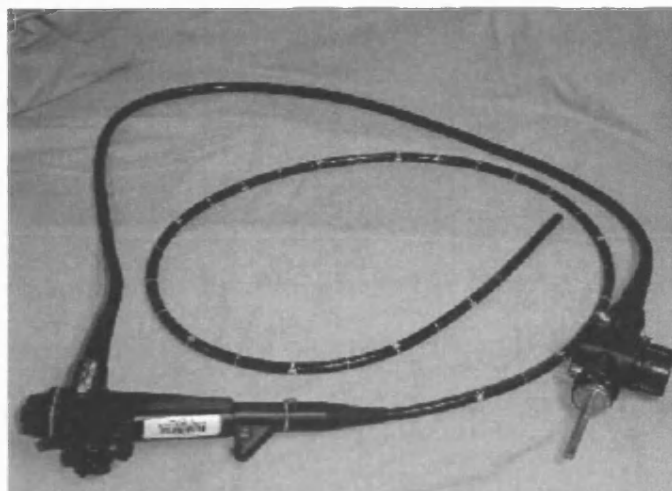


Figure 3-3. A standard colonoscope (Olympus Corp.). The insertion tube has length labels printed in white to determine the distance the tip has been advanced into the colon.

Figure 3-4 is a photograph of the distal end of the colonoscope which has had the outer layers removed.

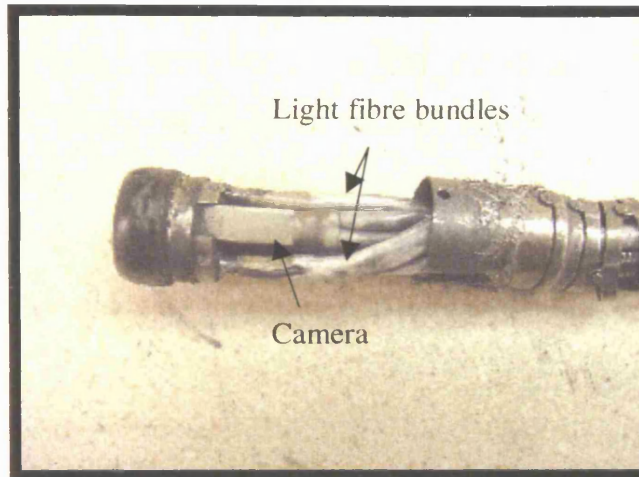


Figure 3-4. The tip of the colonoscope has had the outer layer removed to expose the contents.

The camera module and connecting cables are shown fixed to the tip. The camera module contains an objective lens, imaging array and processing electronics. The two light fibre bundles on each side of the camera provide illumination for the camera. A cold white light source (usually a filtered xenon arc lamp) is used to give the clinician an accurate view of the mucosal surface.

The access channel is on the opposite side from the camera module (not shown). The end cap is smooth and rounded. The entire outer surface of the colonoscope is carefully constructed to reduce sharp edges and is sealed with a lubricious lacquer to ease insertion into the colon.

3.3.1 Techniques in Colonoscopy

Colonoscopists are taught to rotate the scope, pull it back, and various other techniques to overcome the looping problem. Waye states that the most important technique for colonoscopy is the withdrawal and straightening technique (39). This technique involves rotating and pulling back the scope to pleat the colon over the scope. Once this is done, the scope is advanced. Although quite effective, it requires that the operator manipulate the scope in a blind fashion and assumes that the colon will indeed straighten out.

A variable stiffness colonoscope has been used recently as one solution to overcome looping. This type of scope allows the clinician to change the stiffness of the entire length of the scope as needed. If the scope has been advanced through the sigmoid colon, the body could then be stiffened to prevent loop formation as the scope is advanced further. In a review of advances in interventional endoscopy, Seitz reported that the variable stiffness scope was found to be helpful in 90% of colonoscopies (40). Rex (41) reported that, in the hands of an experienced colonoscopist, the variable stiffness scope was useful but did not decrease the time to reach the caecum.

A three dimensional imaging system can be used to provide a real time view of the location of the colonoscope in the colon. This allows the clinician to manipulate the scope to overcome looping without having to guess as to where the looping is occurring. Seitz concluded that although experienced clinicians would not need such a system, it would be useful for training centres (40).

Rex reported on methods of colonoscopy on patients presented after incomplete colonoscopy (42). He successfully completed the colonoscopy in 40 of 42 patients (95%) using techniques such as a different sedation, smaller colonoscopies, external straighteners and guidewire exchange. Looping accounted for 22 of the 42 (52%) initial failures in these patients.

TECHNIQUE EMPLOYED	NO. OF PATIENTS	PERCENTAGE OF TOTAL PATIENTS
Sedation change	2	5%
Standard colonoscope	6	15%
Smaller more flexible scopes (1)	16	40%
Mechanical straightening device (2)	13	33%
Guidewire exchange	3	8%
N=	40	

Table 3-1. Rex data on techniques to complete failed colonoscopies. (1) Paediatric colonoscope or upper endoscope. (2) External straightener.

The various manoeuvres to complete the procedure can be seen in table 3-1. The reason for failure was ascertained in 38 of the 42 cases. When the reason for failure was a narrowed or fixed sigmoid colon, an attempt was first made using a paediatric colonoscope. Smaller and more flexible scopes had the highest completion rate, followed by various mechanical devices to help straighten the scope. But one needs a large channel scope for therapy, therefore a smaller scope

cannot always be used. These data suggest that improving the scope design would provide the clinician with the opportunity to overcome the problem of loop formation.

The guidewire exchange technique was used to simply exchange one scope (paediatric colonoscopy) for another (gastroscope). The gastroscope (smaller diameter and more flexible) would be advanced as far as it could go. The longer paediatric colonoscope would then be exchanged over the guidewire and advanced further to the proximal part of the colon.

3.3.2 Delays in Colonoscopy

One can imagine the difficulty of pushing a rope through a floppy tube. This has been the metaphor used to describe colonoscopy. A good deal of engineering has been applied to the colonoscope to make it possible to push it through the colon without much difficulty. The body (insertion tube) of the colonoscope must be stiff enough to push through the colon, yet the entire body must be flexible enough to pass through the tortuous colon.

Colonoscopists are skilled at pushing, pulling and rotating the colonoscope to advance it further into the colon. The extra time required to advance the colonoscope is considered a part of the normal procedure. As has been mentioned repeatedly, pushing the colonoscope through a loosely affixed structure, such as the colon, can result in loop formation. When these loops form, more push force (insertion force) will increase the size of the loop and not move the tip of the colonoscope forward. Figure 3-5 is a radiograph of multiple loops

within the colon formed by the colonoscope. The articulating section of the colonoscope can be seen clearly in the left upper quadrant.

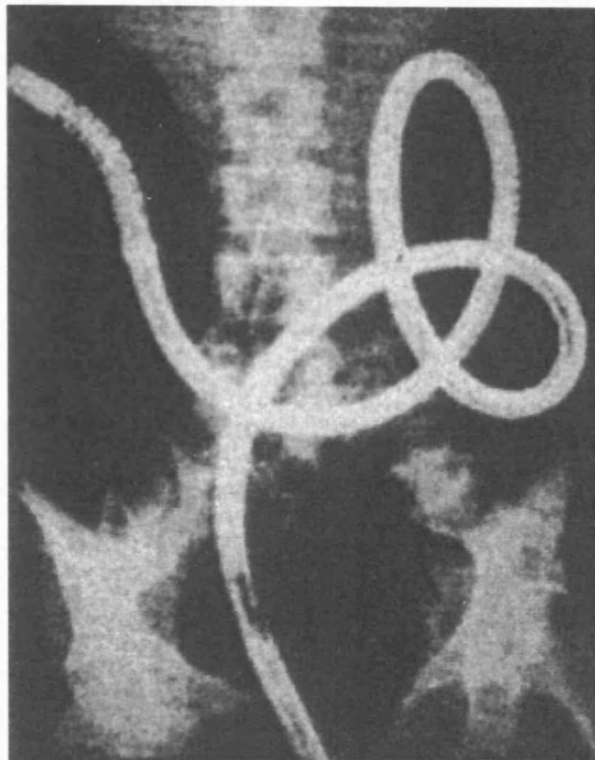


Figure 3-5. Radiograph of a loop which has formed in a colon during a colonoscopy (reproduced from Mosse (43)).

As the insertion force is increased, the colonoscope will eventually slide through the loop. Pushing through these loops can cause pain to the patient and risk a perforation of the colon due to excessive forces (44). In a recent UK study, the caecal intubation rate was reported to be 76.9%. In the cases where the caecum wasn't reached, 34.7% were aborted due to patient discomfort, 29.7% were due to uncontrolled looping, 19.6% were due to poor bowel preparation, and 9.5% were due to diverticulosis (45). The study concluded that better training was needed to improve the rate of caecal intubation.

3.3.3 Measurements of Time Delays During Colonoscopy

For this thesis, data were collected to study in more detail the time delays that routinely occur during colonoscopy. A stopwatch was used during the colonoscopies (n = 29 cases) to record the time during which the tip of the colonoscope moved forward. Delay was defined as any time during which the tip of the endoscope was not moving forwards. Colonoscopists (n = 4) who had performed more than 250 but fewer than 500 procedures were compared with an experienced group (n = 2) who had performed more than 1000 procedures.

Twelve of the procedures performed by experienced (n = 6 cases) and less experienced (n = 6 cases) colonoscopists (separate from the other observations) were compared. In addition to forward movement, times were recorded as the tip of the scope reached anatomical landmarks such as the sigmoid colon, left flexure, right flexure and the caecum.

The mean time (of both groups) to advance the tip of the colonoscope to the caecum was 16 minutes 49 seconds, giving an average speed of 0.124 cm/sec (colon = 1.25 meters). Taking 16 minutes to advance a colonoscope 1.5 metres seems extremely slow.

	EXPERIENCED COLONOSCOPISTS (N=6)	LESS EXPERIENCED COLONOSCOPISTS (N=6)
Mean total time (min)	13.00	20.63
95% confidence interval	9.23 to 16.78	15.25 to 26.02
Mean forward time (min)	3.17	4.37
95% confidence interval	2.23 to 4.10	3.10 to 5.62
Percentage forward	24%	21%
95% confidence interval	21% to 28%	20% to 22%

Table 3-2. Caecal intubation time for 12 colonoscopies. The forward time denotes the time that the tip of the colonoscope was moving forward. The data are in decimal format.

The data in Table 3-2 are the caecal intubation times for the experienced and less experienced clinicians. A statistical analysis showed that the difference in the average times yielded a p value of $p > 0.20$.

There was little difference in percentage forward time for both experienced and less experienced colonoscopists. One could hypothesize that the delays in moving the tip forward are reduced with experience, but that as a percentage of total time the delay does not depend on experience.

It is clear that delays are a part of colonoscopy with both experienced and less experienced colonoscopists. What is not entirely clear is the reason for these delays. As stated before, the relative floppiness of both the colonoscope and the colon make it difficult to advance the tip. A series of forward and backward advancements along with rotation of the colonoscope such as the so-called

“shortening and loop advancement” technique can help to overcome these difficulties (44). But, as has been shown here, these techniques only shorten the overall time to reach the caecum. They do not affect the percentage of time the tip is moving forward. Nor do these techniques entirely eliminate the pain experienced by the patient.

Church showed that completion rate increases with experience (44), where completion was defined as the tip of the colonoscope touching the caecum. Trainees were taught the shortening and loop avoidance technique. This technique is aimed at reducing the pain to the patient by simply pushing through the loops (44).

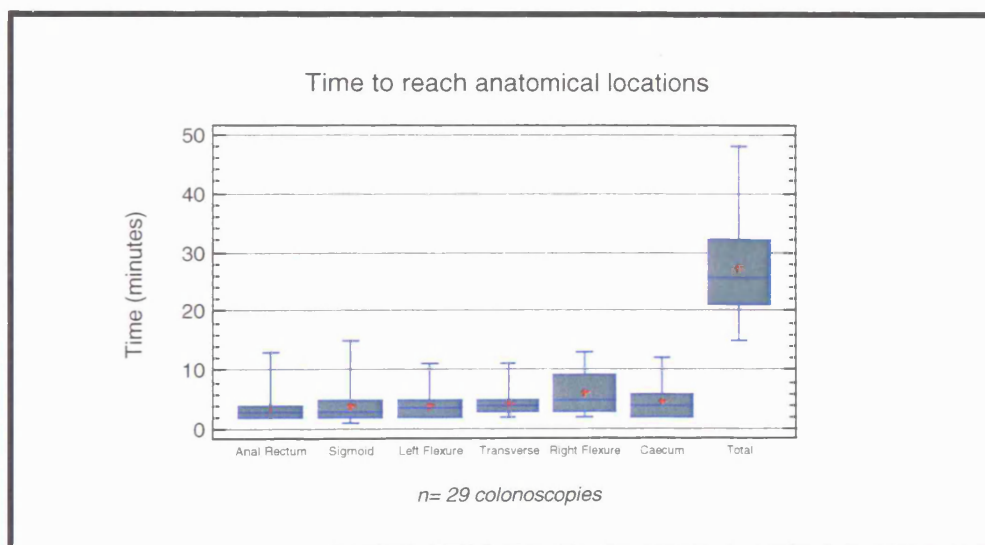


Figure 3-6. Recorded times to reach anatomical landmarks of the colon. These times were recorded with a stopwatch when the colonoscopists indicated that the landmark had been reached.

Figure 3-6 is a chart of the time intervals between each anatomical landmark for the 29 cases (these data were recorded separate from the data in Table 3-2). One such time interval would be the time to advance from the end of the anus/rectum to the end of the sigmoid colon. Another would be the time to advance from the

end of the ascending colon to the left flexure. Again, both experienced and less experienced colonoscopists performed these cases. The mean values are shown in Table 3-3.

Table 3-3. Mean values of times to reach the anatomical landmarks of the colon. See Table 2-2.

	MEAN TIME (MINUTES)	SD
Anus/Rectum	3.97	2.56
Sigmoid	4.07	3.27
Left Flexure	3.93	2.18
Transverse	4.33	1.73
Right Flexure	6.27	3.18
Caecum	4.63	2.79
Total	27.20	8.53

Recent literature has shown that colonoscopy can take up to 40 minutes to complete (27). The caecal intubation time was not reported, but the caecal intubation rate was greater than 90% for only 55% of the endoscopists studied. Given that incomplete colonoscopies are not unusual, and reaching the caecum can be quite time consuming, there exists a need to improve colonoscopy.

3.4 The Guidewire

3.4.1 Background

Arteriographic examination with the aid of a wire has been described as early as 1941 (46). Seldinger described the use of a “leader” to aid the percutaneous introduction of a catheter (47). The leader was essentially an early guide wire, used to help introduce the catheter into the artery through a puncture. The leader was then withdrawn once the catheter was successfully introduced. This early guide wire had a soft end and a relatively rigid body.

It was not until later that the full use of a guide wire would begin to be realized. In 1957 Seldinger published an article describing the use of this catheterization technique in the spleen and liver (48). Carter et. al. had described techniques of catheterization other than for arterial examination in 1952 (49). Catheterization, which was used for years as an aid for arterial examination, was now being used to explore other lumens in the body. The radiologist was still the driving force behind the use of these techniques and tools.

Sargent et. al. described the use of a “wire guide” to aid the insertion of a Cantor tube (50), used for intestinal decompression. This was an early description of the use of a guide wire to selectively stiffen a catheter. This guide wire was 12 feet in length, and was described as a coiled spring wire guide (Figure 3-7).



Figure 3-7. Early "wire guide" manufactured by Cook Inc., Bloomington, Indiana, USA, circa 1962 (reproduced from Sargent (51)).

Although the wire guide was not described in detail, one can infer that the guide wire must have had a solid core and a wire wound around the core to improve flexibility without a risk of kinking. The author describes the technique of pushing and pulling the guide wire while advancing the catheter. In 25 patients where simply pushing the Cantor tube failed, the guide wire technique was successful.

In 1996 a group at the Indiana University Medical Center reported the use of a guide wire to exchange between a small calibre gastroscope and a large calibre colonoscope (52). The small gastroscope could more easily negotiate sigmoid loops and strictures. The guide wire was then introduced through the

gastroscope, left in the patient and back loaded into a colonoscope. The colonoscope could then be advanced past the loop or stricture and continue on to complete the case.

3.4.2 Guidewire Assistance in the Colon

Figure 3-8 is an illustration of typical fixation of the colon. The blue shaded region represents the fixed retroperitoneal sections of the colon.

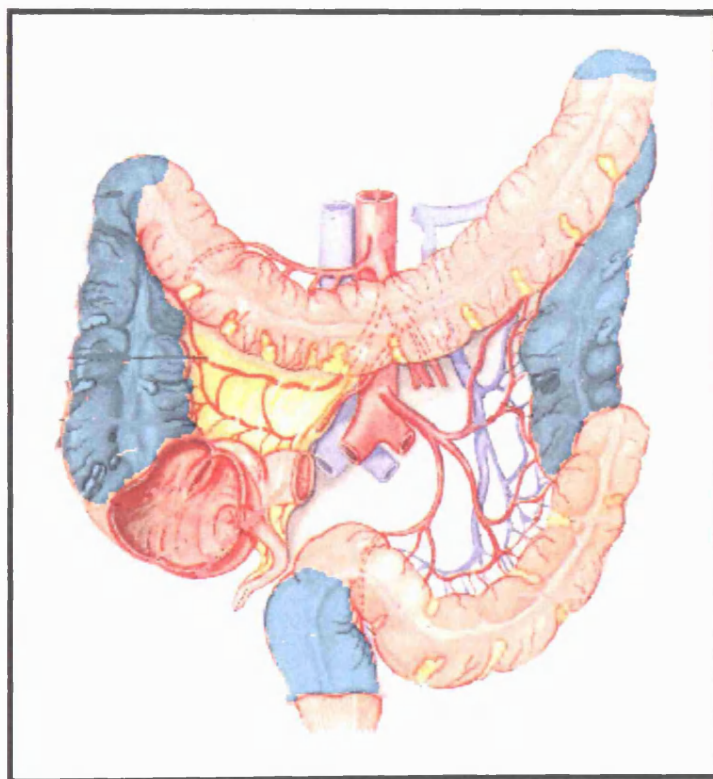


Figure 3-8. The blue shaded region in this illustration represents the fixed retroperitoneal structures. The non-shaded regions are not fixed and tend to move and stretch when pushed by the colonoscope (modified reproduction from Netter (4)).

Experiments were performed in both post-mortem (excised) pig colon and live pigs to determine how a guidewire could aid in the advancement of the

colonoscope. These experiments were performed by the author in both the UK and the USA. The goal of the experiments was to measure the insertion (push) force of the colonoscope when a loop begins to form in the non-shaded areas in Figure 3-8.

Both models (live and post-mortem) have limitations, which can produce misleading test results. The post mortem colon is no longer perfused and can dry out, affecting the lubricity of the tissue and the elasticity. While the live model can overcome this limitation, the pig colon differs anatomically from the human colon.

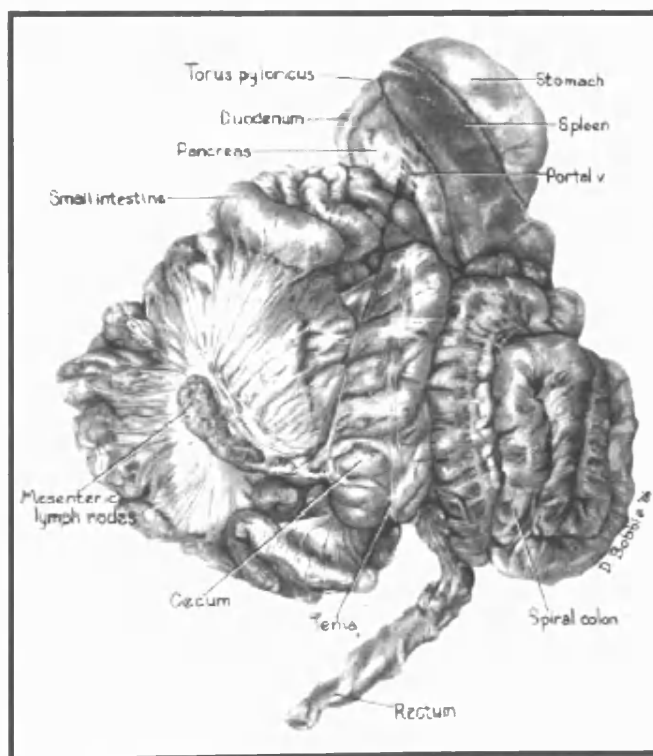


Figure 3-9. An anatomical drawing of the pig gut (reproduced (53)).

The pig colon follows a tight spiral just past the distal colon (Figure 3-9). This would be somewhat analogous to a tortuous sigmoid colon in the human, but the true spiral configuration would be rare in a human.

3.4.2.1 Reduced Insertion Force in a Tissue Model

3.4.2.1.1 Introduction

An experiment was performed to simulate a colonoscope advancing in a colon with and without the aid of a guidewire. A novel guidewire method (*patent pending see appendix I*) was developed to advance more reliably through the colon as compared to a conventional guidewire. Rather than advancing a thin guidewire with a flexible end through the colon, a long guidewire (Jagwire®, Boston Scientific, Boston, USA) was folded back on itself to form a loop end. This end could be advanced through the colon by pushing on one end (leg) of the guidewire. The loop end provided a safe and effective way to advance through the colon regardless of the colon diameter. The loop will contract or expand, depending on the diameter of the colon. The force that the loop applies to the colon will depend on both the stiffness of the wire and the diameter of the colon. If it is difficult to turn a corner, the other leg can be pushed which will typically advance the loop around the corner. Furthermore the orientation of the loop can be changed to help advance further. For instance, if the loop is parallel to the direction of change of the colon, it can be rotated to be perpendicular. This should make it easier to advance the loop further along the colon, rather than into the colon wall.

3.4.2.1.2 Methods

The colonoscope was modelled as a tube (OD = 5.6mm) made of polytetrafluoroethylene (PTFE) and reinforced by a wire strip woven around the outside diameter to prevent kinking.

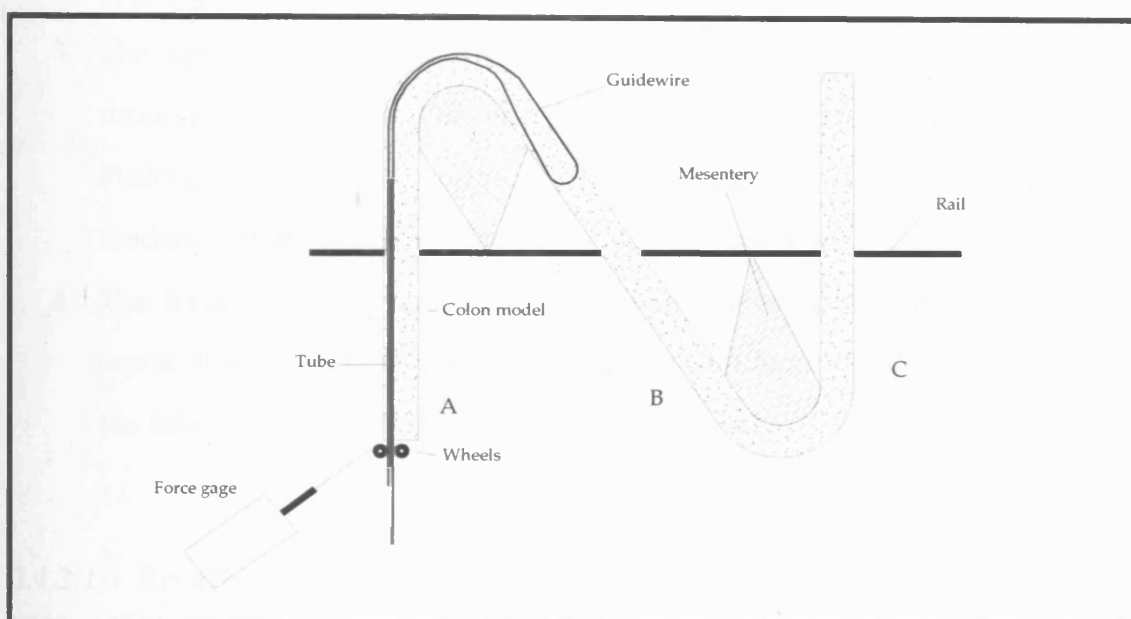


Figure 3-10. Experimental setup of insertion force measurements of a tube in a model of a colon. The force gage measured the force that the wheels applied to advance the tube.

A model of the colon was constructed of porous PTFE (ID=20 mm) attached to a rail system (Figure 3-10) at various points using a thin elastic membrane (cling film) to simulate the mesentery. The rail system allowed the model to be adjusted by sliding the attached membrane along the rail, creating a tortuous path. The guidewire (0.46 mm core, PTFE coating) was doubled to form two legs. The two legs were back loaded into one end of the tube and pulled out the other end of the tube. No lubricants were added; therefore the coefficient of friction is the value for PTFE on PTFE. A force gage (Omega model DFG70, Stamford, CT USA)

was used to measure the force required to advance the tube. The experiment was done as follows:

1. The end on the tube with the folded guidewire was pushed into the colon model until it reached point B in Figure 3-10.
2. One leg of the guidewire was advanced into the model while holding the tube stationary. This advanced the folded end of the guidewire in a "rolling" fashion from point B to point C.
3. The same leg of the guidewire was pulled back while simultaneously rotating two wheels. The wheels advanced the tube by frictional force. Pulling back on the guidewire, while advancing the tube, reduces the tendency of the tube to stretch the colon and mesentery tissues.
4. The force required to advance the tube was measured by pulling on a string attached to the wheels. The maximum force to advance the end of the tube from point B to point C was recorded.

3.4.2.1.3 Results

Table 3-4 presents the data recorded during 20 repetitions of the experiment. The average force required to advance the catheter without guidewire assistance was 5.85 N (0.57 SD). The average force require to advance the catheter with the guidewire was 2.76 N (0.59 SD). Figure 3-11 is a plot of the results.

	Without Guidewire	With Guidewire
	(N)	(N)
1	5.77	2.19
2	6.13	2.65
3	5.34	3.22
4	5.98	3.04
5	6.20	3.47
6	5.69	3.17
7	6.00	2.17
8	7.22	2.94
9	5.83	2.87
10	5.51	2.42
11	6.41	3.10
12	5.54	3.22
13	5.60	2.25
14	4.94	2.97
15	6.73	1.91
16	5.81	2.44
17	6.10	2.28
18	5.92	2.07
19	5.80	4.38
20	4.59	2.43

Table 3-4. Insertion force to advance the tube from B to C in Figure 3-10, with and without the guidewire. The force required to advance the wheels without the tube was subtracted from the values recorded with the tube to yield the total insertion force.

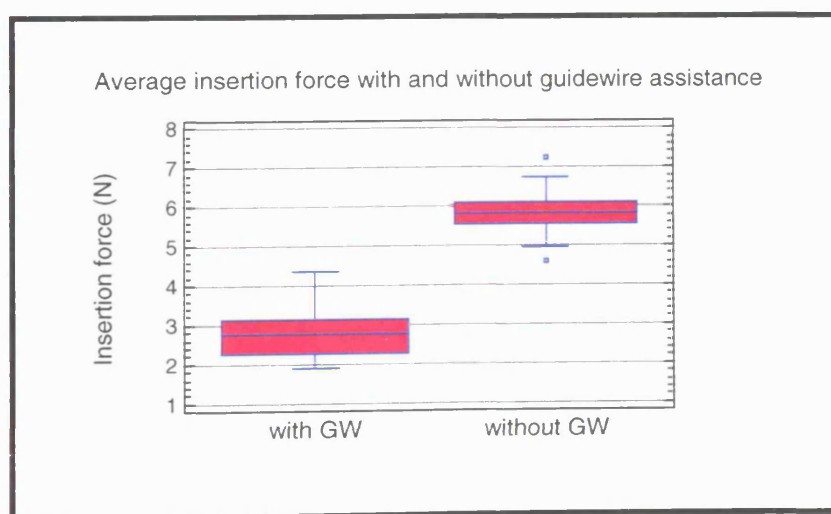


Figure 3-11. Comparison of the insertion force of the tube with and without the assistance of the guidewire.

3.4.2.1.4 Discussion

Using the guidewire to advance the tube reduced the insertion force by 52% (95% confidence interval of $\pm 5\%$). This reduction in insertion force may lead to a reduction in pain. Furthermore, the technique of advancing a folded guidewire is very important for this method to work in the clinical setting. A conventional guidewire is designed with a very flexible end and is advanced under fluoroscopic visualization. When the guidewire is advanced the flexible end will bend when it pushes into the wall of the colon, rather than perforate the wall. It frequently bends and folds back. This technique may assure the operator that the wire is continuing to move through the colon.

The first advantage of this folded method of guidewire advancement is the increased margin of safety. This type of an end will have a very low likelihood of causing a perforation. The second advantage of a loop is the way that it advances naturally. The loop will unroll into the lumen of the colon and can thereby advance quite substantial distances.

It is difficult to model the human colon accurately, therefore there are limitations to this experiment. It was important that the model material had similar properties such as lubricity, elasticity and length and diameter. PTFE has very low coefficient of sliding friction much like the colon, yet is not as elastic as colon (Table 3-5). But a tortuous path with flexible attachment points can be created, which is a very important part of this experiment.

Table 3-5. A comparison of two properties of colon and porous PTFE. * A value for Young's modulus of human colon could not be located in the literature; a value for human aorta was used as a comparison.

	Sliding coefficient of friction	Young's modulus (Gpa)
Colon*	0.15 (43)	0.68X10 ⁻³ +/- 20% (54)
Porous PTFE	0.10 (55)	0.46 (55)

Another limitation is the assumption that a reduction in the insertion force will lead to a reduction in loop formation and pain felt by the patient. Since it is difficult to place transducers in-vivo to measure the actual forces on the mesenteries, one can only infer that the reduction in push force will result in a reduction in the force stretching the mesenteries.

3.4.2.2 Pig Colonoscopy In-Vivo Experiments with Guidewire

Assistance

3.4.2.2.1 Background

The folded guidewire experiment demonstrated that a reduction in insertion force could be realized when a simple tube was used in place of a colonoscope. The next step was to test the wire with a standard colonoscope and a catheter containing a camera, since a simple tube cannot be advanced in a human colon blindly. The Cathcam (see Appendix II) was designed as part of this work. The author worked with a consulting firm (PA Consulting, Cambridge, UK) to complete the design and build the Cathcam devices. The intent of these experiments was to determine whether or not a reduction of force would be realized with a standard colonoscope as well as the Cathcam. The principle

difference between the Cathcam and a standard colonoscope was that the Cathcam did not contain the ability to articulate the end of the tip. If the Cathcam could be advanced without articulation, then a less skilled operator could perform the colonoscopy.

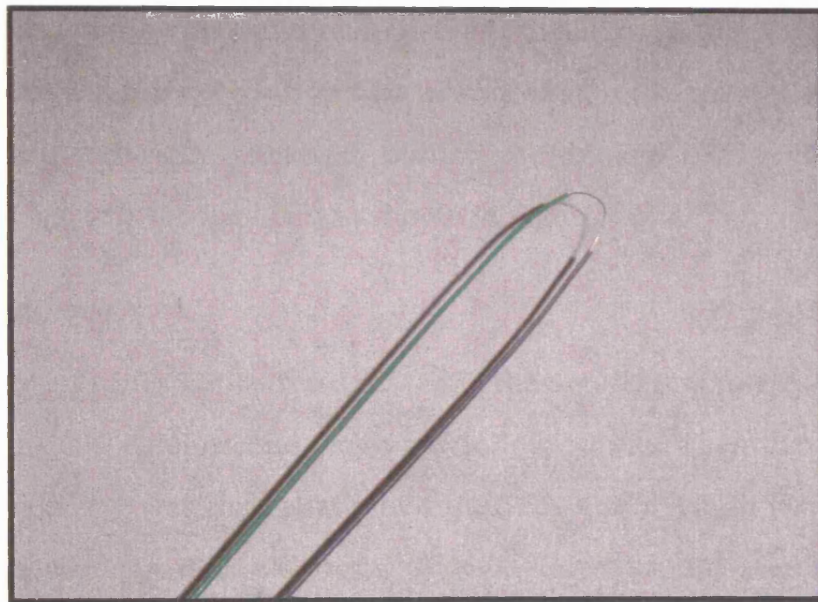


Figure 3-12. Hinged guidewire. The thin section connecting the two “legs” allows the wire to be folded and placed into the working channel of the colonoscope.

A custom guidewire and colonoscope (Cathcam) were built for eventual use in humans, but first were tested on live pigs to measure the insertion force. Insertion force as a function of time was measured during the colonoscopies on the pigs. Three techniques were compared in pigs: colonoscopy using a standard colonoscope; colonoscopy using a standard colonoscope with guidewire assistance; and finally colonoscopy using the Cathcam with guidewire assistance. Each colonoscopy was performed by an experience colonoscopist (more than 1000 colonoscopies) and was assisted by an experienced colonoscopist. This is a single experiment that is meant to illustrate the force measurements and the

histogram analysis. Therefore a statistical analysis will not be provided for this experiment.

The custom guidewire (Lumenguide, see appendix II) was designed to fit through a colonoscope channel. A thinned section connected the two legs of the guidewire. The guidewire could be folded at the hinge (Figure 3-12) to fit down the channel of the colonoscope and be advanced into the colon. One leg of the guidewire could then be retracted, pulling the thinned section back into the channel and leaving a looped end as shown in Figure 3-10.

3.4.2.2.2 Methods

A 52.7 kg pig was anesthetized and placed in the dorsal recumbency position. An Olympus CF-100L colonoscope was used to inspect and clean the colon of the pig. A colonoscopy was then performed until the entire length ($\approx 130\text{cm}$) of the colonoscope was inserted. A model FH6-01 force handle (Figure 3-13, see Appendix II for more technical details) was used to measure the insertion force during the colonoscopy. The force handle contained a load cell with a range of -111 N to 111 N (calibrated over the range of -20 N to 20 N), which was connected to a DAQPad 6020E A/D converter (National Instruments, USA). A program was written in Matlab™ (The Mathworks, USA) to communicate with and collect the data from the DAQPad 6020E (10 Hz sampling).

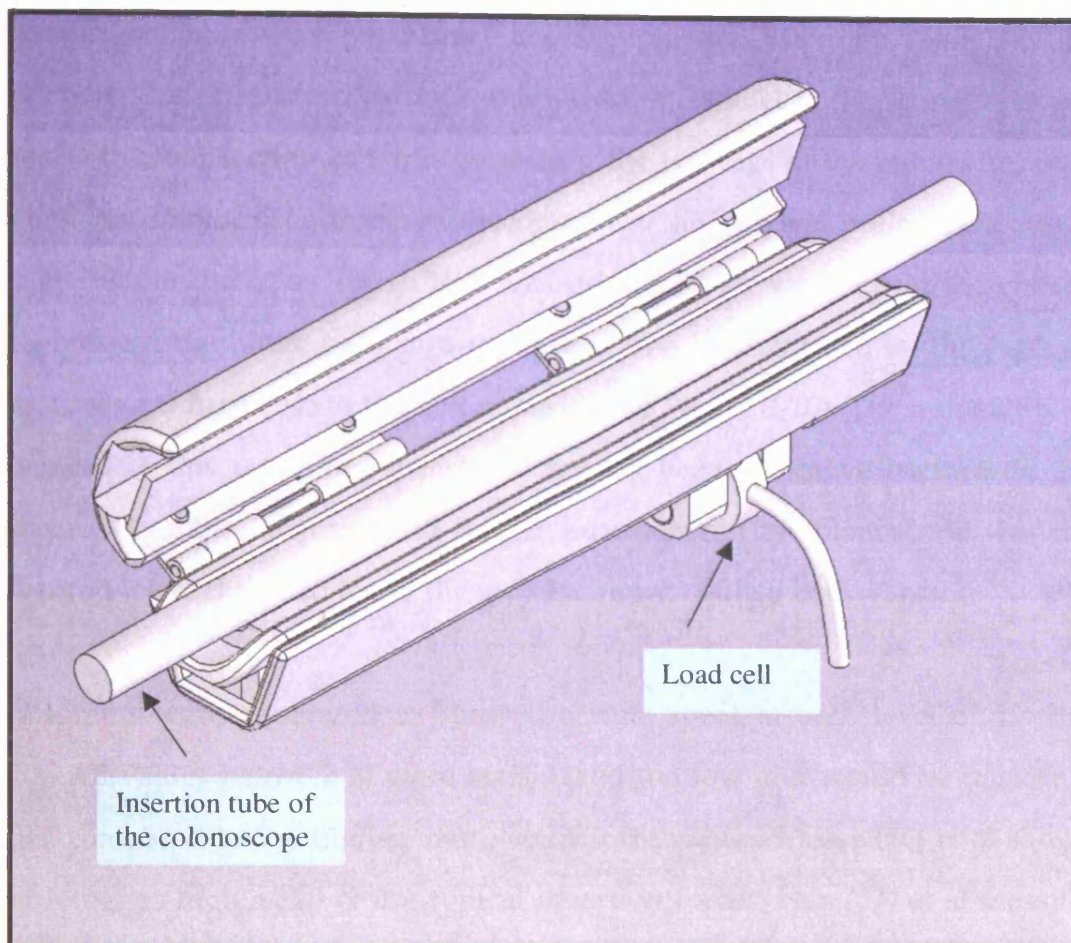


Figure 3-13. Force handle. The load cell is connected to a linear slide which is aligned with the axis of the insertion tube. The top half of the handle squeezes on the insertion tube.

Table 3-6. Colonoscopies performed on the pig. The custom guidewire was used during the 2nd, 3rd, and 4th colonoscopies. *Approximate distances-loops may have formed.

COLONOSCOPY	INSTRUMENT	FORCE HANDLE USED	DISTANCE* (CM)	TIME (MIN.)
1	CF-100L	Yes	100	5
2	CF-100L w/ guidewire	No	na	na
3	CF-100L w/ guidewire	Yes	130	11
4	Cathcam	Yes	70	35

The four colonoscopies performed on the pig are listed in Table 3-6. The guidewire was introduced through the working channel of the scope. When the hinge (a thinned section of wire connecting the two legs of the guidewire) of the guidewire could be seen in the endoscopic view, one leg was pulled back into the channel while the other (push leg) was advanced forward out of the channel. This brought the hinge back into the scope. The loop, formed by the push leg, was advanced further into the colon (similar to Figure 3-10). The guidewire was advanced in this way until the stationary leg began to move backwards. This indicated that the loop was no longer advancing. The colonoscope was then advanced while the push leg of the guidewire was pulled backwards.

Histograms were generated to show the time spent at each level of insertion force. All values below 2 N were considered too low and would be misleading when compared to the higher, more significant values. Mosse (56) et al showed that forces as high as 20 N are typical insertion forces. Han (57) et al measured pressure exerted by the operator and reported that 300 gm/cm² was the minimum pressure which caused pain in a non-sedated patient. But it was unclear how the pressure was calculated. The author stated, "The pain inducing pressure (gm/cm²) initiated by the hand of the colonoscopist was measured with a force gage, and the relationship between the insertion force and location of pain was evaluated." If one were to assume that the pressure referred to here is the pressure by the hand of the colonoscopist, and a hand holding a 1 cm diameter colonoscope is nominally 10 cm wide, then the force would be:

$$\text{Pressure} = \text{Force} / \text{Area}$$

Equation 3-1

$$\begin{aligned}
Force &= 300 \frac{gm}{cm^2} \times 10cm \times \pi \times 1cm \\
&= 9.42kgforce \\
&= 92.5N
\end{aligned}$$

This is much higher (about 5 times higher) than the values measured by Mosse. The only other assumption (the author did not respond to a request for additional information) is that the pressure is being calculated with the distal portion of the colonoscope. This could either be the end or the side of the colonoscope. The end of the 1 cm diameter colonoscope has a fixed area and it would therefore be "easier" to calculate the pressure. The force to generate a pressure of 300 gm/cm² by the end of the tip would be:

$$\begin{aligned}
Force &= 300 \frac{gm}{cm^2} \times \pi \times (0.5cm)^2 \\
&= 0.235kgforce \\
&= 2.30N
\end{aligned}$$

It is unlikely that a colonoscopist would push the end of a colonoscope into the tissue thereby obscuring the view of the colon.

The side of the colonoscope would push and stretch the mesentery to cause pain to the patient. If one were to assume that the colon draped around one third of the colonoscope over a distance of 4cm, then, to a first approximation, the force to generate 300gm/cm² would be:

$$\begin{aligned}
Force &= 300 \frac{gm}{cm^2} \times \frac{1}{3} \pi \times 1cm \times 4cm \\
&= 1.26kgforce \\
&= 12.35N
\end{aligned}$$

Based on these assumptions, the analysis in this thesis will assume a value of 10 N as a threshold of pain. The histograms will highlight the amount of time spent pushing at forces greater than 10N.

3.4.2.2.3 Results

Figures 3-14, 3-15 and 3-16 are the insertion forces measured during the first, third and fourth colonoscopies. Figures 3-17, 3-18 and 3-19 are the histogram plots.

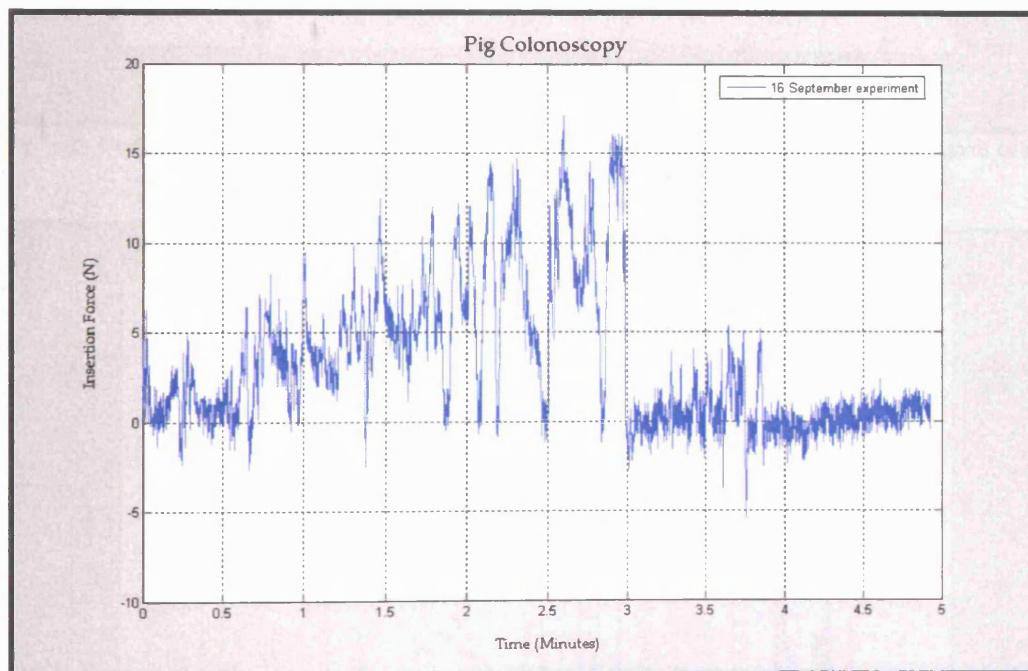


Figure 3-14. Insertion force measured during the first colonoscopy. This colonoscopy was performed with the Olympus colonoscope.

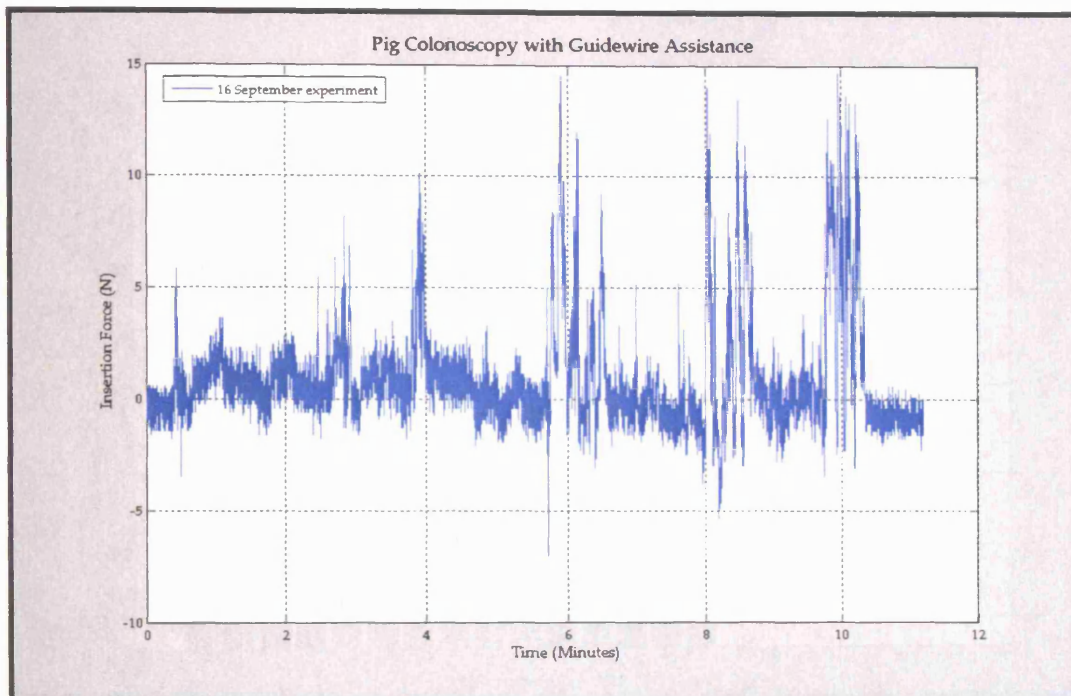


Figure 3-15. Insertion force measured during the third colonoscopy. The guidewire was used to assist the colonoscopy.

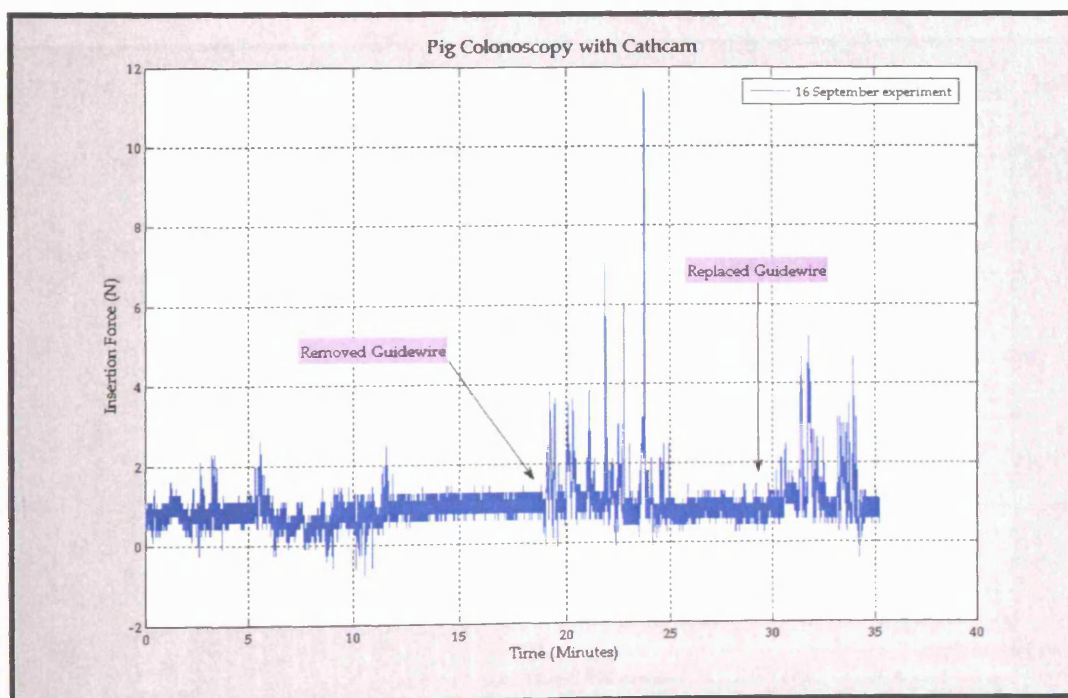


Figure 3-16. Insertion force measured during the fourth colonoscopy. The Cathcam was used to perform this colonoscopy.

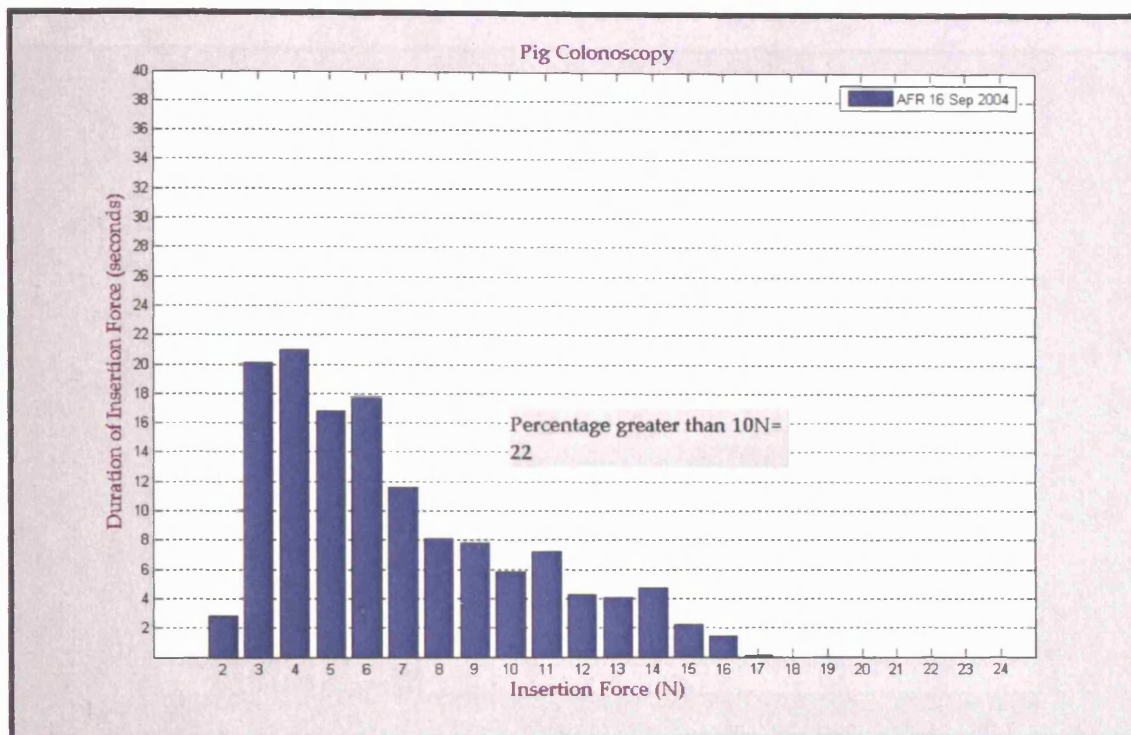


Figure 3-17. Histogram of the time spent at each level of insertion force while performing a colonoscopy on a pig. 22% of the time was spent pushing with a force greater than 10 N.

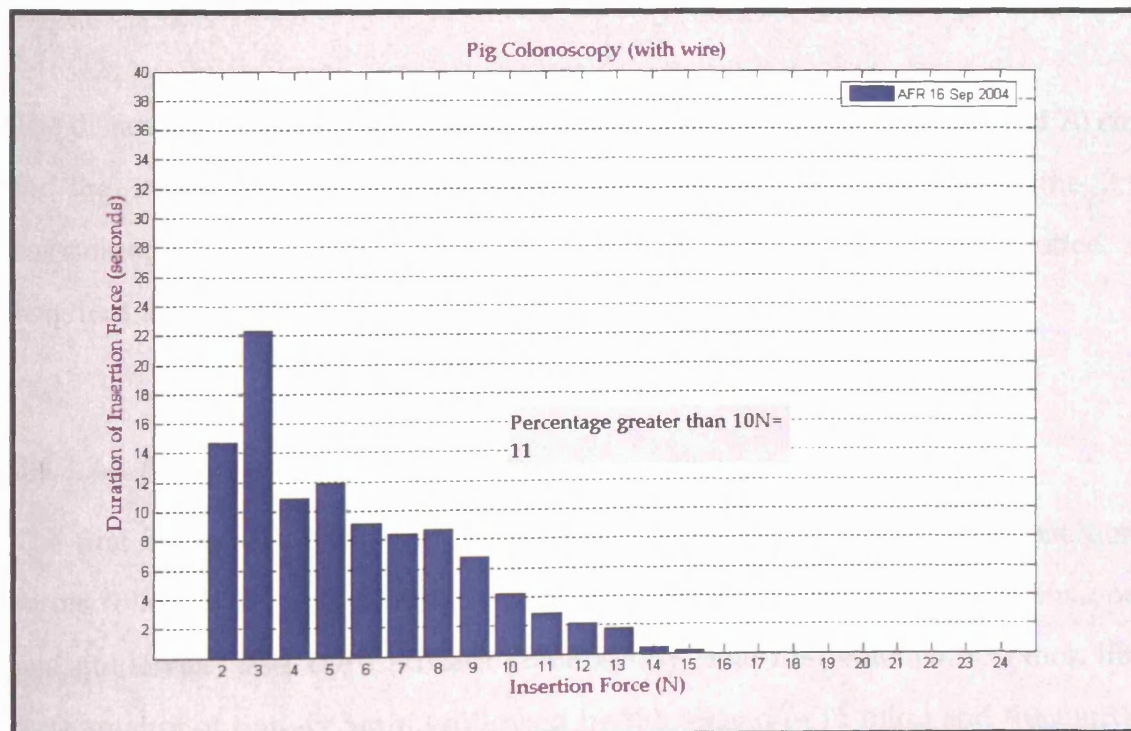


Figure 3-18. Histogram of the time spent at each level of insertion force while performing a colonoscopy with guidewire assistance on a pig. 11% of the time was spent pushing with a force greater than 10 N.

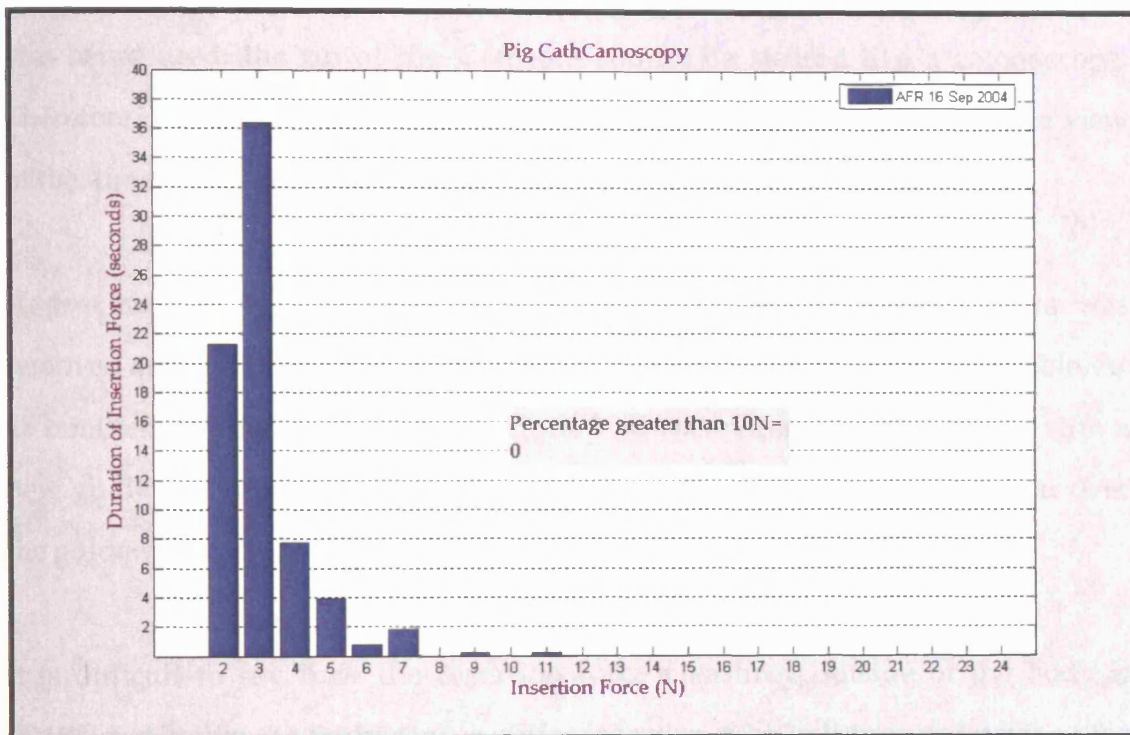


Figure 3-19. Histogram of the time spent at each level of insertion force while performing a Cathcamoscopy on a pig. 0% time was spent pushing greater than 10 N (rounded to zero).

The distances reached during each colonoscopy were 100 cm, 130 cm, and 70 cm for the 1st, 3rd and 4th colonoscopies (the guidewire failed during the 2nd colonoscopy). These distances were approximate and may have included a length of the scope which formed a loop.

3.4.2.2.4 Discussion and Analysis

The first colonoscopy (Olympus colonoscope) produced the greatest insertion forces followed by the guidewire assisted colonoscopy (Olympus colonoscope and guidewire) and the Cathcam colonoscopy. The first colonoscopy took the least amount of time (≈ 5 min.) followed by the second (≈ 11 min.) and the fourth (≈ 35 min.). The colonoscopists weren't able to advance the Cathcam as far as the

colonoscope. This was due in part to the compromised view when the Cathcam was being used; the tip of the Cathcam cannot be steered like a colonoscope. Therefore, it was difficult to manoeuvre the end of the Cathcam to obtain a view of the lumen. This contributed most to the overall procedure time.

Approximately 18 minutes into the Cathcam procedure, the guidewire was removed and then replaced. It had been damaged slightly but was still usable. At 28 minutes into the procedure, the guidewire was removed and replaced with a new guidewire (Figure 3-16). This difficulty with advancing the Cathcam over the guidewire contributed to the overall time of the Cathcam procedure.

It is difficult to say how the insertion force measured outside of the body is distributed inside the body. But, a stiffer insertion tube will transmit more of the force to the colon. This has both advantages and disadvantages; advancing a stiffer tube will advance the tip further, but may also cause more pain to the patient. A more flexible tube will transmit less force to the colon and will cause less pain to the patient. The best outcome would be low insertion force on a flexible tube.

An analysis of the insertion forces greater than 10 N shows that when the colonoscope was used, 22% of the time was spent pushing with an insertion force greater than 10 N, compared to 11% of the time with the assistance of the guidewire and 0% of the time using the Cathcam.

It was fairly easy (opinion of the colonoscopists) to advance the guidewire. Advancing the guidewire was not timed and therefore it is difficult to ascertain how much it contributed to the overall procedure time.

The order of colonoscopies may have had an impact on the difficulty of insertion. A randomization of the procedures would yield a better comparison of the three techniques.

3.4.2.2.5 Results from the Cathcam Clinical Trial

A clinical trial was conducted at the Homerton Hospital (Hackney, London, UK). The protocol was designed to randomize patients in whom a colonoscopy had failed to a standard colonoscopy or an examination with the Cathcam. Upon the advice of the internal ethics committee at the Homerton Hospital, the protocol was rewritten to only perform the examination with the Cathcam. The experience gained from the trial was used to improve the design of the motorized colonoscope (section 3.4.3). 20 patients in whom a colonoscopy failed were enrolled. A single colonoscopist performed the procedure on all of the patients with the assistance of a nurse practitioner. The force handle was used to record the insertion force. Times to reach anatomical landmarks were recorded for each patient.

15 patients received a colonoscopy with the Cathcam. The remaining 5 patients did not receive treatment due to product expiration. Table 3-7 is a summary of the 15 patients. It was difficult for the colonoscopist to advance the wire past the sigmo-rectoid junction for the first 5 patients. This was due, in part, to the lack of angulation control of the tip of the Cathcam. Beginning with patient 6, the wire was preinserted with a colonoscope as far as the colonoscopist felt comfortable. The colonoscope was removed and replaced with the Cathcam, which was then

advanced over the wire. This change in the protocol was made to remove the difficulties encountered by advancing the wire, and still being able to assess how well the Cathcam could be advanced over the wire.

The patients felt little to no pain when the Cathcam was advanced (observation). Each patient had a colonoscopy just after the Cathcam procedure and the patient clearly felt the insertion force during the colonoscopies.

An important outcome from the trial was realizing to what extent the anatomy of the pig colon and the human colon differed. The large folds and thick mucosal tissue in the rectum made it difficult for the colonoscopist to advance the guidewire and the tip of the Cathcam safely (comments from colonoscopist). This difficulty was worsened by the lack of control of the tip of the Cathcam (no articulation). The colonoscopist felt uncomfortable advancing the tip along the colon without "lifting" it away from the lumen wall and into the centre of the lumen.

When the wire was preinserted to the ascending colon, the colonoscopist was able to advance the Cathcam to the transverse colon, and in one case, the caecum. In this particular case, it took 17 minutes for the colonoscopist to advance a standard colonoscope to the descending colon to place the guidewire. It then took only 4 minutes for the colonoscopist to advance the Cathcam to the caecum.

There were no "usable" force data recorded during any of the cases, nor were there a significant number of time data. This was due, in part, to the colonoscopist choosing not to use the force handle as well as some system malfunction.

Each patient had a previously failed colonoscopy and was therefore a “difficult” colon. In retrospect, this was probably not the ideal set of patients on whom to try the Cathcam for the first time. But, as the colonoscopist gained experience with the Cathcam, she became more comfortable with advancing it over the wire.

The colonoscopist concluded that the Cathcam could be a very useful tool for screening colonoscopy if improvements were made to the guidewire. These improvements would increase the chances of advancing the wire further without compromising patient safety.

Table 3-7. Summary of the 15 patients treated with the Cathcam.

<i>Patients</i>	<i>Comments</i>
1 through 5	Could not get beyond the sigmoid colon.
6 through 8	The wire was preinserted to the up to the ascending colon. Reached the descending colon.
9 through 14	The wire was preinserted up to the ascending colon. Reach the ascending colon and the caecum.
15	Product failed

3.4.2.2.6 Conclusions

Using the guidewire with the Olympus colonoscope reduced the insertion force yet increased the overall time to complete the colonoscopy on the pig. The Cathcam produced the lowest insertion forces but did not advance as far as did the colonoscope. The distribution of insertion force values showed that the percentage of high values was shifted lower when the guidewire was used with

the colonoscope. When the Cathcam was used in the animal model, there were essentially no values greater than 10 N, but care should be taken when drawing conclusions from an experiment on a single animal.

The Cathcam human trial did not produce the results that were expected, although the colonoscopist was able to advance the Cathcam to the caecum in the final patient quicker and easier than a colonoscope. The human trials were nonetheless valuable to learn how to make future devices as safe and more effective in humans as possible. The mucosal folds in the human rectum are thicker than those in a pig. It was clear that angulation of the tip was an absolute necessity to advance beyond these folds, therefore any future tests of the Cathcam would include a prototype with tip angulation. Furthermore, this feature was incorporated into the design of the motorized device.

3.4.3 Motorized Guidewire Assistance in Colonoscopy

3.4.3.1 Background

The custom guidewire has been shown to reduce the force required to advance the colonoscope. To take fuller advantage of this technique, it was decided therefore to see if a motor placed at the distal end of the colonoscope could further reduce the insertion force by pulling the colonoscope along the guidewire. It would be difficult to pull the colonoscope along a smooth guidewire since any fluid would reduce the frictional force between the guidewire and the motor coupling mechanism.

A threaded guidewire (*patent pending*) was designed for this application in a way that would not be affected by fluid contamination. The threaded guidewire works much the same as a flexible worm gear. The torque produced by a small motor is used to turn a gear that has a screwed bore which mates with the guidewire.

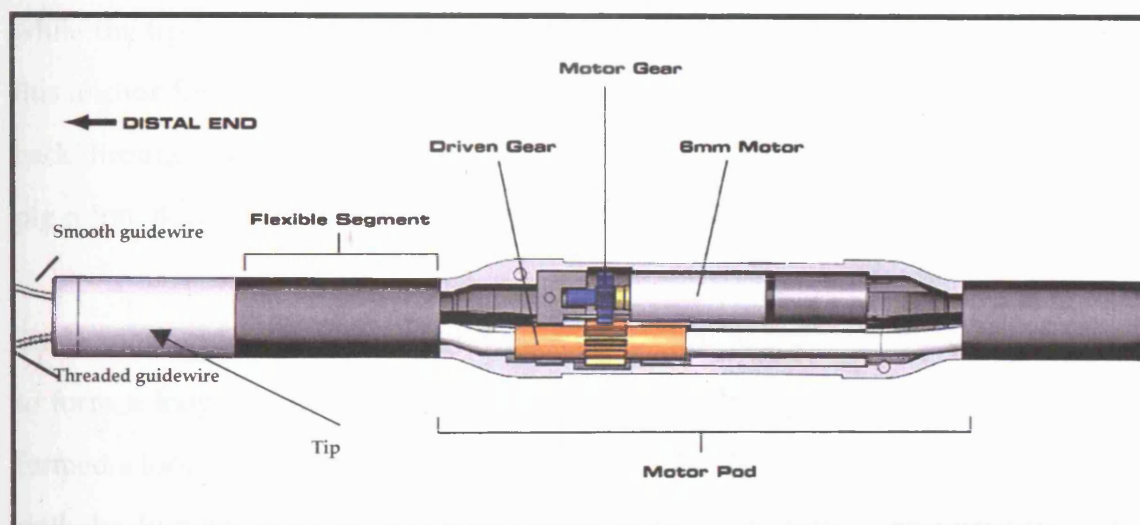


Figure 3-20. Schematic of a motor mounted at the distal end of an experimental colonoscope. The motor turns a gear which pulls the colonoscope along a threaded guidewire. The smooth guidewire is contained within a separate channel of the scope (not shown). The tip can be steered like a standard colonoscope.

Figure 3-20 is an illustration of a motor coupled to a guidewire. The drive gear contains an internal thread which matches the pitch of a guidewire thread. The motor is mounted in the distal end of the colonoscope; therefore the torque from the motor drives the entire colonoscope along the guidewire.

3.4.3.2 Guidewire Force Measurements In-Vitro

3.4.3.2.1 Introduction and Aim

For the motorized colonoscope to function properly, the guidewire is driven away from the tip, along the centre of the colon, to form an anchor. Once this anchor is in place, the motor direction is reversed and the colonoscope is pushed while the tip is pulled along the wire. Measurements were made to understand this anchor force, including the force required to just pull the looped guidewire back through the colon, and the static coefficient of friction between the wire and pig colon. Both smooth and threaded guidewires were tested.

The smooth guidewire was tested on a bench top to measure the force required to form a loop, i.e. the normal force applied to the tissue when the guidewire formed a loop in-vivo and pushed radially inside the colon. The force required to pull the looped guidewire through an excised pig colon was measured. The coefficient of static friction was calculated. The loop forms an “anchor” as the motor pulls the body of the colonoscope along the guidewire, and therefore it is important to maximize this force.

The force required to pull the threaded guidewire was then measured. These data were compared to the pull data for the smooth guidewires to determine how the thread increases the anchor force.

3.4.3.2.2 Methods

Six guidewires (GW03, GW05, GW06, GW06T, GW08, GW09, see appendix II) were tested on a bench top test apparatus and in post-mortem pig colon. The

construction of each guidewire is listed in Table 3-8. The test apparatus used to measure the force that the looped end of the guidewire applied to the colon (normal force) is shown in Figure 3-21. One side of the wire was held fixed while the force gage pushed the other side of the wire into a loop. The force required to form a loop with the same radius which was formed in the colon was recorded. GW06 was used for this experiment.

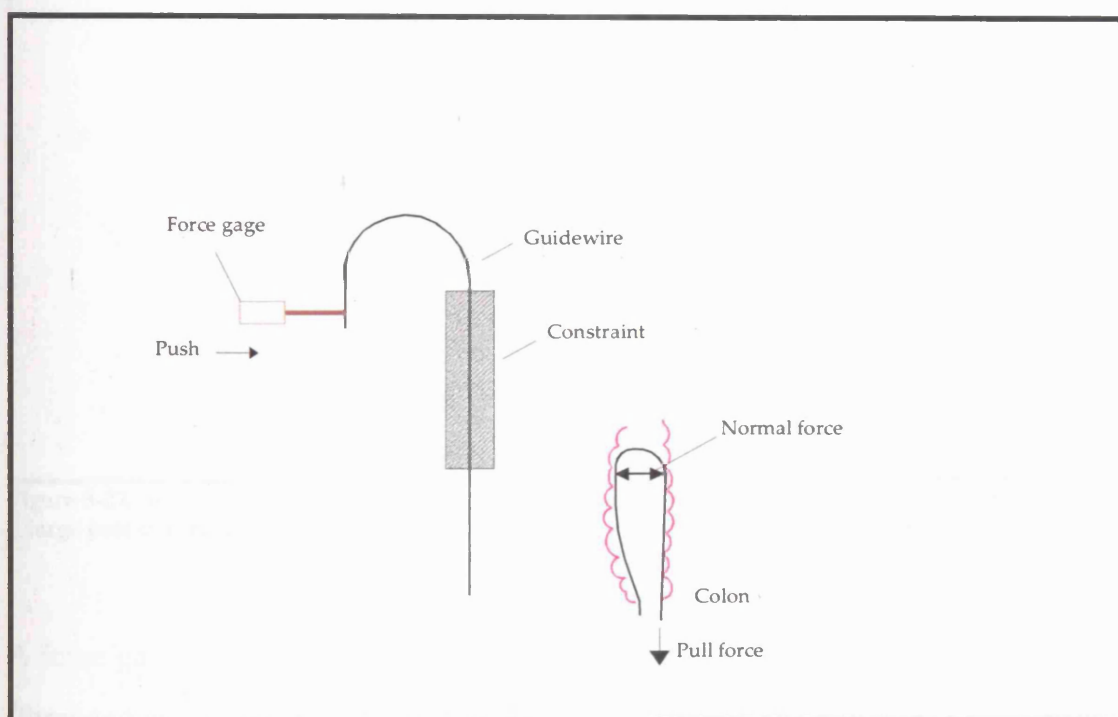


Figure 3-21. Experimental setup to measure the force the looped guidewire applies to the colon (normal force).

Experiments were then performed on thawed post-mortem porcine colon. A section of porcine colon was laid on a flat surface (Figure 3-22). A 10 cm diameter post was used to create a smooth corner around which the colon was placed. Each guidewire was advanced (separately) 80 cm into the colon. The threaded

side of GW03, GW05, GW08 and GW09 were advanced until the threaded half just formed a loop at the end (Figure 3-22).

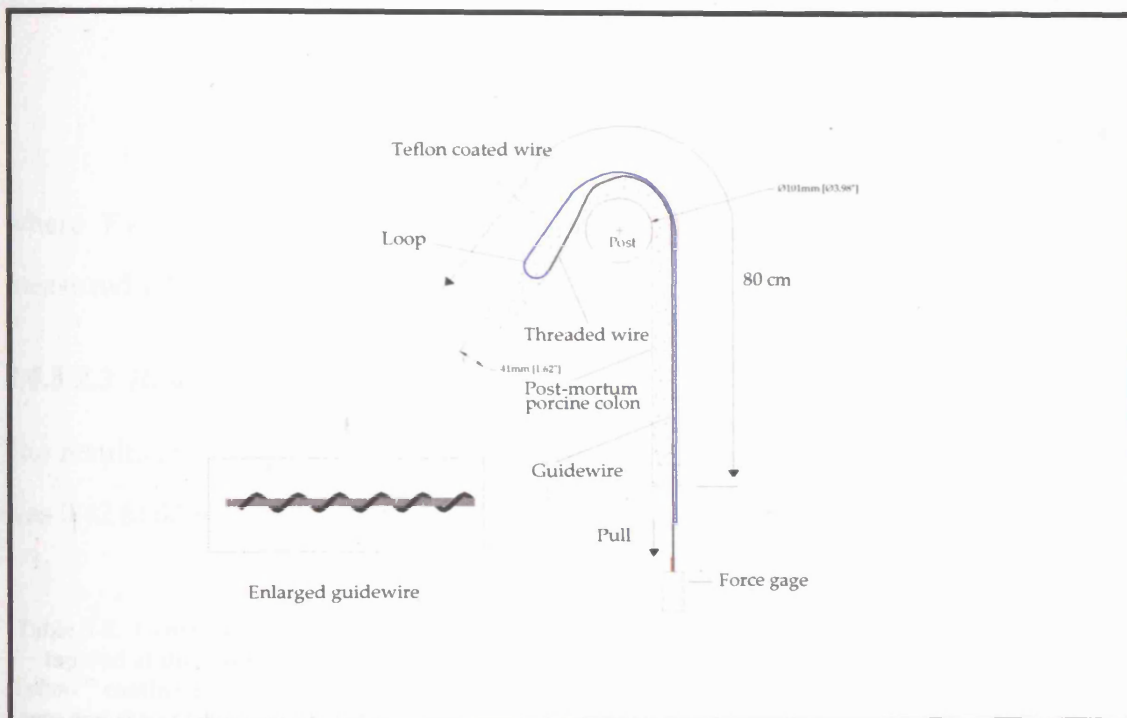


Figure 3-22. Schematic drawing of the porcine colon laying flat on a table top. It is wrapped around a large post to form a smooth turn. The guidewire has been advanced into the colon. The inset is an enlarged view of the guidewire.

A force gage (Omega model DFG70) was attached to the end of the guidewire (threaded end for GW03, GW05, GW08 and GW09) while the other end was free to move. The maximum force, which occurred before slippage between the wire and the colon, was recorded while the wire was pulled by the force gage. The experiment was repeated ten times. Pull force measurements were made with the colon deflated. Water was occasionally added to the colon to prevent a significant change in the tissue lubricity.

These data were then used to calculate the coefficient of static friction, μ between the guidewire and the colon for GW06 and GW06T:

$$\mu = \frac{F}{N}$$

Equation 3-2

where F is the pull (frictional) force measured and N is the normal force measured while forming the loop.

3.4.3.2.3 Results

The results are compiled in Table 3-8. The average coefficient of static friction (μ) was 0.42 (0.07 SD) and 0.25 (0.06 SD) for GW06 and GW06T (Figure 3-235).

Table 3-8. Construction of the guidewires used for testing and comparison. The core diameter was tapered at the midpoint of the wire for GW05 and GW08. NOTES 1-Half of this length had a Teflon[™] coating only on the core (no winding). 2- Wire had an additional tight winding between the core and the outer winding. 3- Wire had a Teflon[™] coating. * Inches is standard denomination for guidewires.

CORE MATERIAL-NITI WIND MATERIAL-SS	CORE DIAMETER (INCHES*)	WINDING DIAMETER (INCHES*)	WINDING PITCH (INCHES*)	AVERAGE PULL FORCE (N)	AVERAGE NORMAL FORCE (N)	NOTES
GW03	0.030	0.012	0.025	1.12	NA	1
GW05	0.022 tapered to 0.018	0.015	0.016	0.67	NA	2
GW06	0.030	NA	NA	0.32	0.79	
GW06T	0.030	NA	NA	0.19	0.76	3
GW08	0.030 tapered to 0.018	0.010	0.008	0.81	NA	1
GW09	0.018	0.010	0.008	0.32	NA	1

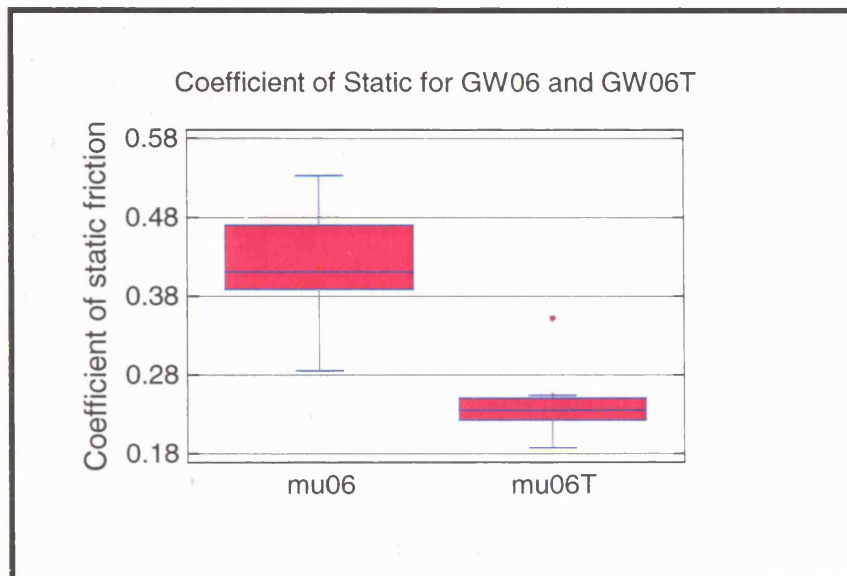


Figure 3-23. Coefficients of static friction for GW06 and GW06T on excised porcine colon. These values were calculated using experimental values of the normal force to form a loop and the pull force in tissue.

3.4.3.2.4 Discussion and Conclusions

The coefficient of friction μ for GW06 (large core, no threads) and GW06T (Teflon coated large core, no threads) were significantly different due to the Teflon[™] coating on GW06T. The pull force for GW03 (large core with threads) and GW08 (large core with threads) are greater than the value for GW06. All three guidewires have the same core material and diameter and therefore have the same static coefficient of friction. The pull forces measured for GW03 and GW08 include the frictional force but also include additional forces which are acting upon the threaded portion of the wire.

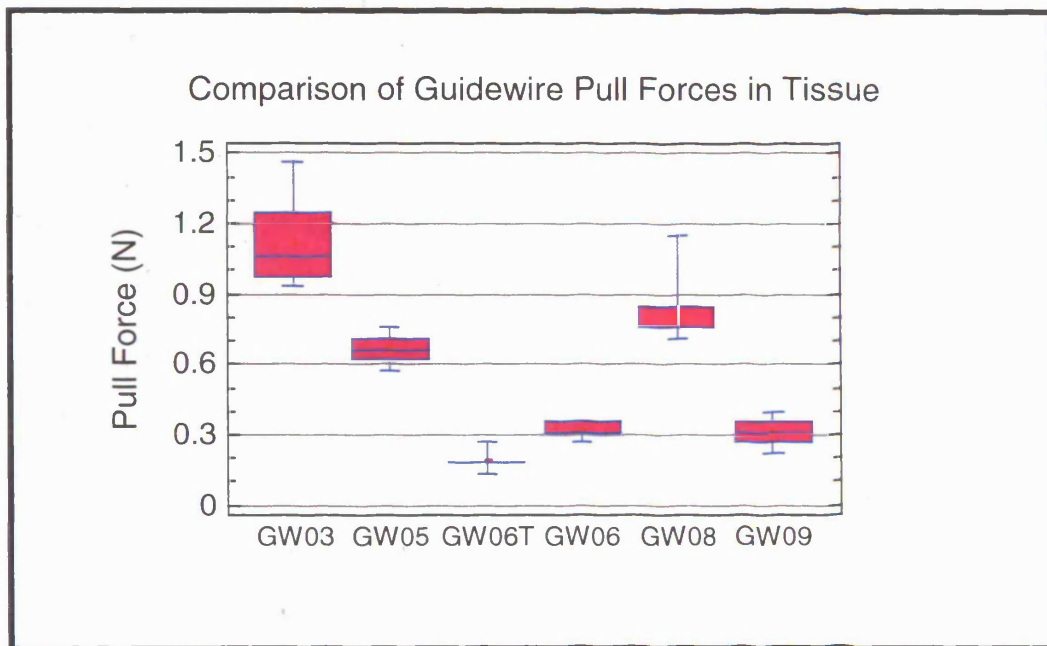


Figure 3-24. Comparison of the pull force of various guidewires. GW03, GW05 and GW06 have the same core diameter. GW09 has approximately half the core diameter of the other three, but like GW03, has threads.

GW09 (small core with threads) produces nearly the same pull force as GW06 even though it has nearly half the core diameter.

A large core diameter wire with threads will maximize the force required to pull the looped guidewire through the colon. Maximizing this force will enable larger forces to be applied to the guidewire, by the motor, to drive the body of the colonoscope forward. But a small core wire will not apply as great a force and therefore it will be easier to push the loop through the colon. A guidewire which tapers from a large core diameter to a smaller diameter (GW08) is the best design to achieve these two goals.

3.4.3.3 Pig Colonoscopy Experiments with Motorized Guidewire Assistance

3.4.3.3.1 Introduction and Aim

With an understanding of how to best use a guidewire to provide an anchor on which to pull the tip of the colonoscope through the colon, a prototype of a motorized colonoscope was built (Coloncam, *patent pending*) to be used in human clinical trials. Before the Coloncam could be used in humans, experiments were conducted in pigs to assess its safety and efficacy. These data were gathered to quantify the difference in insertion force when the motor was pulling the Coloncam along the guidewire and when the Coloncam was simply being pushed. The insertion forces required to perform a colonoscopy with a conventional colonoscope in the same pig were also recorded.

These force-time data were analyzed using the same methods as in Section 3.4.2.2., namely generating histograms. The goal of this design is to reduce the force to a level low enough to reduce the amount of sedation required by the patient, while at the same time allowing a less-skilled practitioner to perform the procedure. It was decided, therefore, that both engineers and physicians should perform these procedures. The following sections describe one of the experiments performed by an engineer.

3.4.3.3.2 Methods

A 51 kg pig was anesthetized and placed in the dorsal recumbency position. The setup for this experiment was the same as for the experiment described in Section 3.4.2.2. The guidewire (COC-GW08) had a core diameter of 0.76mm

(0.030") which tapered to 0.46 mm (0.018") at the midpoint of the wire. The large core diameter section had a 0.254 mm (0.010") diameter wire wound at a 2 mm pitch. A Teflon™ coating covered the small core diameter section.

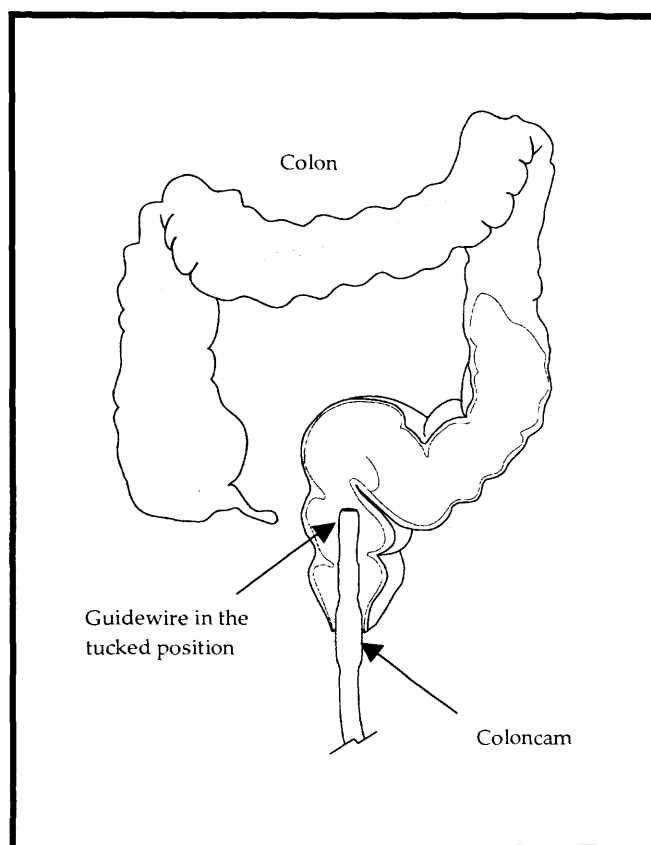


Figure 3-25. Line drawing of the Colonicam in a human rectum. The guidewire is in the tucked position and cannot be seen in the endoscopic view.

The guidewire was placed in the *tucked* position (Figure 3-25 depicts a human colon, but represents how it was used in a pig colon). In this position, the guidewire is out of the endoscopic view. The tip of the Colonicam was introduced through the anus of the pig and a clear view of the rectum was obtained. The force handle was then placed on the insertion tube. Air was introduced into the colon while the smooth leg of the guidewire was advanced approximately 20 cm. The threaded leg was then advanced (Figure 3-26) until the motor current

increased substantially (from 0.090 mA to 0.150 mA). Since the torque produced by a motor is proportional to the current drawn by the motor, the increase in the current indicated that the threaded leg had advanced to the end of the loop or that an excessive amount of force was being applied to the colon by the guidewire. When the threaded leg "turns the corner" to form the loop, the anchor has been formed as described in section 3.4.3.2.2. The motor direction was reversed while the insertion tube was advanced with the force handle. The total distance that the tip advanced into the colon was recorded. The performance of the Colonicam (n = 14), the Colonicam without guidewire assistance (n = 2) and a standard colonoscope (n = 12) were compared.

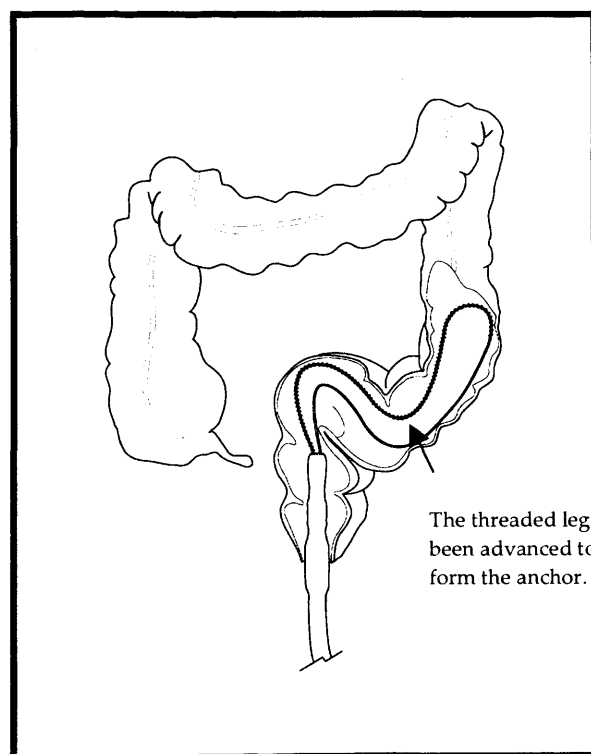


Figure 3-26. The guidewire has been advanced approximately 20 cm. The threaded leg of the guidewire has formed the loop and is now providing an anchor.

3.4.3.3.3 Results

The maximum insertion force measured during the colonoscopy was 37 N, as compared to 21 N for the Colonicam. Figures 3-27 and 3-28 plot the insertion force as a function of time. Figures 3-29 and 3-30 are histogram plots. The total distance traversed was 70 cm for the colonoscope and 145 cm for the Colonicam. Figure 3-31 plots the mean percentages of time spent pushing with a force exceeding 10 N during a larger number of experiments (including the data shown in Figures 3-27 and 3-29).

Figure 3-34 is a fluoroscopic image of the colonoscope at 70 cm. The colonoscope was able to negotiate the first loop but the operator was unable to push it into the spiral colon without an excessive amount of force. Figures 3-32 through 3-35 show fluoroscopic images of the same operator advancing the Colonicam in the same pig. The Colonicam could be advanced much farther (145 cm) than the colonoscope (70 cm) in nearly the same amount of time.

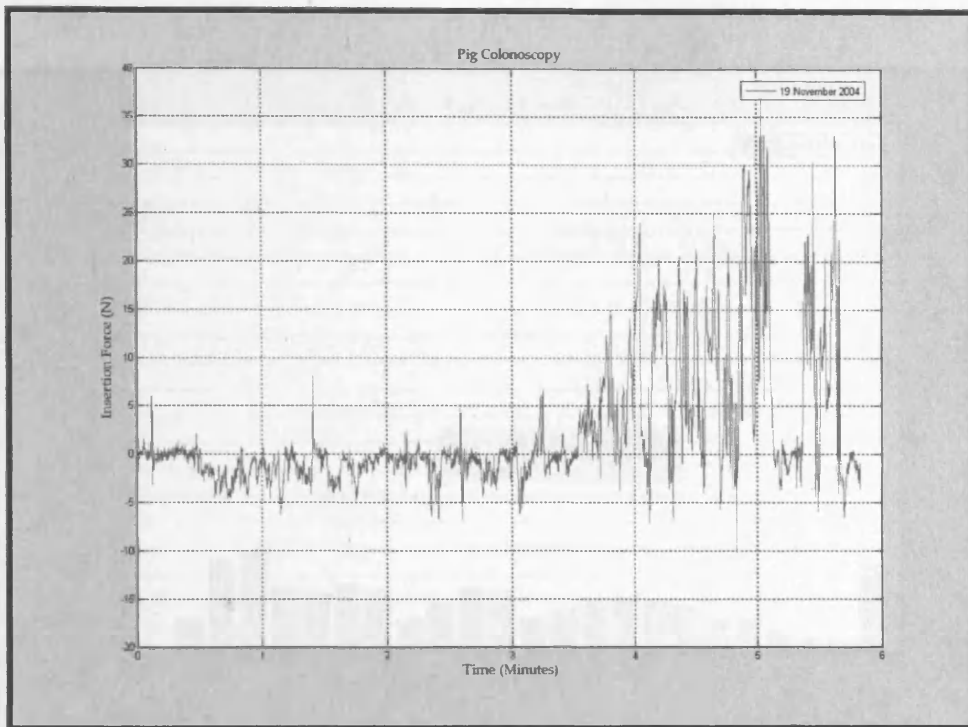


Figure 3-27. Insertion force vs. time of the colonoscope.

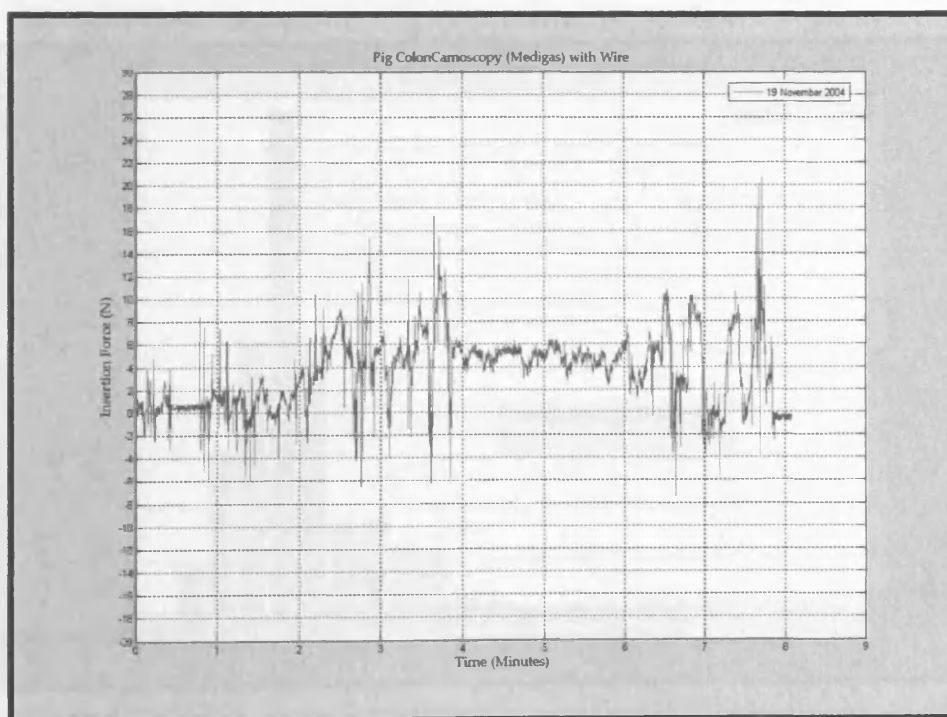


Figure 3-28. Insertion force vs. time of the Colonicam with the aid of the guidewire.

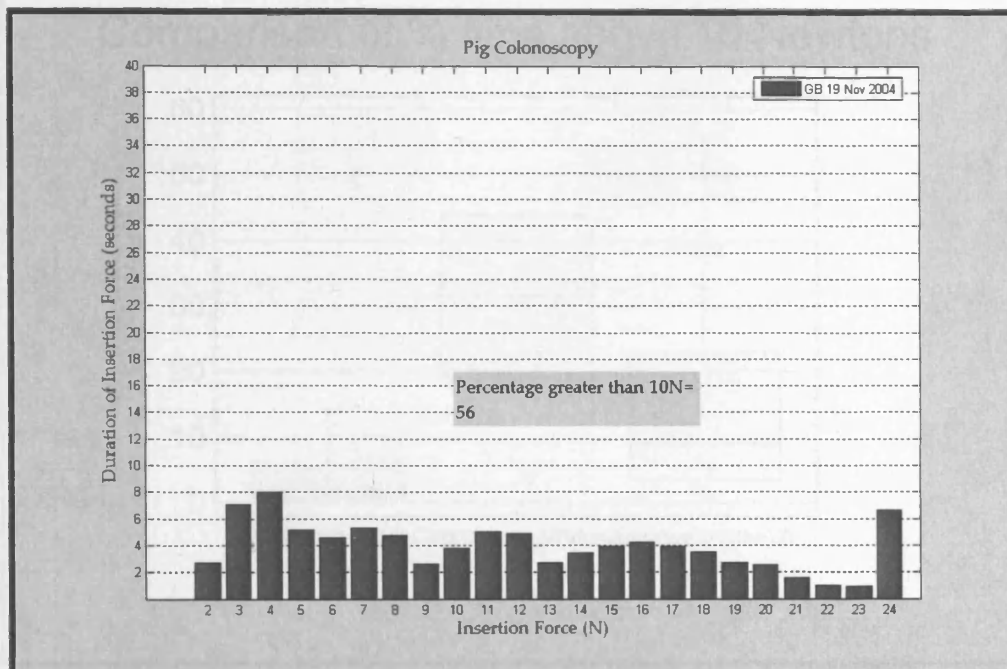


Figure 3-29. Pig Colonoscopy histogram. 56% of the time was spent pushing with an insertion force exceeding 10 N.

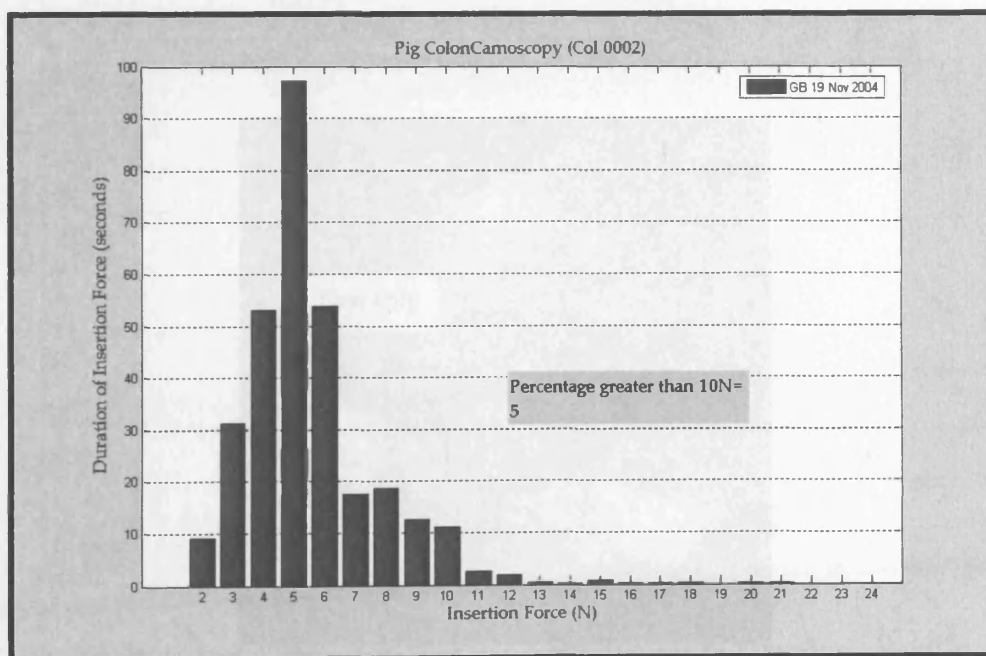


Figure 3-30. Pig Coloncam histogram. 5% of the time was spent pushing with an insertion force exceeding 10 N.

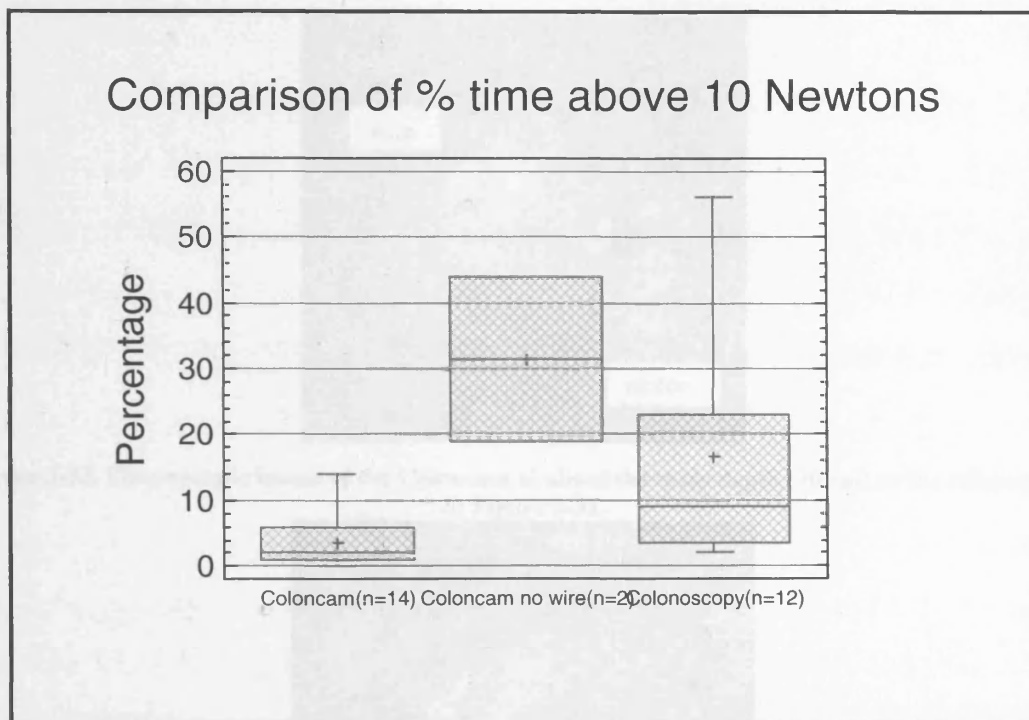


Figure 3-31. A comparison of the means of the percentage of time spent pushing with an insertion force exceeding 10 N. The difference between the colonoscope and the Coloncam is 17% vs. 4% ($p=0.034$). The difference between the Coloncam with and without the guidewire is 4% vs. 32% ($p=0.26$).

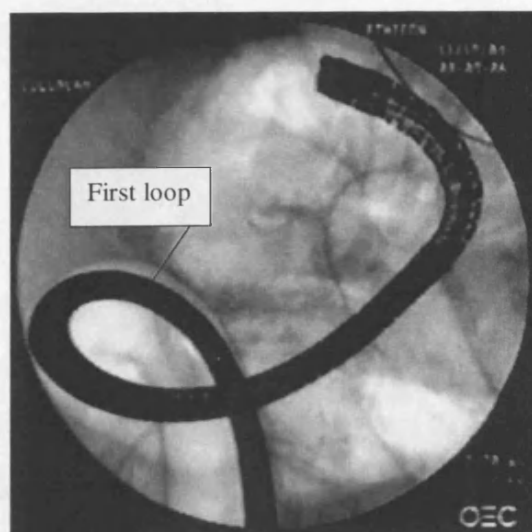


Figure 3-32. Fluoroscopic image of the colonoscope at the furthest point (70 cm) the tip could be advanced in the pig colon.

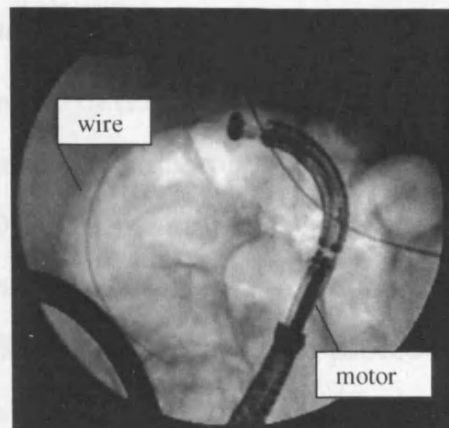


Figure 3-33. Fluoroscopic image of the Colonicam at about the same depth (70 cm) as the colonoscope in Figure 3-32.

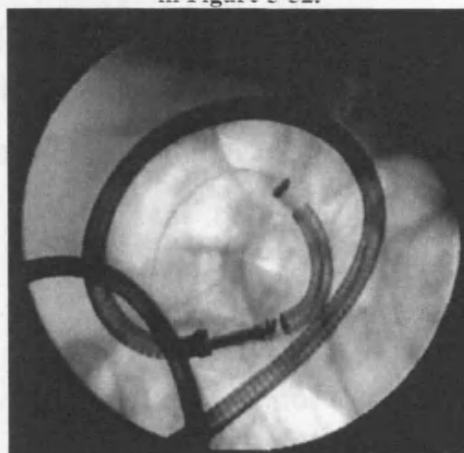


Figure 3-34. Fluoroscopic image of the Colonicam advanced 50 cm further than in Figure 3-33. The tip is entering the spiral colon.

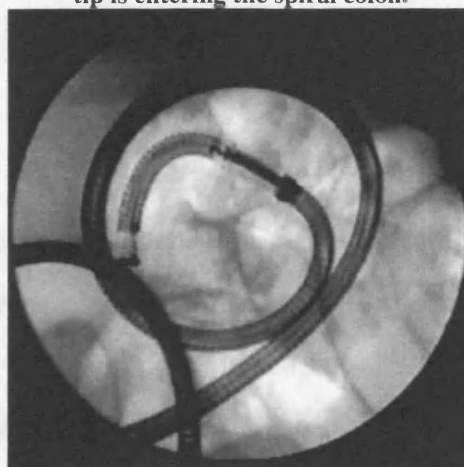


Figure 3-35. Fluoroscopic image of the Colonicam advanced 145 cm in the pig colon.

3.4.3.3.4 Discussion and Conclusion

The means of the percentage of time pushing with a force greater than 10 N were 4%, 32% and 18% for the Colonicam, Colonicam without a wire, and colonoscopy (Figure 3-31). The mean values show that when the wire is used to pull the tip of the Colonicam along, there is a reduction in insertion force, not just at a single point in time, but for most of the procedure. Figures 3-29 and 3-30 illustrate this point. There is a greater difference between the Colonicam with and without the wire. This may be a better comparison, since the same "colonoscope" is being used with and without the wire. Only two experiments could be performed without a wire (due to animal and prototype availability), and therefore a significant difference could not be shown. But there is a significant difference ($p = 0.045$) between the Colonicam and the colonoscopy.

This demonstrates how a less skilled operator can advance the Colonicam further and with less force than a colonoscopy in a pig.

3.4.4 Conclusion

Flexible endoscopy has evolved over the past 200 years to the present day where endoscopes are available to explore the entire digestive tract. The light source had the most impact early on for all scopes. As these scopes were used to examine the upper and lower anatomies, problems were encountered unique to each anatomy. The upper scopes required smaller diameters, flexibility and articulation. The lower scopes required more stiffness to advance through the

proximal part of the colon but at the same time flexibility to manoeuvre the tortuous path.

It has been reported in the literature that looping can cause both delays and pain to the patient. In a UK study (45), it was reported that in 20.7% of the procedures, the endoscopist had to abort the procedure. 64.4% of those procedures that had to be ended prematurely were due to patient pain and uncontrolled looping.

The time delay study showed that even at reasonable caecal intubation rates, the actual forward movement was quite slow (0.124 cm/sec). There was little difference in the percentage of delay between the experienced and less experienced endoscopists. These delays are most likely due to loop formation and the time it takes to apply techniques to eliminate these loops. Continuing to push into these loops can cause pain to the patient.

A guidewire was used to help advance a simple tube through a simulated colon. The guidewire technique reduced the insertion force by 52%. The tube had a relatively small diameter and a small amount of mass compared to a colonoscope. Yet in the animal model experiments, the guidewire assistance reduced the insertion force for both a standard colonoscope and the Cathcam colonoscope.

The use of the guidewire with a colonoscope reduced the level of insertion force when performing a colonoscopy on a pig. When the Cathcam was used in a pig, the time during which the insertion force exceeded 10 N was essentially zero. The human trial did not confirm this advantage (because the data were not recorded), but the colonoscopist did comment (repeatedly) that less force was

required to advance the Cathcam and she was not afraid of hurting the patient. The looped guidewire could not be advanced very far ahead of the tip, therefore the entire concept was not sufficiently tested. Eventually, the Cathcam was advanced to the caecum which was a complete colonoscopy. If angulation had been part of the design, the colonoscopist may have advanced the guidewire further into the colon. It is entirely possible that the Cathcam may have been too heavy compared with the thin guidewire. But since this was a first attempt to use this product on humans, compromises had to be made to assure the safety of the patient.

The Colonicam demonstrated that a less skilled operator could advance the tip of the device further into the pig colon with less force. During the pig colonoscopy, the operator pushed the colonoscope with forces exceeding 10 N for 56% of the time, yet the tip was advanced only 70 cm. When the Colonicam was used in the same pig, the operator advanced the tip twice as far while pushing with forces exceeding 10 N for only 5% of the time.

Reducing the insertion force is the most direct way to reduce the pain felt by the patient. The guidewire and motor technique should be simple and easy for a less skilled practitioner to learn. The looped guidewire tends to find its way through the colon, while the motor will drive the tip of the Colonicam along the path that the guidewire has made. The wire can also be placed in the tucked position, "restoring" the Colonicam to the configuration of a colonoscope.

4 Therapeutic Diathermy in Colonoscopy

4.1 Planar Electrodes for Thermal Denaturation and Tissue Haemostasis

4.1.1 Background

One of the indications for colonoscopy is to screen for colorectal cancer (CRC). Colorectal cancer begins as a small polyp (Section 2.2) in the mucosal layer of the colon wall. A polyp which has been located can be biopsied or removed entirely during a colonoscopy. There is a risk of bleeding associated with the removal of a polyp (polypectomy), which can be reduced or mitigated through the aid of a haemostatic technique. A common haemostatic technique is to heat the tissue, either during the polypectomy or just after the polyp has been removed.

Heat has been used to stop tissue bleeding for more than two millennia. Protell et al reported that tissue proteins coagulate at temperatures of 50 to 100 °C (58). When collagen is coagulated, it shrinks. The contraction of the collagen can lead to a narrowing of the blood vessels contained within, and thus aid in haemostasis (59). There are two ways in which the heat is generated. The first is by thermal conduction; typically, a probe with an embedded heat source is held against the tissue raising the tissue to a sufficiently high temperature for coagulation. The second method is to allow current to flow through the tissue and generate the heat directly through losses in the tissue.

Gilbert et al (60) developed an electrically heated probe to perform the first method. The temperature of the probe was held constant with a feedback loop as it was pressed against the bleeding tissue. It was found that temperatures below 100°C were insufficient in stopping bleeding in artificially created ulcers. A temperature range of 140 to 160°C (as measured in the probe) was needed for consistent stoppage of bleeding. The tip would have to have been at a higher temperature for the heat flow to raise the tissue temperature to the required level. The main disadvantage to this type of probe was the unpredictable depth of injury, which if too deep could lead to a perforation of the GI tract.

The second method of heating tissue is by passing a radio frequency (RF) electric current through it. RF or electrosurgical (ES) generators operate in the frequency range of 300 kHz to 1 MHz. RF currents are used solely to prevent stimulating muscles and nerves. The losses due to the current flow act as a distributed source of heat that can raise the temperature of the tissue to a sufficient level to cause coagulation. There are two types of RF electrodes: monopolar and bipolar, both of which can be delivered to the tissue through an access port in the endoscope.

The term monopolar is somewhat misleading. It generally describes a probe with a single "active" electrode, having a small surface area in contact with tissue, and a second "return" electrode which is placed on the outside of the body. The return electrode surface area is much larger than the active electrode and maintains a current density level low enough so as to not cause damage to the tissue.

In a bipolar device, both electrodes are mounted on a single probe and have equal surface areas in contact with the tissue. The tissue is coagulated

underneath and between both electrodes. The impedance rises rapidly as the tissue is desiccated. This rise in impedance causes the generator to deliver less current, which then reduces further power delivery to the tissue. Likewise monopolar devices will cause a rise in tissue impedance, but bipolar devices operate over a smaller impedance range (Figure 4-4). Bipolar devices are commonly referred to as "multipolar probes" (61).

Separate outputs are available on RF generators for monopolar and bipolar probes. The output for the monopolar probe has a range of operating modes, providing differing voltages and waveforms. For instance, when operating in the fulguration mode, the voltage can reach values as high as 8,000 V_{p-p}. In the fulguration mode, the operator holds the tip just off of the tissue. The high voltage causes a breakdown in the air, forming an arc which can be used to stop large areas of bleeding that were otherwise difficult to stop by placing the probe in contact with the tissue. A range of different waveforms are available in the monopolar cut mode, designed to provide cutting and coagulation effects when the tip is held against the tissue.

Because bipolar probes are used to coagulate tissue rather than cut the tissue, there are fewer output options available. The waveform is a constant sinusoid with peak voltages on the order of 100 V. The bipolar output operates in a constant current mode at low impedances and a constant voltage mode at higher impedances.

Piercey et al (62) showed that monopolar electrodes were unsafe when used in the GI tract. Since the GI tract has a relatively thin wall, a deep injury may cause a perforation. As more or less of the tip makes complete contact with the tissue,

the current density varies and causes an unpredictable depth of coagulation. This work led to the development of a tip which ensured that there was a smaller and more constant amount of metal in contact with the tissue. It provided a more consistent application of energy, but still caused unpredictable depth of coagulation.

Protell et al concluded that bipolar electrocoagulation was safer than monopolar electrocoagulation (63). Less damage occurred with bipolar applications than monopolar applications, even though more total energy was used in the bipolar mode. Despite this conclusion, the authors did not recommend widespread use of bipolar electrocoagulation until more about its effects on tissue were fully understood.

Given these shortcomings of RF devices for endoscopic haemostasis, ways to improve bipolar electrodes were explored. In the course of experimenting, it was observed that when the electrodes of the same size were placed parallel to one another in a plane, the location of the coagulation zone depended on the size and spacing of the electrodes. A specific ratio consistently produced coagulation only between, and not under, the electrodes. This meant that when used endoscopically, the clinician could view the tissue to be coagulated, while the tissue beneath the electrodes was not damaged. Other bipolar devices obscure the tissue to be treated.

The planar electrodes (plan and cross-section views) are shown in Figure 4-1. Figure 4-1 also shows how the electrodes may be placed in the colon to stop bleeding after a polypectomy. In practical terms, the electrodes would be mounted on a structure, such as a clear tube, to hold them against the wall of the

colon. The diameter of the colon is sufficiently large enough that the current along the "long" path is insignificant (Figure 4-1).

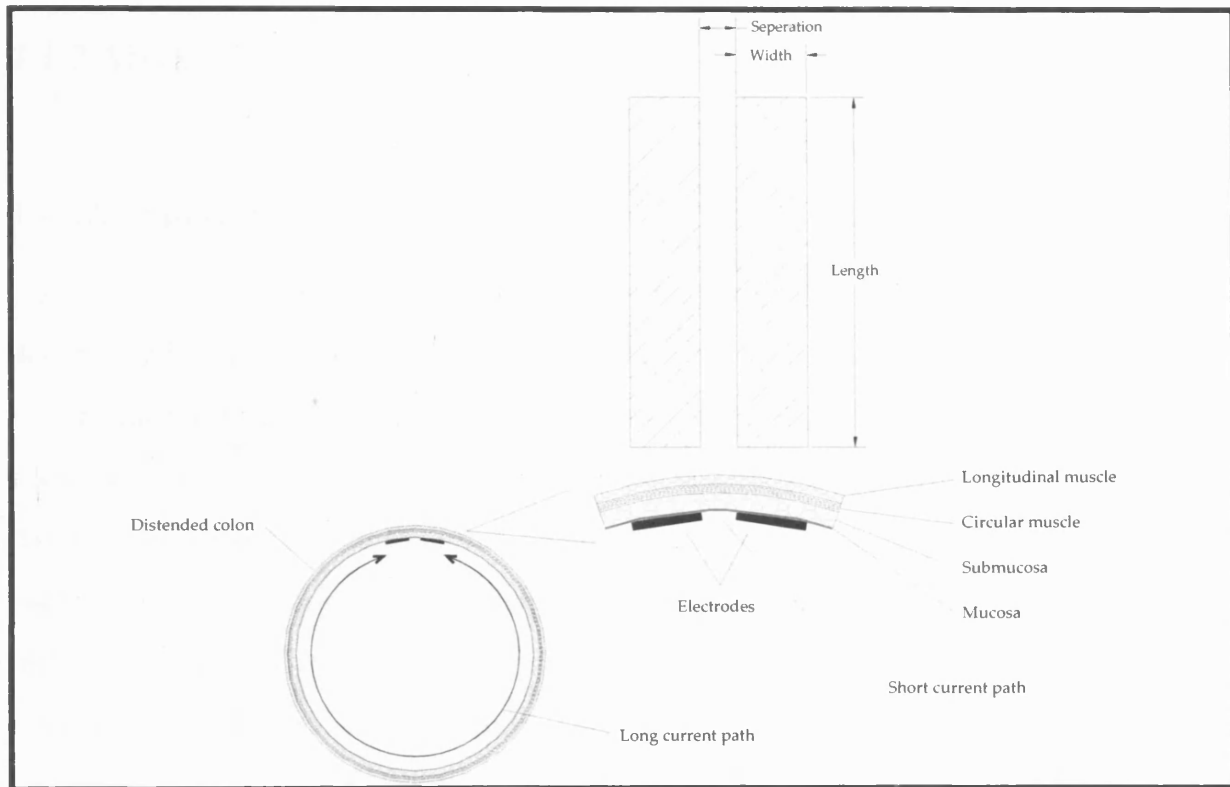


Figure 4-1. Diagram of the planar electrode configuration. The electrodes are in contact with the colon and are shown in both plan and elevation (original design, *patent pending*).

The purpose of this work is to present and discuss the results of in vitro and in vivo experiments designed to assess the performance of the planar electrodes. These results were obtained from experiments performed by the author (in the USA) prior to becoming a Ph.D. student. The author conceived the idea of planar electrodes, generated the data in Table 4-1, participated in the design of the animal experiments, collected and analyzed all of the data. A finite element model (FEM) to solve for the temperature distribution and current density will

be presented, and will be compared to the experimental results, both ex-vivo and in-vivo.

4.1.2 Methods

4.1.2.1 Experiments in Ex-Vivo Tissue

Experiments were conducted to observe the effects of planar electrode geometry (length, width and separation) on coagulation. First, electrodes were made from thin metal strips glued to clear acetate (Figure 4-2). This simple arrangement allowed visualization of the tissue between the electrodes. For each experiment, the two electrodes were of the same dimensions and were placed parallel to one another. Each electrode pair was then connected to an Erbe ICC 350 generator (Erbe, Tübingen, Germany) providing a bipolar output at 330 kHz. The electrodes were placed on ex vivo pork loin obtained from the butcher. When the generator was activated, the tissue between the electrodes was heated to a temperature sufficient to thermally coagulate the tissue and turn it white. The time from generator on to the time that the tissue between the electrodes turned completely white was recorded. If complete coagulation did not occur in a reasonable time (5 to 10 seconds), the generator was switched off. This method was repeated for 33 different pairs of planar electrodes with various lengths, widths and separations (see Table 4-1).

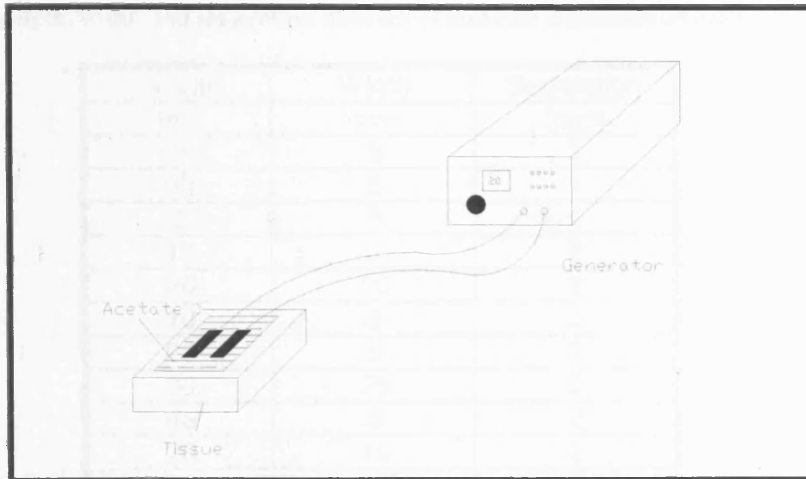




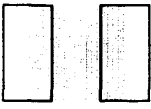
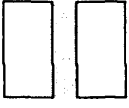
Figure 4-2. Schematic of experiment to test the relationship of electrode geometry to coagulation zone on the tissue.

Table 4-1. Length, width and separation distance of multiple experimental pairs of planar electrodes.

Length	Width	Separation
mm	mm	(mm)
2	3	1
20	5	1
5	5	2
10	10	2
20	20	2
10	5	2
20	5	2
30	25	2
43	5	2
20	10	2
15	15	2
30	5	2
10	20	2
13	2	3
11	4	3
28	2	3
26	4	3
14	16	3
40	5	3
30	15	3
58	2	3
56	4	3
5	5	5
10	5	5
10	10	5
20	5	5
20	10	5
15	15	5
20	20	5
30	5	5
5	5	10
10	5	10
10	10	10

For each coagulation event, the zone of coagulation was then rated using the subjective scale shown in Table 4-2.

Table 4-2. Subjective scale used to describe the coagulation zone for each pair of planar electrodes.

Rating (0 to 10)	Diagram of electrodes (solid outline) and coagulation (shaded areas)	Rating criteria
0 to 2		Coagulation under the electrodes only
3 to 5		Coagulation under and between the electrodes
6 to 8		Coagulation mostly between the electrodes
9 to 10		Coagulation only between the electrodes

4.1.2.2 Experiments In-Vivo

Survival studies were conducted to determine the depth of the coagulation using the planar electrodes on the canine model. The electrodes were mounted on a clear plastic tube through which the endoscope (GIFP140 gastroscope Olympus Corp. USA) was passed (Figure 4-3). The distal oesophagus was treated between approximately 2 and 10 cm proximal to the oesophageal/gastric (OG) junction.

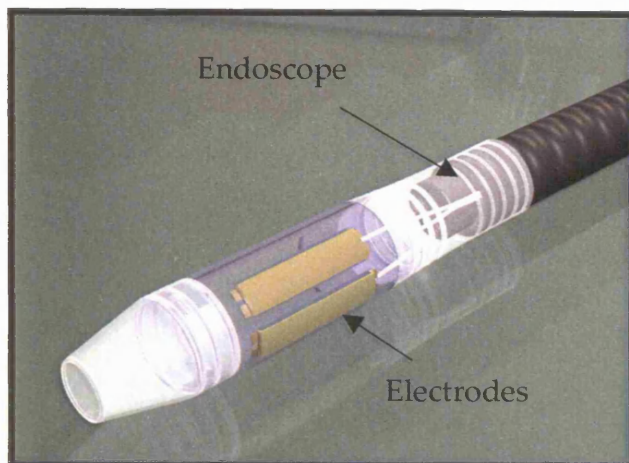


Figure 4-3. Experimental device for in vivo testing.

Six healthy dogs' oesophagi were treated with the planar electrodes to assess the depth of the coagulation over survival periods of 3 days, 2 weeks and 4 weeks. The animals utilized in this study were handled and maintained in accordance with the requirements of the Animal Welfare Act (9CFR Parts 1&2) and its amendments. Compliance was accomplished by conforming to the standards promulgated in the Guide for the Care and Use of Laboratory Animals, 1996 (NCR, ILAR, and National Academy Press USA).

The Erbe ICC 350 was used at a setting of 35 W in the bipolar mode. This produced a voltage of approximately 50 V_{rms} (pure sinusoidal) at the electrodes. Figure 4-4 is a typical power curve of a bipolar generator. These data were generated with non-inductive loads.

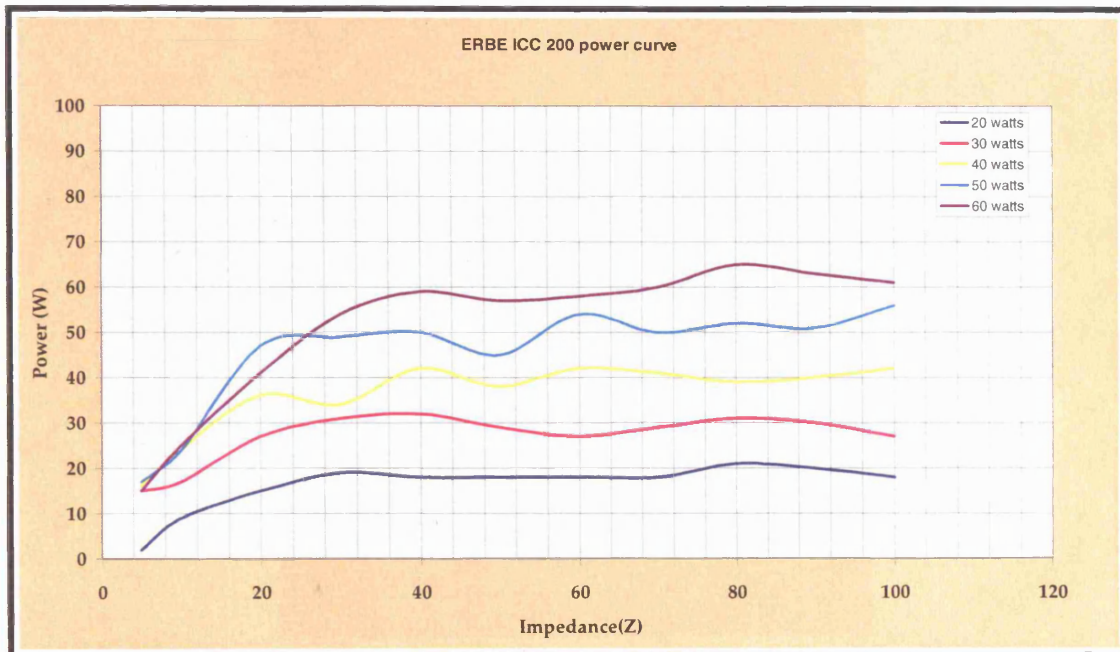


Figure 4-4. Measured power curve of bipolar generator. The load was a non-inductive power resistor.

The dogs were humanely euthanized and the treated tissue was harvested and placed in formalin and forwarded to the pathologist. The tissue was trimmed and processed into haematoxylin and eosin (H&E) and tri-chrome-stained micro slides (to increase the contrast between cells). The pathologist examined the slides and measurements of depth of coagulation were made.

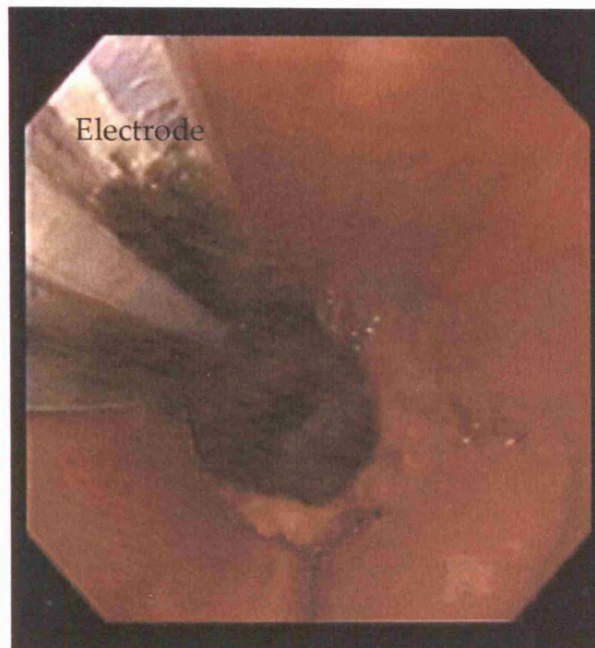


Figure 4-5. Endoscopic view of the electrodes supported by a clear plastic tube in a canine oesophagus. The white stripe is the coagulated tissue between the electrodes.

Figure 4-5 is an endoscopic view of the coagulation of canine oesophagus between the electrodes. The endoscope is placed down the clear tube and introduced through the mouth of the dog. The entire circumference of the oesophagus can be viewed as seen in Figure 4-5. The tube was rotated independent of the endoscope to align the space between the electrodes with the tissue to be treated. The endoscope (and the view of the tissue) therefore could be held in a fixed position.

4.1.2.3 Finite Element Model

A finite element model of the electrodes on a slab of tissue was created using Femlab™ (Comsol, Cambridge, UK). This model was used to solve for the current density, electric field and temperature distribution. The electrical solution was used as the heat source in the heat equation, while a damage

integral was used to assess tissue death. Although the numerical results should be treated with caution, the thermal distribution is a useful way to assess tissue damage. Such a model can reduce the time to complete a device design as well as reduce the number of animals required to measure efficacy and safety.

Figure 4-6 shows a Femlab model of the tissue slab and electrodes. The tissue slab was 40 mm wide by 30 mm long and 10 mm thick, and the electrodes were 5 mm wide.

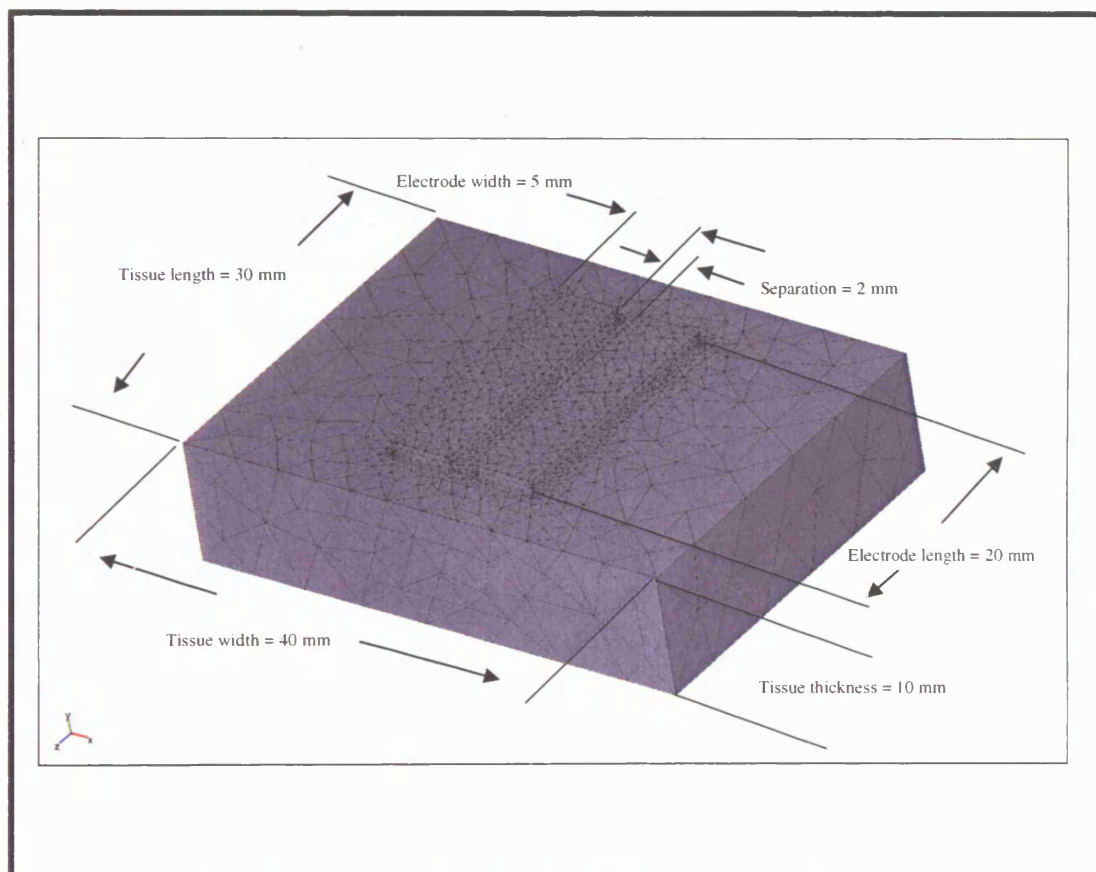


Figure 4-6. Electrodes on a tissue slab, showing width (W) , length (L) and separation (S) of the electrodes. The finite element mesh is shown.

The total number of grid element for the slab of tissue and two electrodes was 41,338. This was a prohibitively high number of elements to solve the partial differential equations with such complex coefficients with limited memory and computational power. Chang (64) showed that symmetry could be used to reduce the number of elements and achieve convergence and a solution with fewer elements. Therefore, to reduce solution time, a model of a quarter of the slab and electrode was used (Figure 4-7).

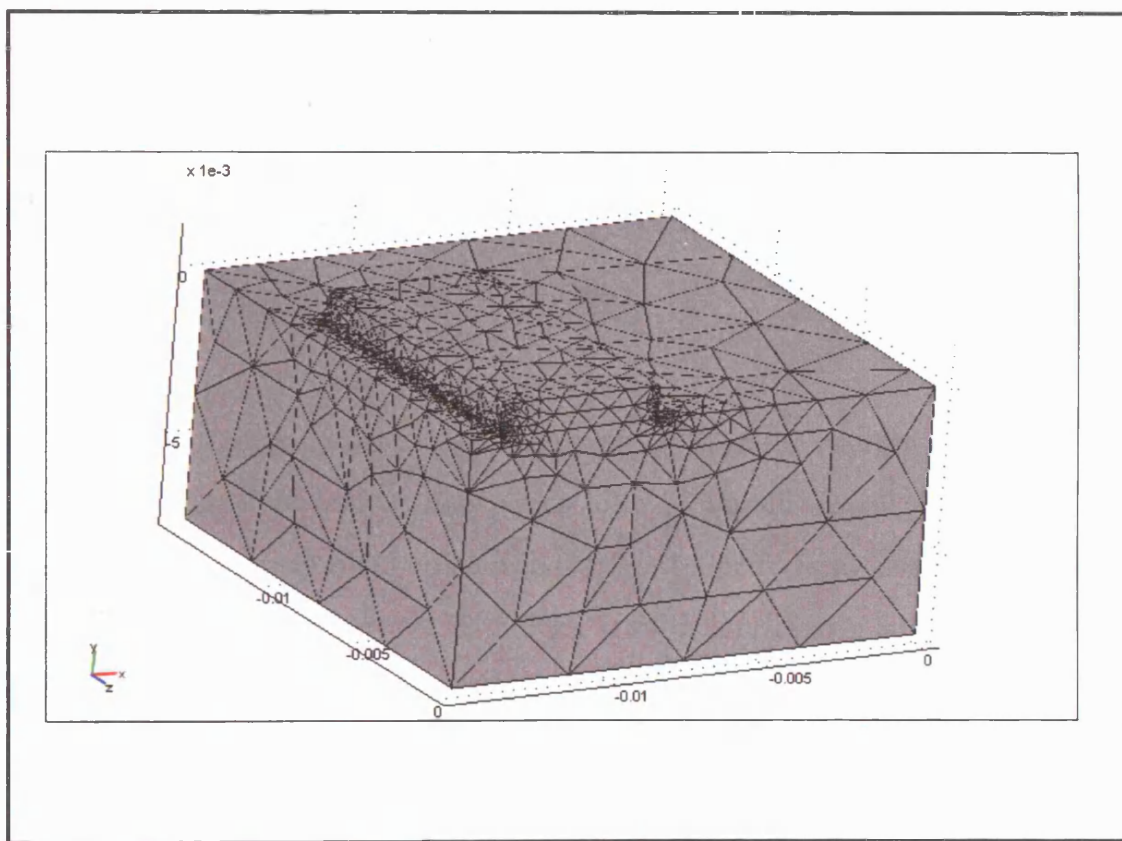


Figure 4-7. Model of 1/4 of the slab of tissue and the electrode. The number of mesh elements is 8,191.

Stainless steel was chosen as the material for the electrodes. The material properties for the electrodes and the tissue are listed in Table 4-3.

Table 4-3. Electrical and thermal properties used for the finite element model.

	Tissue	Stainless Steel
Conductivity (Sm ⁻¹)	0.471 (65)	700X10 ⁹
Density (kgm ⁻³)	1000 (65)	7930
Heat capacity (Jkg ⁻¹ K ⁻¹)	3500 (65)	500
Thermal conductivity (WK ⁻¹ m ⁻¹)	0.556 (65)	150

Tissue conductivity σ is the ratio of the current density (J) to the electric field (E) at a point in the tissue:

$$\sigma = \frac{J}{E}$$

Equation 4-1

In the range of frequencies that RF probes operate at, the heating of the tissue is mostly the result of power dissipation due to ohmic losses (64). Heating is primarily due to movement of charge from one electrode to another. At higher frequencies such as microwave (27 MHz), heating is primarily due to vibration of particles in the tissue. For this analysis, a quasi-static (DC) electrical conduction model was used with the following governing equations. Equation 4-1 can be rearranged:

$$J = \sigma E$$

Equation 4-2

The electric field can be defined as the gradient of the voltage V:

$$E = \nabla \bullet V$$

Equation 4-3

Substituting (3) into (2) and taking the gradient (equation of continuity):

$$\nabla \bullet J = -\nabla \bullet (\sigma \nabla \bullet V) = 0$$

Equation 4-4

A solution for the electric field can be obtained:

$$-\nabla \bullet (\sigma \nabla \bullet V) = 0$$

Equation 4-5

This is the equation used to solve for the electric field in the finite element model.

In the model, the voltage of the electrode was set to 50 VDC while the midline surface was set to 25 V_{DC}. 50 V_{rms} was the actual voltage value during the experiments described earlier. Since the generator operated in a constant voltage mode (Figure 4-4) within the impedance range of the experiments, a constant voltage was used in the model.

The product of the current density and the electric field is the source term in the heat equation (Equation 4-6):

$$\rho C \frac{\partial T}{\partial t} - \nabla \cdot (k \nabla T) = Q$$

Equation 4-6

where:

Tissue density	ρ	$\text{Kg} \cdot \text{m}^{-3}$
Specific heat	C	$\text{Jkg}^{-1} \cdot \text{K}^{-1}$
Thermal conductivity	k	$\text{W} \cdot \text{K}^{-1} \cdot \text{m}^{-1}$
Temperature	T	K
Heat source	$Q = J \cdot X \cdot E$	J

For this first model, perfusion was not considered. Due to the high water content of tissue, a change in phase must be considered. Phase transition with latent heat is modelled in Femlab by modifying the heat equation:

$$\rho(C + D\lambda) \frac{\partial T}{\partial t} - \nabla \cdot (k \nabla T) = Q$$

Equation 4-7

where λ is the latent heat of vaporization ($2.256 \times 10^6 \text{ Jkg}^{-1}$ for water) and D is a normalized pulse around the transition temperature T_{trans} :

$$D = \frac{e^{\frac{-(T - T_{\text{trans}})^2}{\partial T^2}}}{\sqrt{\pi \partial T^2}}$$

Equation 4-8

This is the way Femlab mathematically includes the term for latent heat during the phase change, namely by multiplying a Gaussian pulse, D with λ . The constant, δT , determines the width of the pulse and therefore the “width” around the phase change temperature (100°C). This modification of the heat equation accounts for the energy consumed during the phase transition of the fluid in the tissue. The value k_T was substituted for k in equation 4-7 to account for the temperature dependence of thermal conductivity:

$$k_T = k \times (1 + \alpha \times (T - T_b))$$

Equation 4-9

where k is the thermal conductivity, α ($\alpha=0.02$ (65)) is the rate at which the temperature increases the conductivity, and T is the temperature (K).

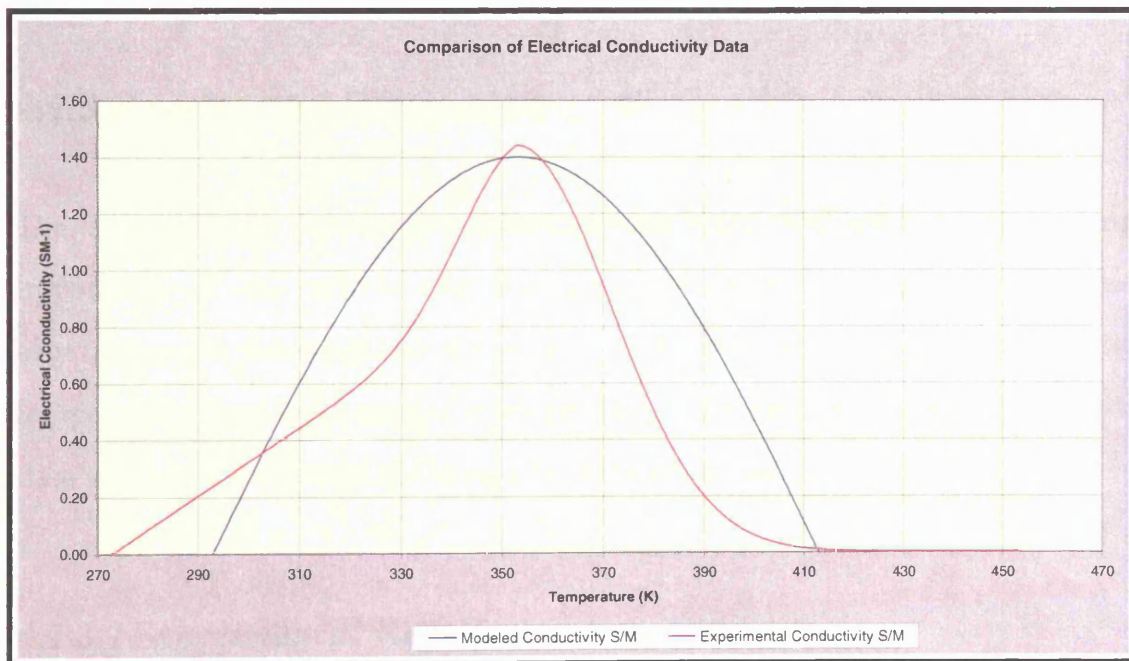


Figure 4-8. Electrical conductivity as a function of temperature, experimental vs. modelled curve.

The electrical conductivity is a temperature dependent quantity. Conductivity data were supplied in pairs (lookup table) of conductivity and temperature. Femlab accepts a partial differential equation (PDE) coefficient rather than pairs of data. Therefore a 6th order curve fit was applied to the data which consumed both time and memory in Femlab. A simpler curve was fit to the data (Figure 4-8). The fitted equation is:

$$\sigma_T = 1.4 \sin((T - 293) \frac{3.14}{120})$$

Equation 4-10

The value of conductivity at low temperatures is not zero, but very low – for example, frozen cow muscle has a value of approximately 0.80 μSM^{-1} (65). Since this analysis dealt with tissue heating, the conductivity values at and above body temperature from Figure 4-8 were used.

4.1.3 Results and Discussion

The experimental data were statistically analyzed and plotted. A working hypothesis of the relationship between the electrode length, width and separation with the coagulation zone was explored. Voltage, current density and temperature plots were created from the finite element model. The experimental data were then compared to the results of the finite element model.

4.1.3.1 Experimental Results

The subjective rating (from Table 4-2) was added to the spreadsheet containing various geometric configurations for planar electrodes (Table 4-1); each row

defines an individual experiment. Current density, J is part of the heat source ($Q=JXE$) which causes the tissue to coagulate. Therefore maximizing J between the electrodes will cause preferential heating of the tissue between the electrodes. For instance, as the distance between the electrodes, S decreases, the current density, J should increase. But since current density is current per m^2 , then increasing the width will likewise affect the current density. Increasing the width of the electrodes affects the depth of tissue through which the current flows and thus the current density J .

The next step was to quantify how a combination of electrode geometry and spacing may follow a pattern. A range of geometries was tested on an ad hoc basis. Each quantification took the form of a dimensionless index Φ , for example

$$\Phi = \frac{W^2}{(L+W)^2} \text{ (bearing in mind that the current density should be maximized}$$

between the electrodes). Additional columns were created to calculate the indices from the many experimental planar electrode configurations. The values in each index column were calculated and sorted in ascending order, and the index was plotted against the experimental "rating". Most of the indices tested did not correlate with the subjective ratings; however, the ratio of the perimeter of the electrodes to their separation (for those data where $L \geq W$) appeared to correlate well. Figure 4-9 shows a plot of the rating versus the index, Φ where:

$$\Phi = \frac{2 \times (W + L)}{S}$$

Equation 4-11

where:

Φ = index

W = width of the electrodes

L = length of the electrodes

S = separation

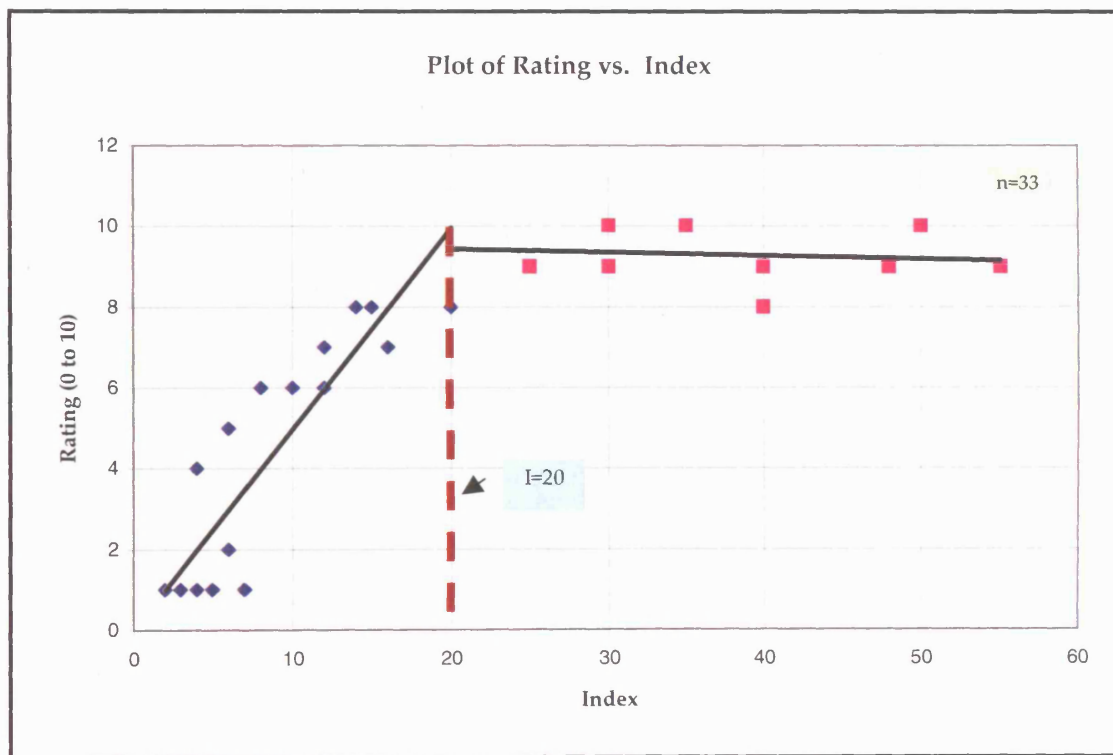


Figure 4-9. Simple curve fit of the subjective rating versus the index for the experimental data. The red line indicates the value at which the two lines converge. Above this value ($I=20$), the rating remains between 8 and 10.

4.1.3.2 Experimental Results Discussion

Figure 4-9 is a simple curve fit of the rating vs. the index (Table 4-1). An index above 20 yields a rating of 9 or 10, although a rating of 8 falls above and below an index of 20.

This simple linear regression analysis demonstrates a reasonable fit of the data to two lines which converge to a point. Above this value ($I = 20$) the coagulation will likely occur between the electrodes. Therefore, if the length, width and separation are chosen such that $\Phi > 20$, then coagulation will occur between the electrodes.

The practical value of equation 4-11 is that it can be used in designing bipolar electrodes for specific coagulation zones. For instance, if a polyp were 1.5 mm in diameter, then a separation of 2 mm and a length of 15 mm may be chosen. Then the electrode width required to assure coagulation only between the electrodes (only the tissue surrounding the polyp) can be calculated. Using the value of $\Phi > 20$ (from Figure 4-8) as the minimum index value for coagulation only between the electrodes, the width required would be calculated as:

$$20 = \frac{2 \times (W + 15mm)}{2mm}$$

$$W = 5mm$$

4.1.3.3 *In Vivo Results*

Figure 4-10 is a microscopic view of the canine oesophagus at 14 days healing, showing a clear demarcation between tissue which has not been damaged, tissue which has been damaged (absence of secretion glands) and is being regenerated. The secretion glands will regenerate in time (personal communication with pathologist). There is no evidence of damage to the tissue directly beneath the electrodes. The dark lines have been added to show approximately where the electrodes were placed. The treatment area between the electrodes is less than 2 mm, due to the shrinkage of the tissue during the healing response.

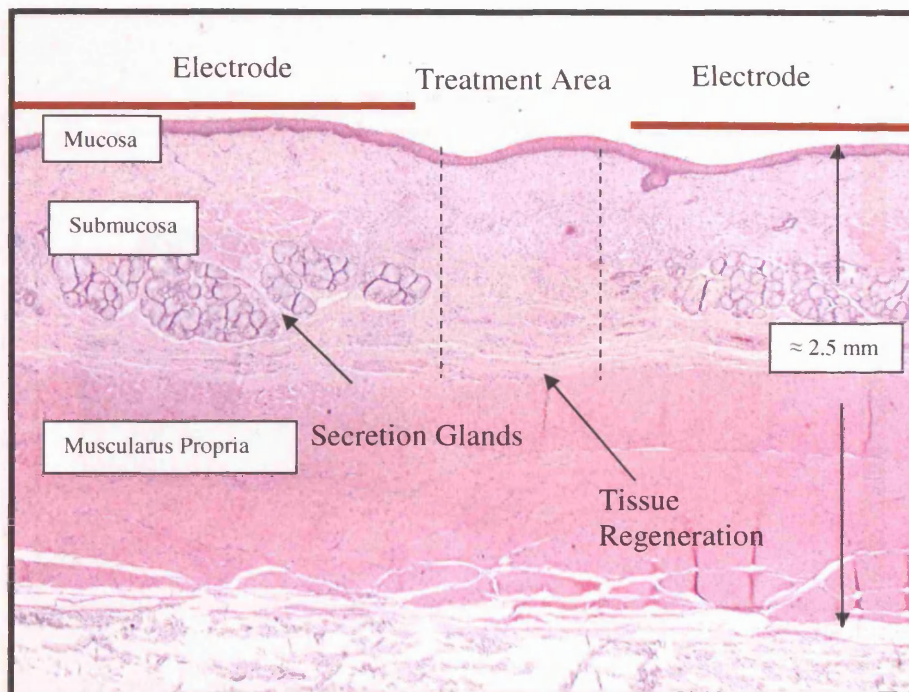


Figure 4-10. Canine oesophagus cross-section at 14 days.

4.1.3.4 *Finite element results*

4.1.3.5 Electrical model

Figure 4-11 is a graphical representation of the steady state voltage at the electrodes and along the surface of the slab of half symmetry. Figure 4-12 is the steady state voltage at the electrode of a quarter symmetry slab. The stainless steel electrodes have a very high value for conductivity and therefore there will be a zero voltage drop across them. The value of conductivity of the tissue was held constant for this solution. Although conductivity is a function of temperature, this analysis is simply looking at the steady state values of voltage and current density before a substantial amount of heating occurs ($<0.1 \mu\text{sec}$).

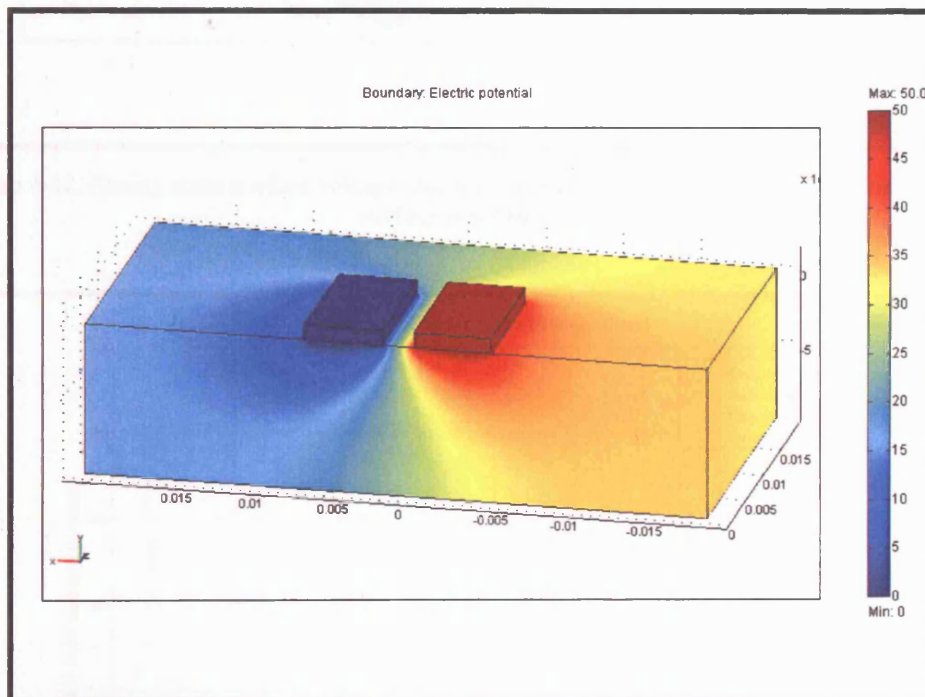


Figure 4-11. Graphical representation of the voltage profile on a half symmetry model. The model has been sliced in half across the electrodes. Figure 4-12 is a quarter symmetry slab.

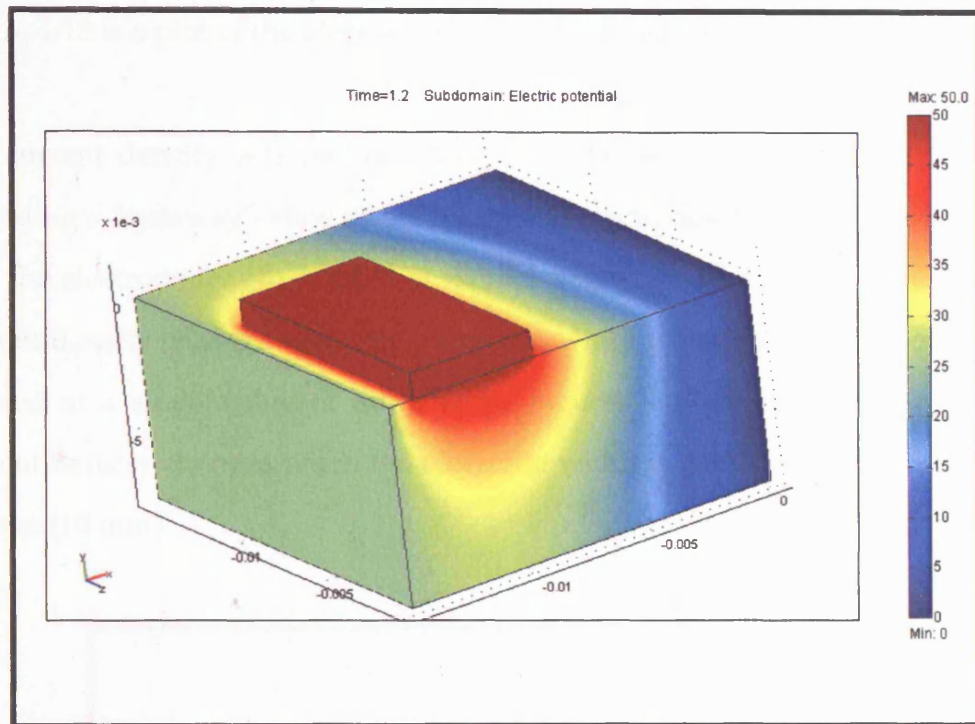


Figure 4-12. Steady state surface voltage plot for the quarter symmetry planar electrode. The left surface is set to 25 V.

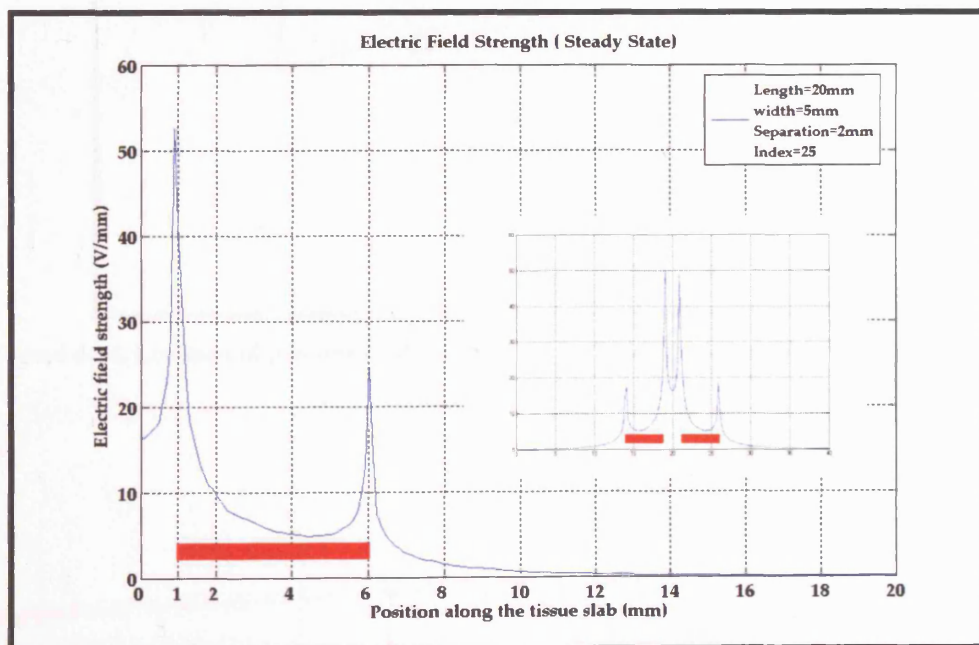


Figure 4-13. The electric field along the tissue surface (red bars represent the electrodes). The inset shows the full width plot of the electric field, illustrating the symmetry.

Figure 4-13 is a plot of the electric field along the tissue/electrode interface.

The current density was plotted along the cross-section shown in Figure 4-14, providing a “cutaway” view of the tissue and electrodes. In Figures 4-15 through 4-18 the electrode length is fixed at 20 mm. Figures 4-15 and 4-16 illustrate how current density changes when the electrode width is varied while the separation is fixed at a small value (2 mm), while Figures 4-17 and 4-18 show how the current density changes when the electrode width is varied while the separation is large (10 mm).

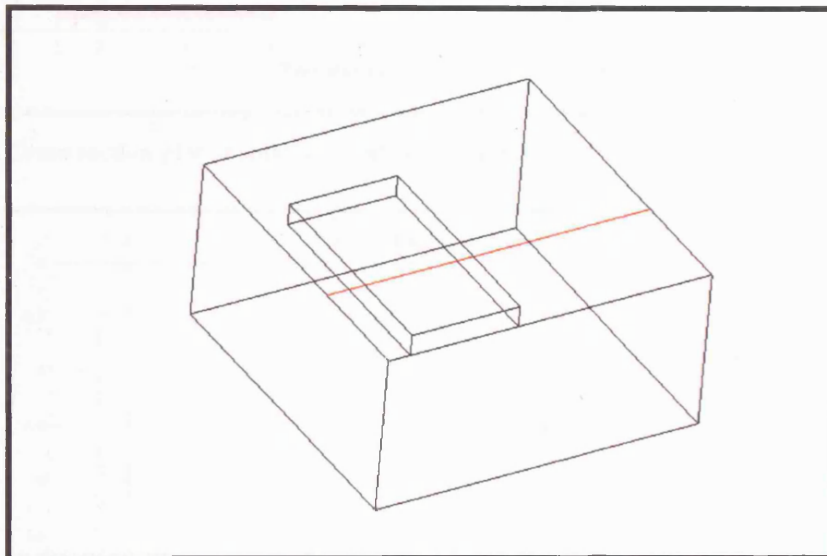


Figure 4-14. Location of plot line (red broken line) for cross section in Figures 15 through 18.

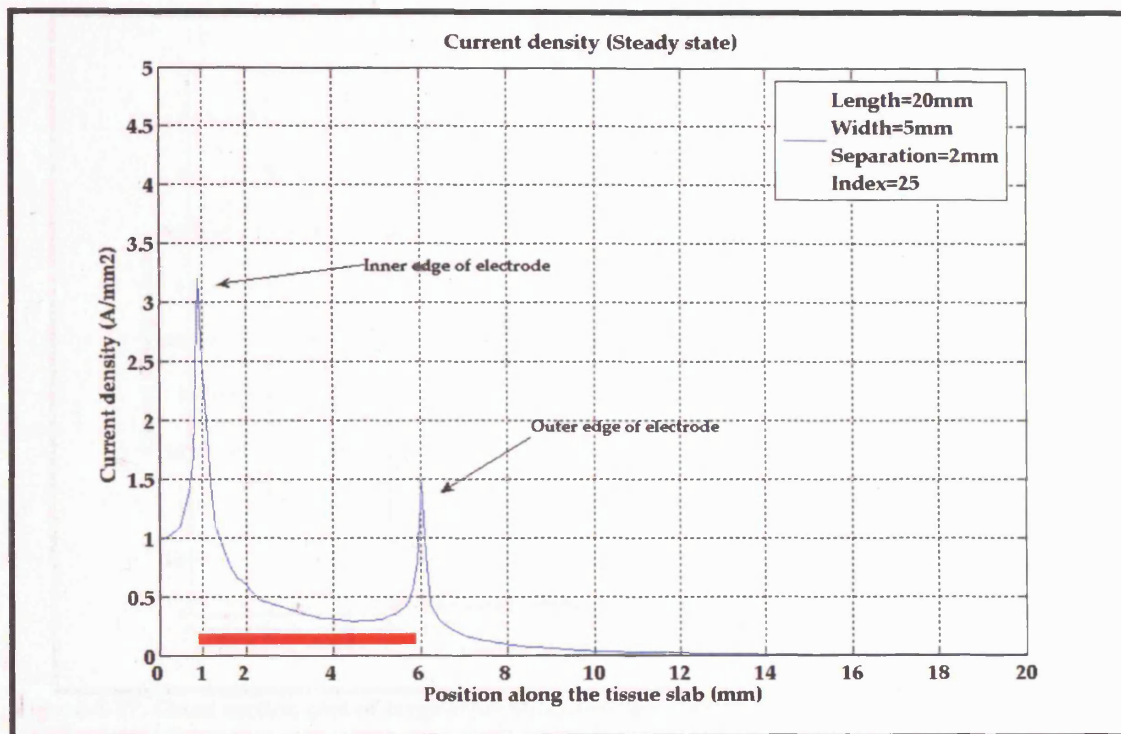


Figure 4-15. Cross section plot of small separation and large width (red bar represents the electrode).

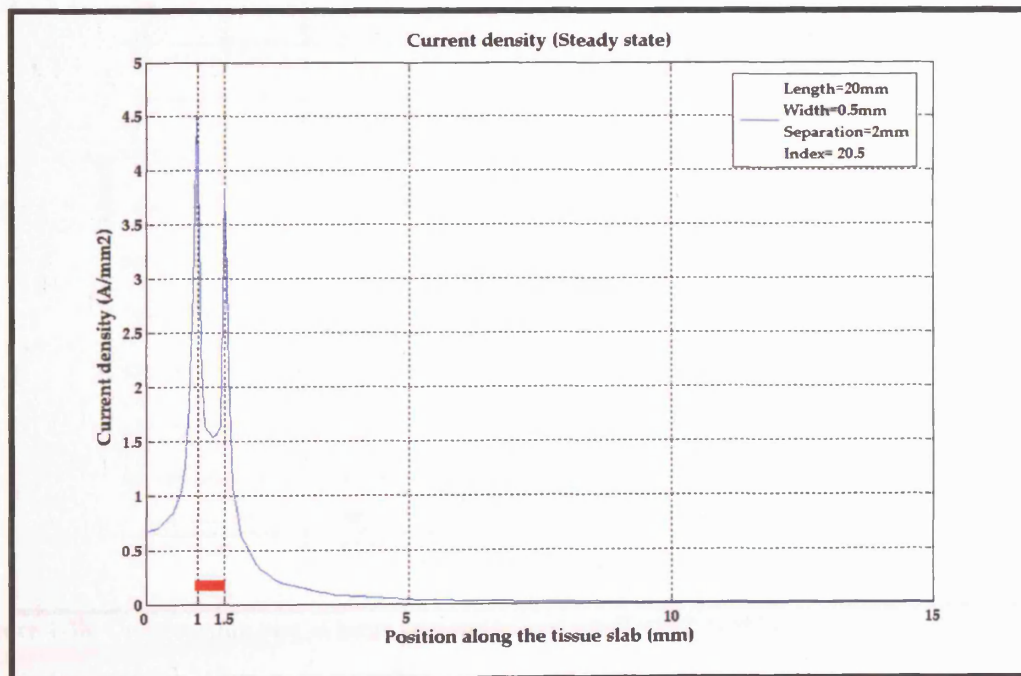


Figure 4-16. Cross section plot of small separation and small width (red bar represents the electrode).

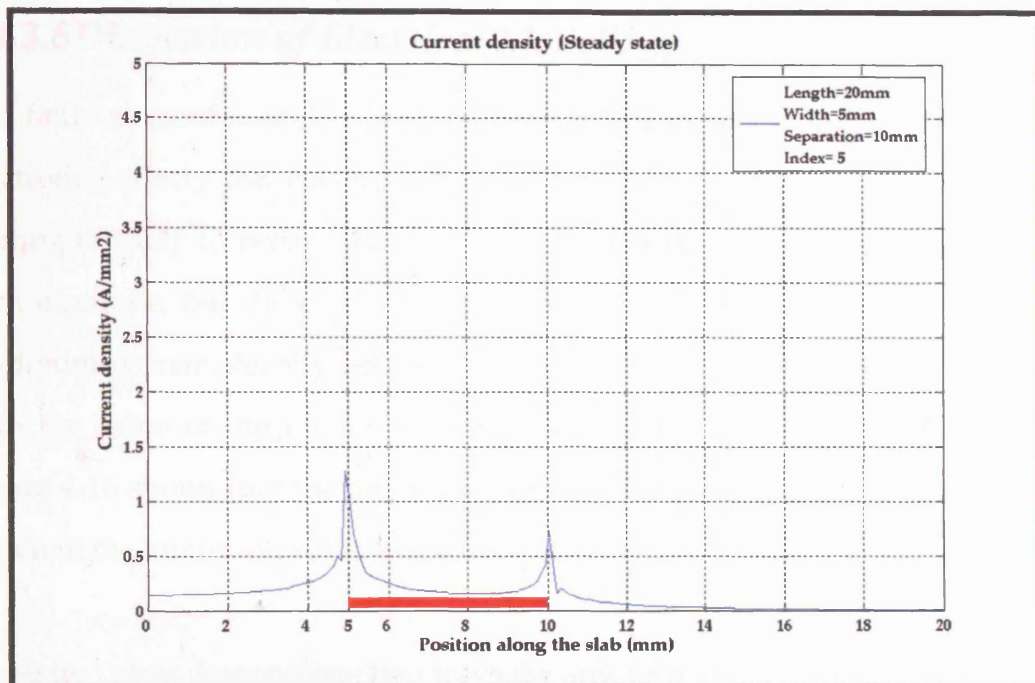


Figure 4-17. Cross section plot of large separation and large width (red bar represents the electrode).

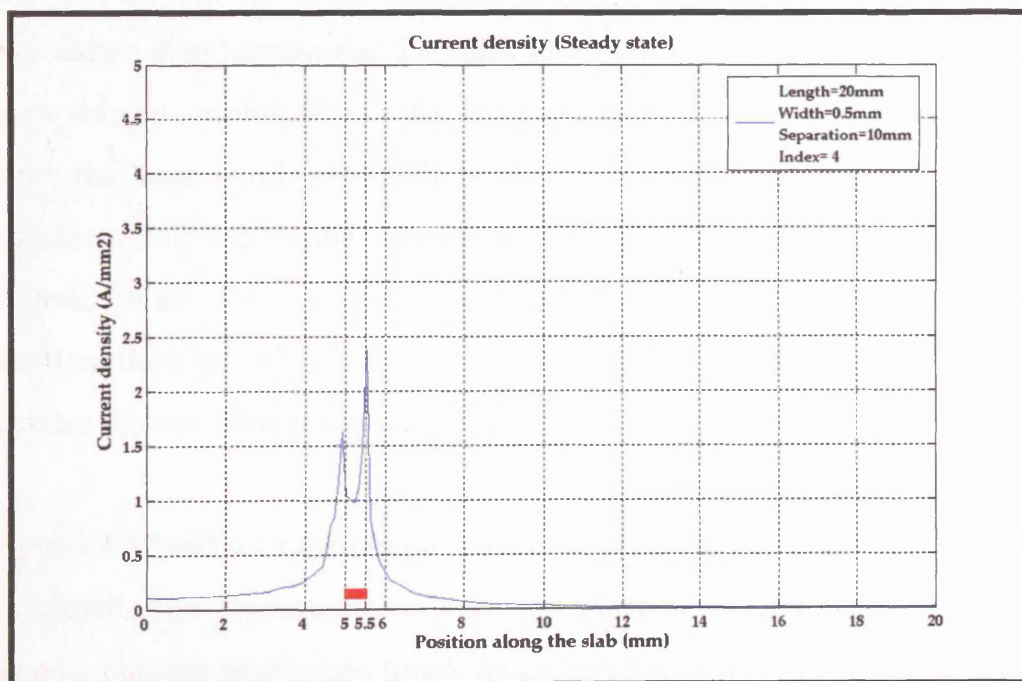


Figure 4-18. Cross section plot of large separation and small width (red bar represents the electrode).

4.1.3.6 Discussion of Electrical Modelling

The finite element models were generated to quantify how the geometry of the electrodes affects the current density flowing in the tissue and thus where heating is likely to occur. The peak current density occurs at the inner edge of each electrode, but there is also a peak at the outer edges. In Figure 4-15, the minimum current density between the electrodes (1.0 A/mm^2) is much greater than the value of the minimum along the electrode (0.3 A/mm^2). By contrast, Figure 4-16 shows that the minimum between the electrodes (0.7 A/mm^2) is less than half the minimum value along the electrode (1.5 A/mm^2).

These two plots demonstrate two ways the arrangement of the electrodes and the separation distance affect the current density. First, placing the electrodes in a plane, rather than having the flat sides face each other, creates a difference in current density amplitude between the inner and outer edges of the electrodes. Second, the large width of the electrodes causes the current density along the electrode to fall below the minimum between the electrodes (Figure 4-15). Therefore, when the width of the electrodes is large compared to their separation, the current density is higher between the electrodes than along the electrodes (ignoring the peaks at the edges).

In Figures 4-17 and 4-18 the separation S is fixed at a large value while the width W is varied. The asymmetry between the inner and outer edges can still be observed, but the width has much less effect. In both figures, the minimum current density between the electrodes is equal or less than the minimum current density under the electrode. Therefore the highest current densities occur either under the electrodes (Figure 4-18) or under and between (Figure 4-17), rather

than only between. A large separation distance S will yield a smaller value of the index, Φ . A smaller value of Φ will predict that the coagulation zone will occur under the electrodes or under and between the electrodes.

An inference can be made from equation 4-11. The width has less of an effect on the *index* Φ , than the separation, since the width and the length are summed in the numerator (twice the sum of the width and the length of the electrode i.e. its perimeter). It might seem that the larger the perimeter, the smaller the current density. But this only takes into account the average current density flowing from the electrode. The current density at the edges is affected by the ratio of width to length. The separation is inversely related to the index and can substantially change the current density.

It has been shown here that the current density varies throughout the tissue and has peak values at the edges of the electrodes. The current density maxima occur at the edge of the electrodes as has been reported in the literature (66). This is due to the profile of the electric field. Recall that the electric field is proportional to the current density by a factor equal to the reciprocal of the conductivity (Equation 4-1). The electric field is the divergence of the voltage. In this model, the voltage has been set at the electrode surface in contact with the tissue slab. Since the divergence is the rate of change of the voltage with respect to space coordinates, then the electric field should peak at the edges. Likewise the current density will peak at the edges.

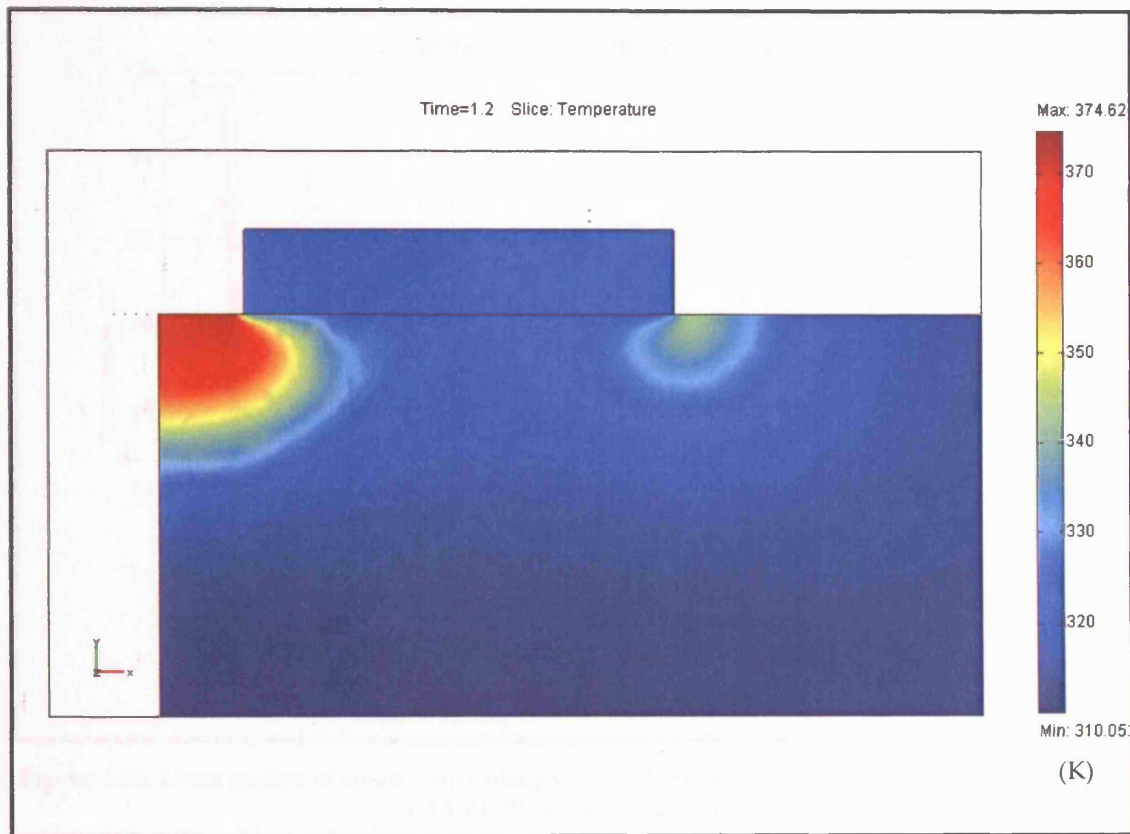


Figure 4-19. Graphical representation of the solution for temperature. The scale to the right is in Kelvins .

4.1.3.7 Thermal model

Figure 4-19 is a graphical representation of the thermal solution. This is a “slice”, or two-dimensional cross section view of an electrode on a slab of tissue (Figure 4-12). The heating occurs between the electrodes as expected for this particular geometry, which has an index of 25.

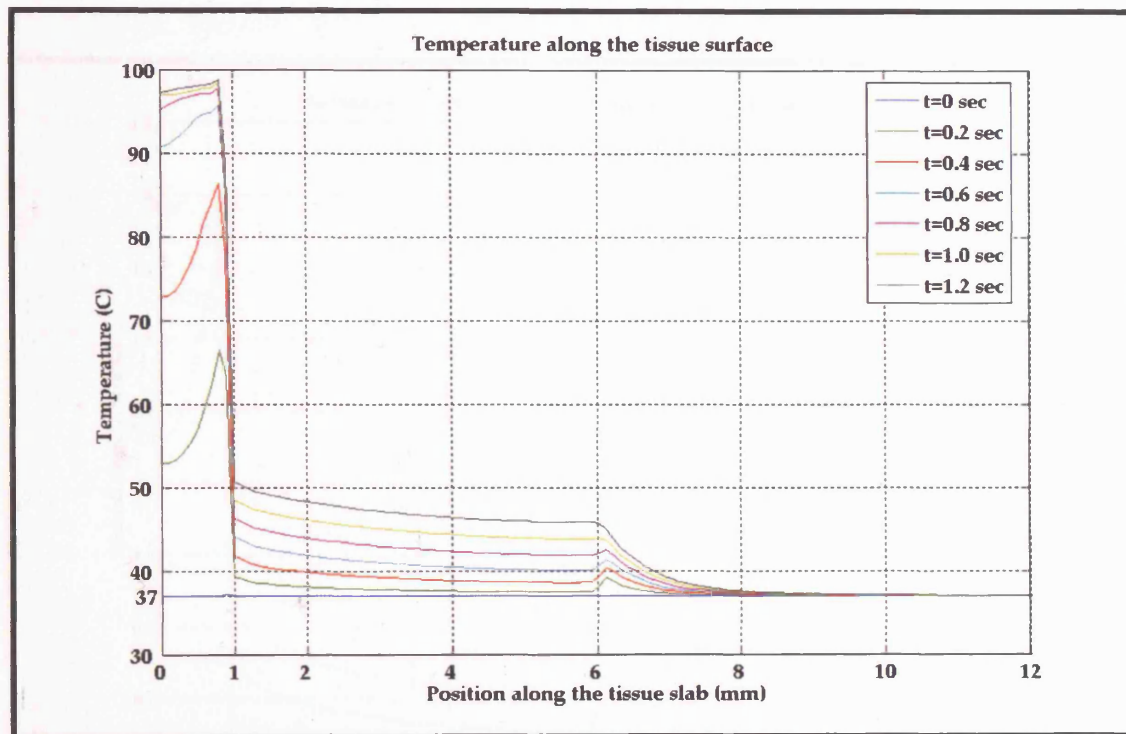


Figure 4-20. Cross section of temperature along the tissue/electrode interface, for time = 0 seconds to 1.2 seconds in 0.2 second steps.

Figure 4-20 plots the temperature profile at the tissue/electrode interface as a function of time. One can see that the temperature rises rapidly ($75^{\circ}\text{C}/\text{S}$ to $150^{\circ}\text{C}/\text{S}$) until it approaches 100°C . The temperature rise under the electrodes is in part due to conduction from the heating in the tissue. During the initial heating, the temperature at the inner edge of the electrode is slightly higher than at the outer edges, which is due to the very high current density spike. It is possible that the thermal mass of the electrode acts to cool the tissue in contact, and therefore contribute to the preferential heating between the electrodes.

Figure 4-21 plots the electrical conductivity along the tissue/electrode as a function of time. This pattern is similar to the temperature profile between the electrodes (Figure 4-19).

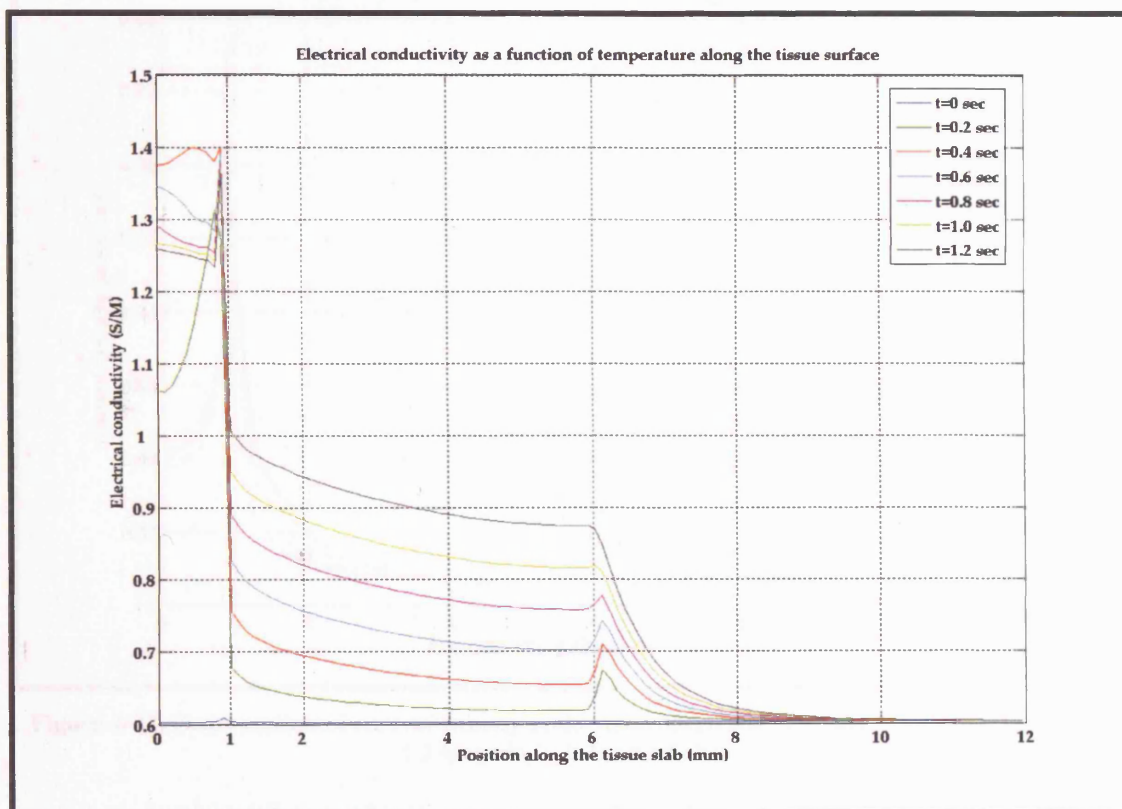


Figure 4-21. Cross section of conductivity at the tissue/electrode interface at time = 0 seconds to 1.2 seconds, in 0.2 second steps. These values are calculated with equation 4-10, therefore $\sigma=0.60$ S/M at time=0 sec.

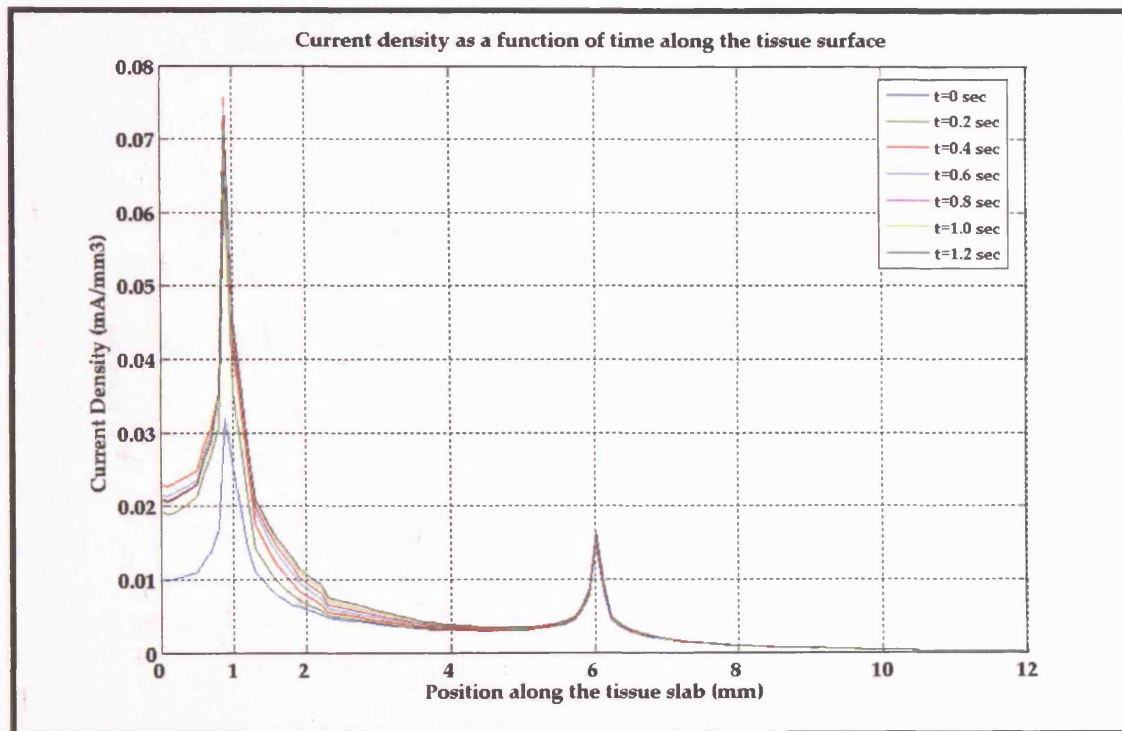


Figure 4-22. Cross section of current density at the tissue/electrode interface at time = 0 seconds to 1.2 seconds, in 0.2 second steps.

Figure 4-22 contains multiple plots of the current density as the time is increased from 0 to 1.2 seconds.

Figure 4-23 plots the temperature rise midway between the electrodes and at a distance 1.5mm into the tissue. The rate of temperature rise (35°C/S) is slower than at the surface (75°C/S Figure 4-20).

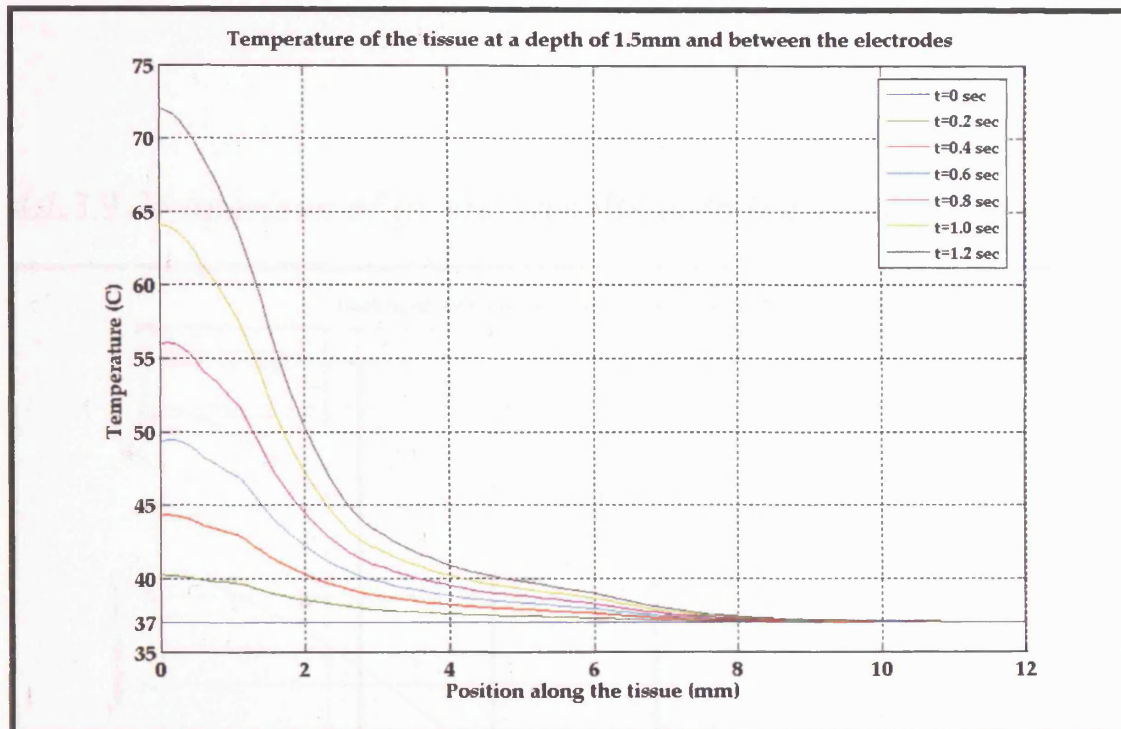


Figure 4-23. The temperature rise between the electrodes at a distance 1.5 mm into the tissue.

4.1.3.8 Thermal Model Discussion

As the temperature increases, the current density increases. The rate at which this increases is not the same at all points along the tissue. The current density between the electrodes doubled while the current density along and outside the electrodes has remained nearly the same.

Figures 4-15, 4-19 and 4-20 demonstrate how the concentrating of the current density further contributes to the heating between the electrodes. The current density is higher between the electrodes than under or outside the electrodes, heating the tissue between the electrodes more rapidly than elsewhere. The increase in temperature causes a further increase in the conductivity and current density between the electrodes.

4.1.3.9 Comparison of In-vivo results with the model

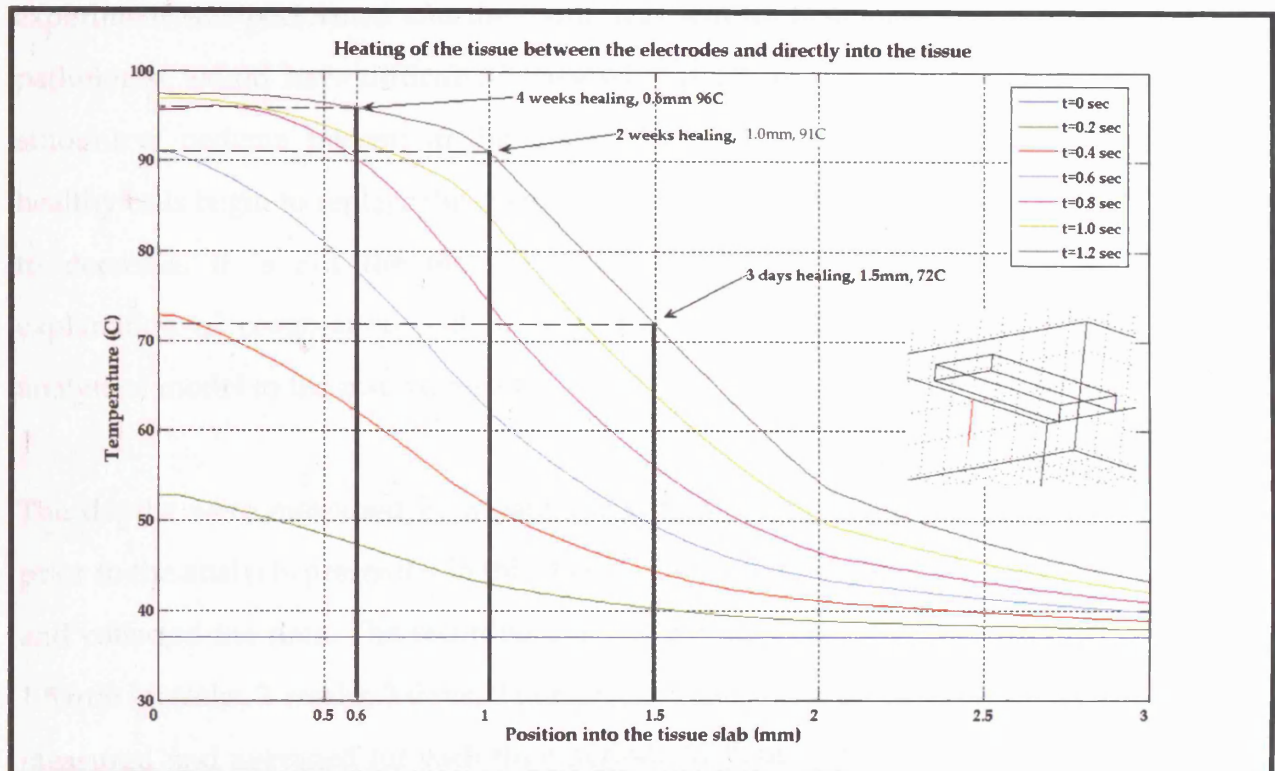


Figure 4-24. Temperature of the modelled tissue from time = 0 seconds to 1.2 seconds. This plot begins at the midpoint between the electrodes and ends 3 mm directly into the tissue (inset figure). The maximum temperature reached for the depths of coagulation determined by a pathologist are labelled.

Figure 4-24 contains multiple plots of the tissue temperature as a function of depth in the model. Each plot represents the temperature at intervals of 0.2 seconds from time = 0 to time = 1.2 seconds. These data were produced to compare with the histological results from the canine study. Depth of coagulation was reported for survival times of 3 days, 2 weeks and 4 weeks (67). The 3 dotted lines in Figure 4-24 represent the maximum temperature in the

model at locations of maximum depth of coagulation as reported by the pathologist.

The depth of coagulation in-vivo is somewhat difficult to assess. If an acute experiment was performed and the tissue was sent for histological analysis, the pathologist would have difficulty in assessing depth of coagulation due to the amount of oedema present in the tissue. As the tissue heals over time and healthy cells begin to replace the necrotic cells, the coagulation depth will appear to decrease. It is not the intent of this discussion to provide a detailed explanation of coagulation and healing response, but rather to compare the analytical model to the in-vivo results.

The depths were measured by a pathologist in an animal study(68) conducted prior to the analysis presented in this thesis. The author participated in the study and collected the data. The recorded average depths were 0.6 mm, 1.0 mm and 1.5 mm (4weeks, 2 weeks, 3 days). Four single applications of the electrodes were measured and averaged for each time period. All four applications were in the same animal. The temperatures at these depths were 96° C, 91° C, 72° C (4 weeks, 2 weeks, 3 days). After a healing response of 3 days, the greatest damage can be observed in tissue which has incurred a thermal injury (personal communication with pathologist). The depths recorded for 2 weeks and 4 weeks would not represent the maximum depth of injury, or coagulation, because of the substantial healing that has occurred. The 3 day data will be, therefore compared to the results of the finite element model.

At a depth of 1.5mm, the tissue reached a temperature of 72° C in the model. The tissue will remain at an elevated temperature until the heat dissipates into the

surrounding tissue. Figure 4-25 is a plot of the temperature of the tissue as it cools. To obtain these plots, the solution (at 1.2 seconds of the heat equation with the ohmic losses as the source term) was used as an initial condition. The heat source term (which represents the generator) was then set to 0 and the heat equation was solved for a time period of 4 seconds in 0.5 second steps.

At 1.5 mm into the tissue the temperature dropped from 72°C to 64°C during 4 seconds of cooling. Since this model analyzes only the heat flow due to conduction, it will underestimate the effects of cooling due to perfusion.

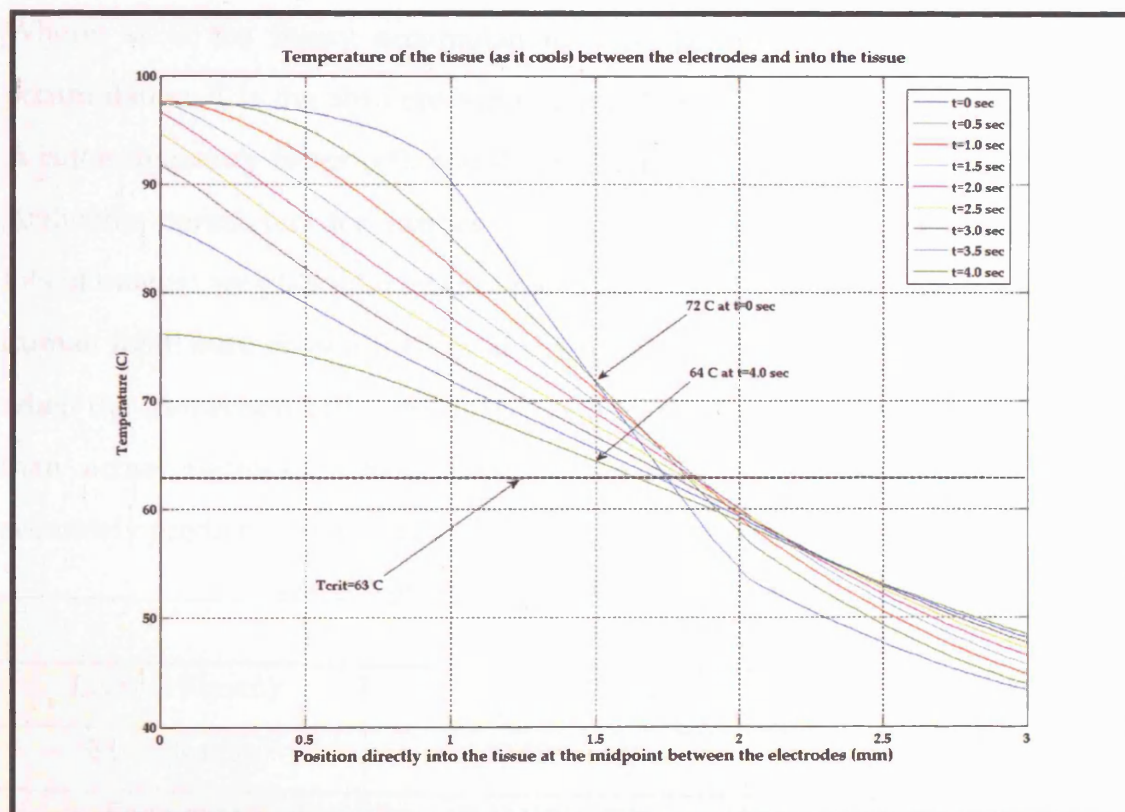


Figure 4-25. Multiple plots of the tissue cooling after the heat source has been removed. This is the temperature of the tissue, midway between the electrodes, from the surface to 3.0 mm into the tissue. Figure 4-26 plots the thermal history of a point in the tissue midway between the electrodes, from the surface to 2.0 mm below the surface.

Heriques and Moritz (69-72) performed thermal damage experiments and applied rate process models to their experimental results. The Arrhenius rate process model was used to predict tissue damage in skin. The basis of this rate process model of thermal damage can be obtained from chemical reaction kinetics (73). The damage integral is given as:

$$\Omega = \int_0^{\tau} A e^{\left[-\frac{E}{RT} \right]} dt$$

Equation 4-12

Where: Ω is the injury accumulation, τ is the time (seconds) for damage accumulation, T is the absolute temperature, E is the activation energy (J/mole), A is the frequency factor (s^{-1}), and R is the universal gas constant. Table 4-4 lists Arrhenius parameters for various tissues. Mucosa and submucosa (producing lots of mucus) are glandular tissues, much like liver, therefore the parameters for human liver were chosen for this analysis (the values for aorta were measured when the connection between collagen and elastin weakened in the aorta rather than actual necrosis). Chang (74) showed that the values for liver could accurately predict cell death when RF energy was used to heat the tissue.

Table 4-4. Arrhenius parameters for various tissues.

	A (s^{-1})	E _a (J·mole ⁻¹)
Liver (Human)	7.39 X10 ³⁹ (74)	2.577X10 ⁵ (74)
Skin (Human)	3.1X10 ⁹⁸ (73)	6.28X10 ⁵ (73)
Egg white	3.8X10 ⁵⁷ (73)	3.85X10 ⁵ (73)
Kidney (porcine)	6X10 ³⁴ (75)	2.38X10 ⁵ (75)
Aorta (Human)	5.6X10 ⁶³ (73)	4.3X10 ⁵ (73)

Pearce (73) defined a critical temperature such that the damage accumulation rate is 1:

$$\frac{\partial \Omega}{\partial t} = 1$$

Equation 4-13

Therefore,

$$T_{crit} = \frac{E_a}{R \ln(A)}$$

Equation 4-14

The damage rate of tissue below this temperature is negligible. This is a characteristic behaviour of the kinetic damage model (73). For our parameters, the critical temperature is:

$$\begin{aligned} T_{crit} &= \frac{2.577 \times 10^5 \text{ Jmol}^{-1}}{8.32 \text{ Jmol}^{-1} \text{ K}^{-1} \ln(7.39 \times 10^{39} \text{ s}^{-1})} \\ &= 337\text{K} (64^\circ\text{C}) \end{aligned}$$

A dotted line has been drawn in Figure 4-26 denoting the critical temperature. At a depth of 1.5mm the temperature of the tissue stays above this critical temperature from approximately 1.0 second into the heating cycle through 4 seconds of cooling (Figure 4-26).

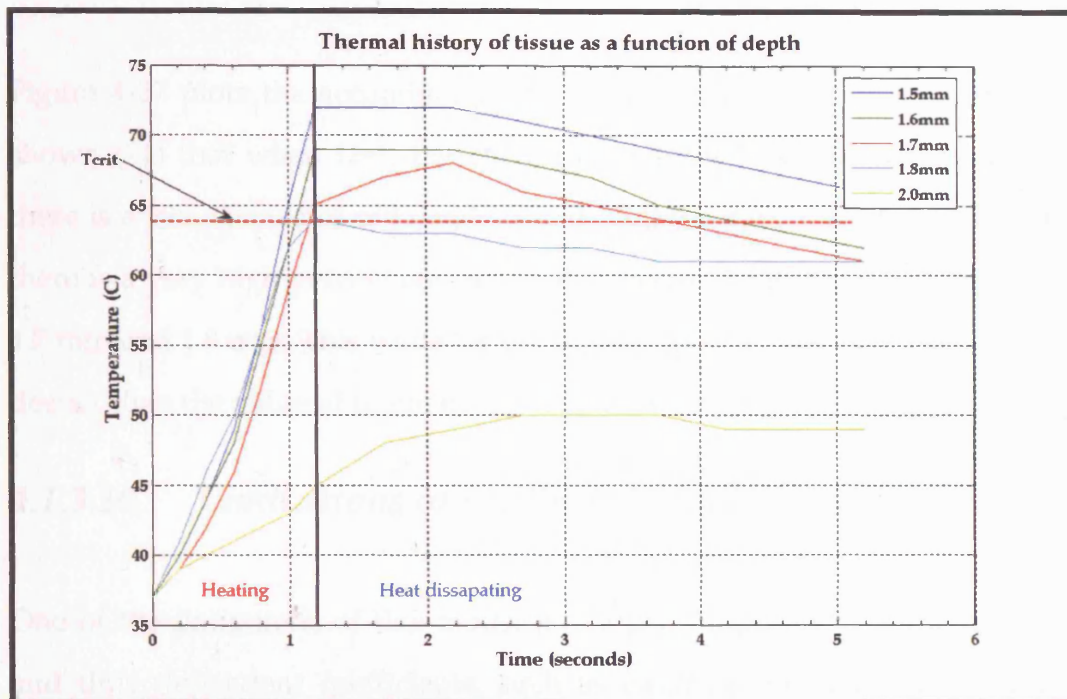


Figure 4-26. Temperature history at a point midway between the electrodes and at depths of 1.5 through 2.0mm The tissue is heating up to 1.2 seconds, while the heat is dissipating beyond 1.2 seconds. The critical temperature ($T_{crit}=64^{\circ}\text{C}$) has been labeled).

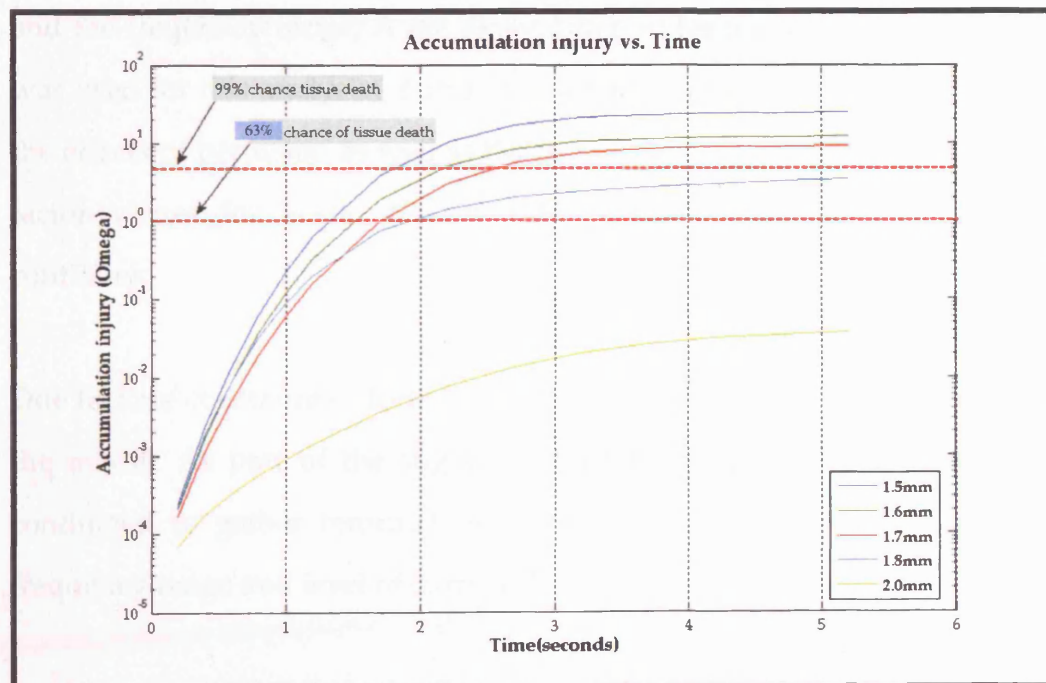


Figure 4-27. Total accumulated injury for tissue midway between the electrodes and at depths of 1.5mm through 2.0mm. The horizontal, dotted, red lines indicate values at which the chance of cell death is between 63% and 99%.

Figure 4-27 plots the accumulated injury, Ω as a function of time. It has been shown (74) that when $\Omega=1$, the chance of cell death is 63% while when $\Omega=4.5$ there is a 99% chance of cell death. Based on these data, this model predicts that there is a very high percentage chance that necrosis will occur at depth between 1.7 mm and 1.8 mm. This value for depth of tissue necrosis is approximately 15% deeper than the value of tissue necrosis determined by a pathologist.

4.1.3.10 *Limitations of the finite element model*

One of the limitations of this model is the poor availability of the temperature and time dependent coefficients, such as electrical and thermal conductivity. These values are known for some tissues (such as liver), but there is limited data available for mucosal and submucosal tissue. Likewise the activation energy E and the frequency factor, A are likely different for mucosa than for liver (which was used for this analysis). Future work will include an analysis which includes the effects of perfusion as well as the use of the activation energy and frequency factor values for aorta. A search for mucosa and submucosa parameters continues.

Due to time constraints, electrode contact impedance was also not considered in the model. As part of the suggested further work, a literature search will be conducted to gather information of the effects of contact impedance in this frequency range and level of current flow.

4.1.4 Conclusions

It has been shown both experimentally and analytically that the configuration of the planar electrodes can determine the coagulation volume and location. By contrast, multipolar probes are similar in the way in which the electrodes lie in a plane when they are placed on the tissue. The geometrical relationship of those electrodes is such that quite the opposite occurs (61). That is, when the multipolar probe is placed on tissue, it will coagulate the tissue independent of the orientation and surface area in contact. The planar electrodes have been designed with two key attributes- visualization and control. The entire surface of the tissue to be coagulated can be visualized and so ensure accurate targeting of the treatment.

The length, width and separation of the electrodes affect the current density under and between the electrodes, causing preferential heating of the tissue. The experimental data led to an index which helped to predict the location of the coagulation zone. The finite element model tested the index and showed that by placing these electrodes in a plane and by varying the width, length and separation of the electrodes, the current density could be maximized between the electrodes. Since the heating of the tissue is due to the power dissipated by the current flow through the tissue, maximizing the current density between the electrodes will lead to coagulation between the electrodes. The damage integral quantified the depth of tissue necrosis. This value was within 15% of a value determined by histological examination.

The in-vivo tests demonstrated no irreversible tissue damage under the electrodes. These electrodes could be designed to surround a polyp and provide

haemostasis to the base as the polyp is removed, without causing damage to the polyp.

Both the index and finite element modelling may be of practical use in designing and testing a planar electrode device for haemostasis in the gastrointestinal tract. Such a device could provide visualization to the clinician and assure a consistent depth of coagulation. The planar electrodes could be mounted on an over tube as a safe and effective way to treat bleeding in the colon. Other tissue pathologies, such as ulcers and varices, could also be treated with these planar electrodes.

And finally, as part of the suggested further work, the index hypothesis will be further explored. It is possible that a more reasonable index could be formulated as a quantity per unit length or width. Limitations of the index such as time will be explored. More experimental data will be gathered to test the limits of the index.

5 Conclusion

This thesis began with a quote from Lord Kelvin which stated the importance of measuring and quantifying in order to reach a logical conclusion; this notion was applied to current methods used to screen for and treat colorectal cancer. Two major topics were covered:

1. Diagnostic capability of colonoscopy (Guidewire Endoscopy)

Experiments were performed with guidewires to show how they may make it easier for the physician (or a less-skilled practitioner) to access diseased, gastrointestinal tissue. The Cathcam and the Colonicam, two new devices that make use of guidewires, were designed, built, and tested in-vivo, ultimately reducing the insertion force.

2. Therapeutic capability of colonoscopy (Planar Electrodes)

A unique geometrical relationship for a pair of planar electrodes was discovered which coagulates tissue between rather than under the electrodes, for improved visualization. This phenomenon was modelled and analyzed using finite element techniques. The planar electrodes could improve treatment of gastrointestinal lesions by precisely controlling depth and area of coagulation.

5.1 Guidewire Endoscopy

Colonoscopy is an important step in the prevention of colon cancer throughout the world. Colonoscopy is a simple, minimally invasive procedure which can be painful to the patient. Trained colonoscopists can reach the caecum using rotation and straightening techniques, but the time spent advancing the tip of the

colonoscope forward as a percentage of total time is low. The percentage of time spent advancing the colonoscope forward was shown to be independent of experience. Looping is a major contributor to incomplete colonoscopies, and to pain felt by the patient. The guidewire technique was developed as a way to prevent negative consequences of loop formation in the colon. As the result of this work, two devices were built and tested in humans: the Cathcam and the Colonicam. In-vivo testing showed that the amount of force to advance the insertion tube was significantly reduced when aided by a guidewire. This reduction in force will reduce the pain and discomfort the patient will experience during the procedure, possibly to the point where sedation would not be required. A more comfortable colonoscopy may also increase the likelihood that the patient will return and have routine examinations for polyps.

It was shown that a less experienced person could advance the tip of the Colonicam further and with less force than a traditional colonoscope. The nurse assistant may someday be able to perform the caecal intubation with the Colonicam, while the gastroenterologist performs the withdrawal examination. This could lead to more patients being screened for CRC by the gastroenterologist.

5.1.1 Cathcam

The Cathcam design was based on the data which showed that a guidewire could reduce the insertion force (by 52%) required to advance a thin catheter along a tortuous path. The animal study showed that the percentage of time spent pushing the Cathcam above the human pain threshold was 0%.

This simple catheter did have some difficulties advancing in humans along the hinged guidewire due to the lack of tip articulation. Although insertion force could not be measured with the Cathcam, it was observed that patients appeared to feel little discomfort while the Cathcam was in use. In order to incorporate the functions needed to perform a colonoscopy, the final Cathcam prototype was by necessity larger and heavier than the original catheter. What was learned from the Cathcam human trial was incorporated into the design of the motorized Colonicam.

5.1.2 Colonicam

The Colonicam accomplished the main goal of guidewire endoscopy, namely, to reduce the insertion force and the pain felt by the patient. Figure 3-3 showed that 17% of the total time was spent pushing a traditional colonoscope above the human threshold of pain (10 N), while 4% of the total time was spent pushing the Colonicam above the pain threshold ($p = 0.034$). The Colonicam performed all the essential functions of a colonoscope along with the option of using the guidewire only when necessary. This reduction in insertion force might benefit a patient living in a country where sedation is not routinely available, or a patient who chooses not to be sedated.

5.2 Planar Electrodes

Experimental data showed that the configuration of planar electrodes controls the location and depth of tissue heating when diseased tissue is treated with RF current. Testing of over thirty planar electrode configurations, and curve fitting these data, led to a simple equation for designing a device which could

predictably coagulate tissue. Since the colon has a thin wall and care must be taken to not cause irreversible damage to the entire thickness of the wall, it is paramount to be able to control the depth of tissue damage. One specific planar electrode configuration allows coagulation only between the electrodes, which allows for a clear endoscopic view of the tissue to be coagulated.

A finite element model of the planar electrodes was created that closely correlated to the experimental results, providing some insight as to why the length and width of the electrodes and the separation distance can affect where the tissue is heated. Temperature data from the model were used to calculate the accumulated damage to the tissue with the Arrhenius integral. The calculated value (1.75 mm) of depth of tissue necrosis was within 15% of the depth assessed by a pathologist (1.5 mm) on live animals. There are naturally limitations and sources of error in both the model and the assessment by the pathologist, but given the uncertainty of each assessment, the model appears to have predicted the depth of necrosis accurately.

With this model of the planar electrodes, an instrument could be designed which can aid in the removal of a polyp from the colon with two benefits. Firstly, the planar electrodes can surround the polyp and simultaneously provide haemostasis as the polyp is removed; the polyp will not be damaged by the heat and therefore can be examined by a pathologist for the presence of cancer. Secondly, the physician can be assured that the depth of necrosis does not extend into the outer layers of the colon and cause a perforation. Using this model could also shorten the design cycle and reduce the number of animals sacrificed to produce a prototype which can be safely used in humans.

5.3 *Further Work*

- Guidewire Endoscopy
 - A plan is in place to measure the insertion force and pain felt during colonoscopies in patients who have been sedated those who have not. These data will be used to determine how successfully pain may be reduced by use of the Colonicam rather than a colonoscope.
 - A new prototype which incorporates the “best” characteristics of both the Cathcam and the Colonicam has been prototyped and is presently being tested.
- Planar Electrodes
 - The finite element model will be run with perfusion taken into account. The bioheat equation will be used in place of the heat equation. The accumulated damage will be calculated with aorta parameters. The depth of coagulation will be compared to the depth calculated with parameters for liver.
 - A prototype of the planar electrodes is being constructed to aid in the removal of large polyps.
 - A variation of the planar electrodes will be developed to treat gastric and duodenal ulcers and oesophageal varices.
 - The finite element model will be used to determine the affect that time has on the location of the coagulation.

6 Acknowledgements

I would like to thank Tim Mills and Sandy Mosse for their support and helpful advice during this work. It was an opportunity for me to learn a good deal from them and become friends as well. I very much enjoyed the many conversations Tim and I had along the way, while Sandy's earlier work helped pave the way for more improvements in colonoscopy.

I would like to thank Paul Swain and Annette Fritcher-Ravens for their help in evaluating and developing these ideas for pre-clinical and clinical use. They helped me understand how experimentation can always yield useful results that are never too small.

I would like to thank Adam Gibson and Martin Fry for their invaluable guidance and advice. Students under their guidance are in good hands.

I would like to thank Ken Dobler and Duane Linenkugel for giving me an opportunity to become a student again and remind myself that learning never ends. I appreciate their support and confidence.

I would like to thank Greg Bakos and Omar Vakharia for their help on prototyping the force handle and the Coloncam. They are talented and valuable co-workers.

Finally, I would like to thank my wife Lynn for all of her efforts in editing this document. She has a true talent for transforming simple text into a clear and concise message.

7 References

Reference List

- (1) Ransohoff DF. Screening colonoscopy in balance. Issues of implementation. *Gastroenterol Clin North Am* 2002;**31**(4):1031-44, vii.
- (2) Yamada T. Colon: Anatomy and structural anomalies. Textbook of Gastroenterology. J.B. Lippincott Company, 1997: 1739.
- (3) Deyoe LA, Balfe DM. Cross-Section anatomy. Textbook of Gastroenterology. J.B. Lippincott Company, 1997: 2655.
- (4) Frank H.Netter MD. Atlas of Human Anatomy. 2 ed. Novartis Medical Education, 1998.
- (5) Guyton AC, Hall JE. General Principles of Gastrointestinal Function-Motility, Nervous Control, and Blood Circulation. W.B Saunders Company, 2000.
- (6) Guyton AC, Hall JE. Secretory Functions of the Alimentary Tract. Textbook of Medical Physiology. W.B Saunders Company, 2000.
- (7) F.Cervero. Neurophysiology of gastrointestinal pain. *Bailliere's Clinical Gastroenterology* 1988;**2**(1):183-99.
- (8) Guyton A.C, Hall J.E. General principles of gastrointestinal function-motility, nervous control, and blood circulation. Gastrointestinal Physiology. 2000.
- (9) Guyton AC, Hall JE. Somatic Sensations II. Pain, Headache, and Thermal Sensations. Textbook of Medical Physiology. W.B Saunders Company, 2000.
- (10) Ransohoff DF. Screening colonoscopy in balance. Issues of implementation. *Gastroenterol Clin North Am* 2002;**31**(4):1031-44, vii.
- (11) Yamada T, Alpers DH, Owyang C *et al.* Colonic Polyps: Benign and Premalignant Neoplasms of the Colon. Textbook of Gastroenterology. J.B. Lippincott Company, 1997.

- (12) Imperiale TF, Wagner DR, Lin CY *et al.* Risk of advanced proximal neoplasms in asymptomatic adults according to the distal colorectal findings. *N Engl J Med* 2000;**343**(3):169-74.
- (13) Fearon E, Vogelstein B. A genetic model for colorectal tumorigenesis. *Cell* 1990;**61**:759-67.
- (14) Hisamuddin, Irfan M. and Yang, Vincent W. Genetics of Colorectal Cancer. Medscape . 2004. Medscape.
Ref Type: Electronic Citation
- (15) Boyles, S. New colon cancer test shows promise. WebMD . 2004.
Ref Type: Electronic Citation
- (16) Trowbridge B, Burt RW. Colorectal cancer screening. *Surg Clin North Am* 2002;**82**(5):943-57.
- (17) Ransohoff DF. Screening colonoscopy in balance. Issues of implementation. *Gastroenterol Clin North Am* 2002;**31**(4):1031-44, vii.
- (18) American Gastroenterological Association. Digestive disease education. AGA . 2004.
Ref Type: Electronic Citation
- (19) Rozen P. The OMED Colorectal Cancer Screening Committee: a report of its aims and activities. Organisation Mondiale d'Endoscopie Digestive. *Gastrointest Endosc* 1999;**50**(3):449-53.
- (20) Levine MS, Rubesin SE, Laufer I *et al.* Contrast Radiolgy. Textbook of Gastroenterology. J.B. Lippincott Company, 1997.
- (21) CB Williams, J Waye. Colonoscopy and Fexible Sigmoidoscopy. Gastroenterology. 2004: 2571.
- (22) Waye, Rex, Williams. Colonoscopy: Principles and Practice. Blackwell Publishing Ltd., 2003.
- (23) Inadomi JM, Sonnenberg A. The impact of colorectal cancer screening on life expectancy. *Gastrointest Endosc* 2000;**51**(5):517-23.
- (24) Winawer SJ, Stewart ET, Zauber AG *et al.* A comparison of colonoscopy and double-contrast barium enema for surveillance after polypectomy. National Polyp Study Work Group. *N Engl J Med* 2000;**342**(24):1766-72.

- (25) Rex DK. Barium studies/virtual colonoscopy: the gastroenterologist's perspective. *Gastrointest Endosc* 2002;**55**(7 Suppl):S33-S36.
- (26) Lieberman DA, Weiss DG, Bond JH *et al.* Use of colonoscopy to screen asymptomatic adults for colorectal cancer. Veterans Affairs Cooperative Study Group 380. *N Engl J Med* 2000;**343**(3):162-8.
- (27) Cotton PB, Connor P, McGee D *et al.* Colonoscopy: practice variation among 69 hospital-based endoscopists. *Gastrointest Endosc* 2003;**57**(3):352-7.
- (28) Wu TK. Occult injuries during colonoscopy. Measurement of forces required to injure the colon and report of cases. *Gastrointest Endosc* 1978;**24**(5):236-8.
- (29) Shah SG, Brooker JC, Thapar C *et al.* Patient Pain During Colonoscopy: An analysis Using Real-Time Magnetic Endoscope Imaging. *Endoscopy* 2004;**067**:435-40.
- (30) Rex D, Atkin W, Hoff G *et al.* The flexible sigmoidoscope. *Gastrointest Endosc* 2000;**52**(4):587-9.
- (31) Cipolletta L, Bianco MA, Rotondano G *et al.* Endoclip-assisted resection of large pedunculated colon polyps. *Gastrointest Endosc* 1999;**50**(3):405-6.
- (32) Jerome D.Waye. Polypectomy-Basic Principles. Colonoscopy Principles and Practice. Blackwell Publishing Ltd., 2003.
- (33) Edmonson JM. History of the instruments for gastrointestinal endoscopy. *Gastrointest Endosc* 1991;**37**(2 Suppl):S27-S56.
- (34) Jerome D.Waye, Douglas K.Rex, Christopher B.Williams. History of endoscopy in the rectum and colon. Blackwell Publishing Ltd., 2003.
- (35) Edmonson JM. History of the instruments for gastrointestinal endoscopy. *Gastrointest Endosc* 1991;**37**(2 Suppl):S27-S56.
- (36) Edmonson JM. History of the instruments for gastrointestinal endoscopy. *Gastrointest Endosc* 1991;**37**(2 Suppl):S27-S56.
- (37) Novis BH, Bank S, Brown AA. A review of colonoscopy in 200 patients. *S Afr Med J* 1976;**50**(35):1358-61.

- (38) Trowbridge B, Burt RW. Colorectal cancer screening. *Surg Clin North Am* 2002;**82**(5):943-57.
- (39) Jerome D.Waye. The most important technique for colonoscopy. gastro-pro . 2004.
Ref Type: Electronic Citation
- (40) Seitz U, Seewald S, Bohnacker S *et al.* Advances in interventional gastrointestinal endoscopy in colon and rectum. *Int J Colorectal Dis* 2003;**18**(1):12-8.
- (41) Rex DK. Effect of variable stiffness colonoscopes on cecal intubation times for routine colonoscopy by an experienced examiner in sedated patients. *Endoscopy* 2001;**33**(1):60-4.
- (42) Rex DK, Goodwine BW. Method of colonoscopy in 42 consecutive patients presenting after prior incomplete colonoscopy. *Am J Gastroenterol* 2002;**97**(5):1148-51.
- (43) Mosse CA. University College London Medical Physics and Bioengineering Department, 1999.
- (44) Church J, Oakley J, Milsom J *et al.* Colonoscopy training: the need for patience (patients). *ANZ J Surg* 2002;**72**(2):89-91.
- (45) Bowles CJ, Leicester R, Romaya C *et al.* A prospective study of colonoscopy practice in the UK today: are we adequately prepared for national colorectal cancer screening tomorrow? *Gut* 2004;**53**(2):277-83.
- (46) Farinas PL. A new technique for arteriographic examination of the abdominal aorta and its branches. *Am J Roentgenol* 2003.
- (47) Seldinger SI. Catheter replacement of the needle in percutaneous arteriography; a new technique. *Acta Radiol* 1953;**39**(5):368-76.
- (48) Seldinger SI. A simple method of catheterization of the spleen and liver. *Acta Radiol* 1957;**48**(2):93-6.
- (49) Carter RF, Saypol GM. Transabdominal cholangiography. *JAMA* 1952;**148**:253.

- (50) Sargent EN, Meyers HI. Wire guide and technique for Cantor tube insertion. Rapid small bowel intubation. *Am J Roentgenol Radium Ther Nucl Med* 1969;**107**(1):150-5.
- (51) Sargent EN, Meyers HI. Wire guide and technique for Cantor tube insertion. Rapid small bowel intubation. *Am J Roentgenol Radium Ther Nucl Med* 1969;**107**(1):150-5.
- (52) Ness R, Gottlieb K, Rex D *et al*. Difficult sigmoid colon intubation: guide wire exchange technique. *Gastrointestinal Endoscopy Online* 1996.
- (53) Sinclair Research. Pig anatomy. Internet . 2005.
Ref Type: Electronic Citation
- (54) Duck F. Mechanical Properties of Tissue. *Physical Properties of Tissue; A Comprehensive Reference Book*. Acedemic Press, 1990.
- (55) Matweb. Overview - Polytetrafluoroethylene (PTFE), Extruded. internet . 2005.
Ref Type: Electronic Citation
- (56) Mosse CA, Mills TN, Bell GD *et al*. Device for measuring the forces exerted on the shaft of an endoscope during colonoscopy. *Med Biol Eng Comput* 1998;**36**(2):186-90.
- (57) Han Y, Uno Y, Munakata A. Does flexible small-diameter colonoscope reduce insertion pain during colonoscopy? *World J Gastroenterol* 2000;**6**(5):659-63.
- (58) Gilbert DA, Silverstein FE, Auth DC *et al*. Nonsurgical management of acute nonvariceal upper gastrointestinal bleeding. *Prog Hemost Thromb* 1978;**4**:349-95.
- (59) Farin, Grund. Polypectomy. *Colonoscopy Principles and Practice*. 2004: 394-5.
- (60) Protell RL, Rubin CE, Auth DC *et al*. The heater probe: a new endoscopic method for stopping massive gastrointestinal bleeding. *Gastroenterology* 1978;**74**(2 Pt 1):257-62.
- (61) Auth, David C.(Bellevue W, Opie et al, inventors. Multipolar electrosurgical device and method. patent **4,532,924** . 1985 1985.

- (62) Piercey JR, Auth DC, Silverstein FE *et al.* Electrosurgical treatment of experimental bleeding canine gastric ulcers: development and testing of a computer control and a better electrode. *Gastroenterology* 1978;**74**(3):527-34.
- (63) Protell RL, Gilbert DA, Silverstein FE *et al.* Computer-assisted electrocoagulation: bipolar vs. monopolar in the treatment of experimental canine gastric ulcer bleeding. *Gastroenterology* 1981;**80**(3):451-5.
- (64) Chang I. Finite Element Analysis of Hepatic Radiofrequency Ablation Probes using Temperature-Dependent Electrical Conductivity. *Biomed Eng Online* 2003;**2**(1):12.
- (65) Duck Francis. Electrical Properties of Tissue. Physical Properties of Tissue. 2003.
- (66) Krasteva VT, Papazov SP. Estimation of current density distribution under electrodes for external defibrillation. *Biomed Eng Online* 2002;**1**(1):7.
- (67) Freeman L. Evaluation of Prototype RF Devices for Mucosal Ablation of the Distal oesophagus in the Canine Animal Model. E-04-0007. 2004.
Ref Type: Report
- (68) Freeman, Lyn DVM. EndoWindow Pre-Clinical. 2002. Ethicon Endo-Surgery CONFIDENTIAL.
Ref Type: Report
- (69) Moritz AR HF. Studies of thermal injury II. The relative importance of time and surface temperature in the causation of cutaneous burns. *Am J Pathol* 1947;**23**:695-720.
- (70) Moritz AR. Studies of thermal injury III. The pathology and pathogenesis of cutaneous burns: An experimental study. *Am J Pathol* 1947;**23**:915-34.
- (71) Henriques FC, Moritz AR. Studies of thermal injury in the conduction of heat to and through skin and the temperatures attained therein: A theoretical and experimental investigation. *Am J Pathol* 1947;**23**:531-49.

- (72) Henriques FC. Studies of thermal injuries V. The prediction and significance of thermally induced rate processes leading to irreversible epidermal injury. *Arch Pathol* 1947;**43**:489-502.
- (73) Pearce J, Thompsen S. Rate process analysis of thermal damage. In: Welch AJ, van Gemert MJC, editors. Optical-thermal response of laser-irradiated tissue. 1995: 594-6.
- (74) Chang IA, Nguyen UD. Thermal modeling of lesion growth with radiofrequency ablation devices. *Biomed Eng Online* 2004;**3**(1):27.
- (75) Pop M, Molckovsky A, Chin L *et al*. Changes in dielectric properties at 460 kHz of kidney and fat during heating: importance for radio-frequency thermal therapy. *Phys Med Biol* 2003;**48**(15):2509-25.
- (76) Dark, G. On-line medical dictionary. internet . 2004. 10-13-2004.
Ref Type: Electronic Citation
- (77) Pttrie A, Sabin C. Case-control studies. Medical statistics. 2004.

8 Glossary of Terms

Adenoma: A benign tumour of a glandular structure or glandular origin-*adenomontous*.

Afferent: Moving or carrying to a central part(76).

Anoscope: an instrument for facilitating visual examination of the anal canal.

Assay: Examination and determination as to characteristics (as weight, measure, or quality).

CRC: Colorectal cancer

Carcinoma: A malignant tumour of epithelial growth.

Case-control study: A case-control study is a retrospective study that compares the characteristics of a group of patients with a particular disease outcome (the case) to a group of individuals without a disease outcome (the controls), to see whether any factors occurred more or less frequently in the cases than the controls(77).

Chyme: the semi fluid mass of partly digested food expelled by the stomach into the duodenum.

Colposcope: an instrument designed to facilitate visual inspection of the vagina.

Distal: Away from the origin.

Endothelial: See mucosal.

Epithelium: a membranous cellular tissue that covers a free surface or lines a tube or cavity of an animal body and serves especially to enclose and protect the other parts of the body, to produce secretions and excretions, and to function in assimilation.

Extrinsic: originating or due to causes or factors from or on the outside of a body, organ, or part.

Fulguration: The removal of diseased tissue using a controlled electric current.

Homoeostasis: The maintenance of relatively stable internal physiological conditions (as body temperature or the pH of blood) in higher animals under fluctuating environmental conditions.

Hypertrophy: Excessive development of an organ or part.

Ischaemia: A low oxygen state usually due to obstruction of the arterial blood supply or inadequate blood flow leading to hypoxia in the tissue.

Malignant: Tending to produce death or deterioration. Tending to infiltrate, metastasize and terminate fatally.

Metastasise: To spread by metastasis.

Mitosis: a process that takes place in the nucleus of a dividing cell, involves typically a series of steps consisting of prophase, metaphase, anaphase and telephase, and results in the formation of two new nuclei each having the same number of chromosomes as the parent nucleus.

Mucosal: Having to do with the mucous membrane- the inner lining of the GI tract.

Neoplastic: Of relating to, or constituting a neoplasm or neoplasia.

Neoplasm: A new growth of tissue serving no physiological function.

Oncogenes: a gene having the potential to cause a normal cell to become cancerous.

Parenteral: situated or occurring outside the intestine. Administration by intravenous, intramuscular, or subcutaneous.

Parasympathetic: The parasympathetic nervous system slows the heart rate, increases intestinal and gland activity, and relaxes sphincter muscles.

Pathology: The science which deals with the causes of, and changes produced in the body by, disease.

Perfused: To cause a flow or spread.

Polyp: A projecting mass of swollen and hypertrophied or tumourous membrane.

Proximal: Near the origin.

Sympathetic: The sympathetic nervous system that accelerates the heart rate, constricts blood vessels, and raises blood pressure.

Villous: covered or furnished with or as if with villi.

9 Appendix I: Publications

The Cath-Cam- A new concept in colonoscopy

Gary Long, Annette Fritscher-Ravens MD, C Alexander Mosse PhD, Tim Mills PhD, Paul Swain MD.

Submitted to GI Endoscopy April 2005

US Patent application 10/310,365

Title: Locally propelled Intraluminal Device with Cable Loop Track and Method of Use

Abstract: A medical device for performing medical procedures inside a lumen (such as the GI tract) of a patient is provided comprising a capsule, a cable, and a propulsion means. The cable can have one end anchored to the patient, and can extend from this anchored portion to the capsule. The cable can include a loop forward (distal) of the capsule in the GI tract. The propulsion means is operably connected to the cable to vary the length of cable between the anchored end and the capsule, so that the capsule is repositioned inside the GI tract of the patient.

Inventor:

Gary Long

US Patent application 10/406020

Title: Medical Device with Track and Method for Use

Abstract: A medical device for performing medical procedures inside a lumen (such as the GI tract) of a patient is provided. The device includes an elongate flexible member which can be advanced along a track. The track can include a

loop portion which can be advanced ahead of the elongate flexible member. The distal end of the flexible member can include a camera, light source, vacuum opening, and a working channel for receiving medical instruments.

Inventor:

Gary Long

US Patent application 10/409,207

Title: Guide Wire Structure for Insertion into an Internal Space

Abstract: A method is described of inserting guide wires into a lumen, for example into the human gastrointestinal tract. A guide wire structure is employed which comprises at least two guide wires each having a leading end portion which terminates in a leading end, the guide wires being connected to one another by a junction at or adjacent their leading ends, the guide wires have a first position in which the leading end portions are substantially parallel to one another, a second position in which the leading end portions are curved, and a third position in which at least one of the leading end portions forms a loop. The guide wire structure is steered through the gastrointestinal tract by selectively advancing or retracting a single guide wire or advancing more than one guide wire simultaneously, according to the path which is required to be followed.

Inventors:

Swain, Paul, Christopher

Long, Gary

*US Patent application 10/729,754*Title: Guide Wire having Bending Segment

Abstract: A guide wire including a continuous, unitary wire having a first segment, a second segment, and a third segment is shown and described. The third segment has a bending moment of inertia less than the bending moment of inertia of the first and second segments. The guide wire can be used to advance a medical device within a body lumen.

Inventors:

Bakos, Gregory, J.

Gee, Kevin, K.

Tierney, Scott, J.

Swain, Christopher, Paul

Long, Gary

US Patent application 60/571,118

Title: Medical Device with Propulsion Mechanism

Abstract: A medical device is provided with a propulsion mechanism positioned near a distal end. The medical device may be advanced manually at a proximal location outside the body by a user, and at a distal location by the propulsion mechanism to reduce the instances of forming loops in an elongated body of the medical device. The medical device may also include a camera and a guidewire.

Inventors:

Gary Long

Greg Bakos

Omar Vahkaria

US Patent application (11/128,084)

Title: Guidewire Structure

Abstract: A first guidewire structure includes a medical guidewire extendable beyond a distal end of a medical instrument and having first and second segments, wherein the bending moment of inertia of the first segment is less than the bending moment of inertia of the second segment. A second guidewire structure includes a medical guidewire extendable beyond a distal end of a medical instrument having a mechanized guidewire drive assembly. The medical guidewire has an exterior surface including a repetitive series of spaced-apart surface elevation features. One example of surface elevation features is external threads. The spaced-apart surface elevation features are adapted for operable engagement with the mechanized guidewire drive assembly.

Inventors:

Gary Long

Greg Bakos

Omar Vahkaria

US Patent application (11/128,036)

Title: Medical Instrument Having a Medical Guidewire

Abstract: A first medical instrument includes a flexible catheter and a medical guidewire extendable beyond a distal end of the catheter. The medical guidewire has first and second segments, wherein the bending moment of inertia of the first segment is less than the bending moment of inertia of the second segment. A second medical instrument includes a flexible catheter, a mechanized guidewire assembly, and a medical guidewire extendable beyond a distal end of the catheter. The medical guidewire has an exterior surface including a repetitive series of spaced-apart surface elevation features. One

example of surface elevation features is external threads. The spaced-apart surface elevation features are adapted for operable engagement with the mechanized guidewire drive assembly.

Inventors:

Gary Long

Greg Bakos

Omar Vahkaria

US Patent application (11/128,023)

Title: Medical Instrument Having a Controlled Guidewire Drive

Abstract: A medical instrument includes a flexible catheter, a medical guidewire, and a mechanized guidewire drive assembly. The catheter has a distal end insertable into a body lumen of a patient. The mechanized guidewire drive assembly is adapted for operable engagement with the medical guidewire. The mechanized guidewire drive assembly includes a motor and includes a controller which drives the motor with a driving force. The driving force has a predetermined upper limit.

Inventors:

Gary Long

Greg Bakos

Omar Vahkaria

US Patent application (11/128,012)

Title: Medical Instrument Having a Catheter and a Medical Guidewire

Abstract: A first medical instrument includes a flexible catheter having a distal end which has a substantially bullet-nose shape, which is insertable into a body lumen of a patient, and which has at least one guidewire passageway opening. The first medical instrument also includes a medical guidewire having a working portion extendable beyond the at-least-one guidewire passageway opening. A second medical instrument includes a flexible catheter, a medical guidewire having a working portion extendable beyond the distal end of the catheter, and at least one wire length counter which is operably connectable to the medical guidewire to measure a length of the working portion being extended beyond the distal end of the catheter. A third medical instrument includes a flexible catheter, a medical guidewire, and a force/torque-limiting clutch operatively connectable to the medical guidewire.

Inventors:

Gary Long

Greg Bakos

Omar Vahkaria

US Patent application (11/128,072)

Title: Medical Instrument Having a Guidewire and Articulated Catheter

Abstract: A first medical instrument includes a flexible catheter and a medical guidewire extendable beyond a distal end of the catheter. The catheter has an articulated section. The medical guidewire has first and second segments, wherein the bending moment of inertia of the first segment is less than the bending moment of inertia of the second segment. A second medical instrument includes a flexible catheter, a mechanized guidewire assembly, and a medical guidewire extendable beyond a distal end of the catheter. The catheter has an

articulated section. The medical guidewire has an exterior surface including a repetitive series of spaced-apart surface elevation features. One example of surface elevation features is external threads. The spaced-apart surface elevation features are adapted for operable engagement with the mechanized guidewire drive assembly.

Inventors:

Gary Long

Greg Bakos

Omar Vahkaria

US Patent application (11/128,108)

Title: Medical Instrument Having a Guidewire and an Add-To Catheter

Abstract: A first medical instrument includes a flexible catheter and a medical guidewire extendable beyond a distal end of the catheter. The catheter is adapted to slidably receive a rail-coupling portion of an adjunct medical device. The medical guidewire has first and second segments, wherein the bending moment of inertia of the first segment is less than the bending moment of inertia of the second segment. A second medical instrument includes a flexible catheter, a mechanized guidewire assembly, and a medical guidewire extendable beyond a distal end of the catheter. The catheter is adapted to slidably receive a rail-coupling portion of an adjunct medical device. The medical guidewire has an exterior surface including a repetitive series of spaced-apart surface elevation features. One example of surface elevation features is external threads. The spaced-apart surface elevation features are adapted for operable engagement with the mechanized guidewire drive assembly.

Inventors:

Gary Long

Greg Bakos

Omar Vahkaria

10 Appendix II: Technical Specifications

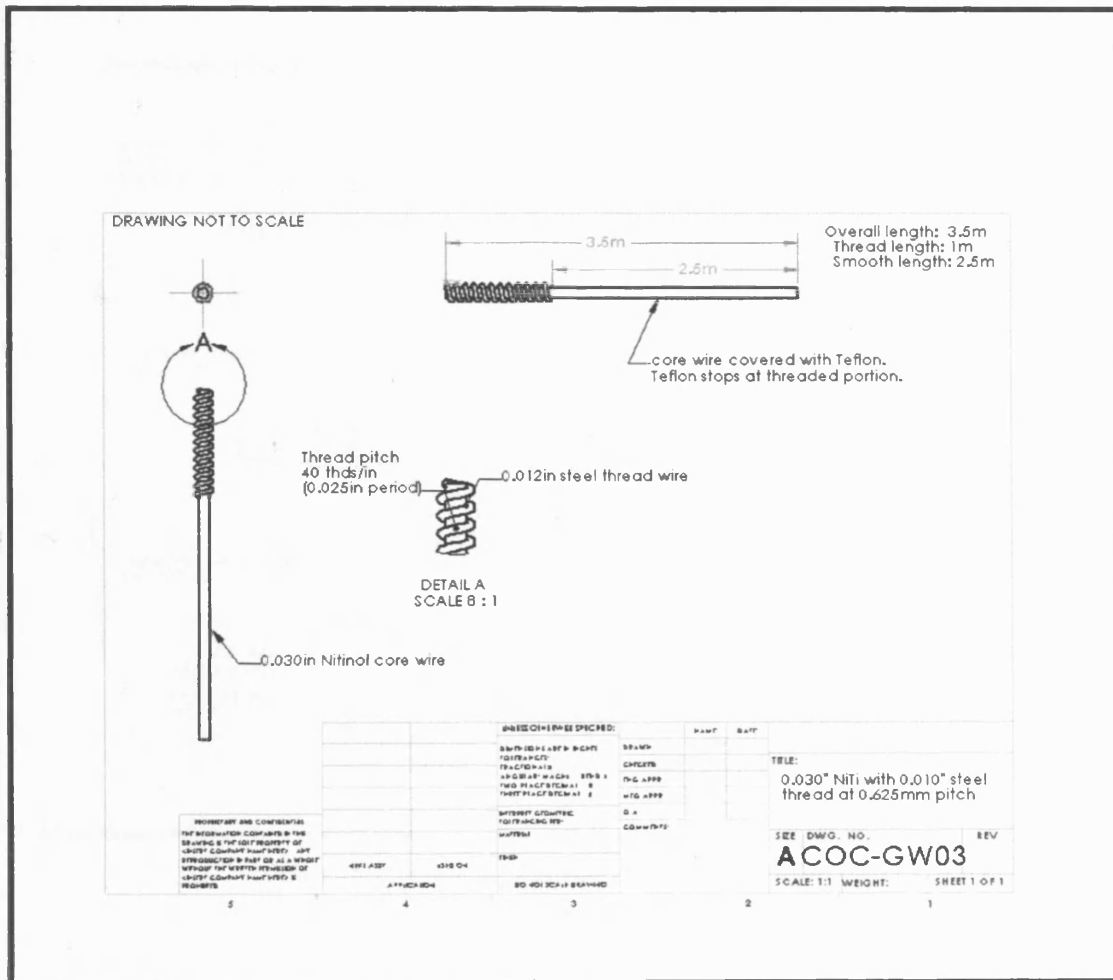


Figure 10-1. Schematic drawing of guidewire GW03.



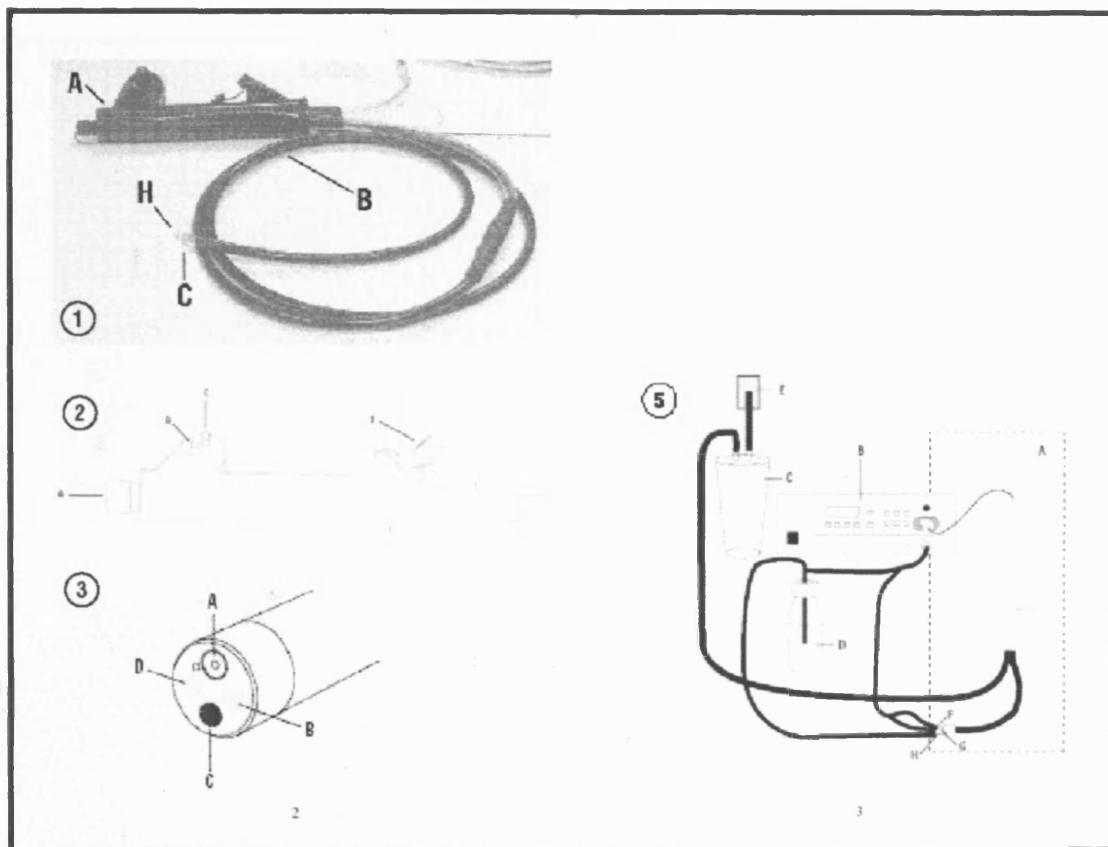


Figure 10-7. Photograph and drawing of the Cathcam. See Table 10-1 for details.

Table 10-1. Details of Cathcam drawing.

Drawing	Label	Description
①	A	Handle
	B	Insertion tube or body of the Cathcam
	C	Distal tip
	H	Protective cap
②		Handle
③	A	Camera
	B & D	Light source
	C	Access channel
⑤	A	Handle
	B	Console
	C	Suction trap
	D	Water bottle
	E	Wall suction

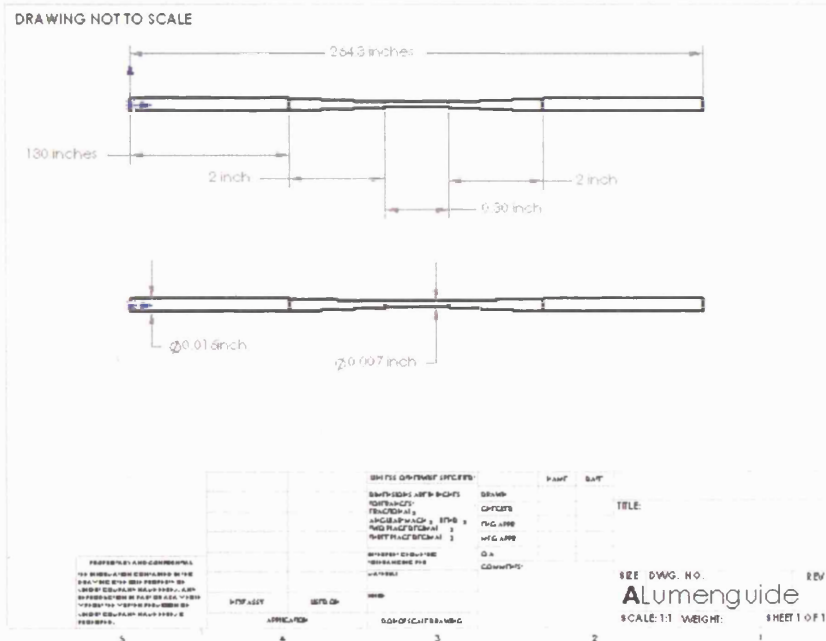


Figure 10-8. Schematic drawing of the Lumenguide guidewire.

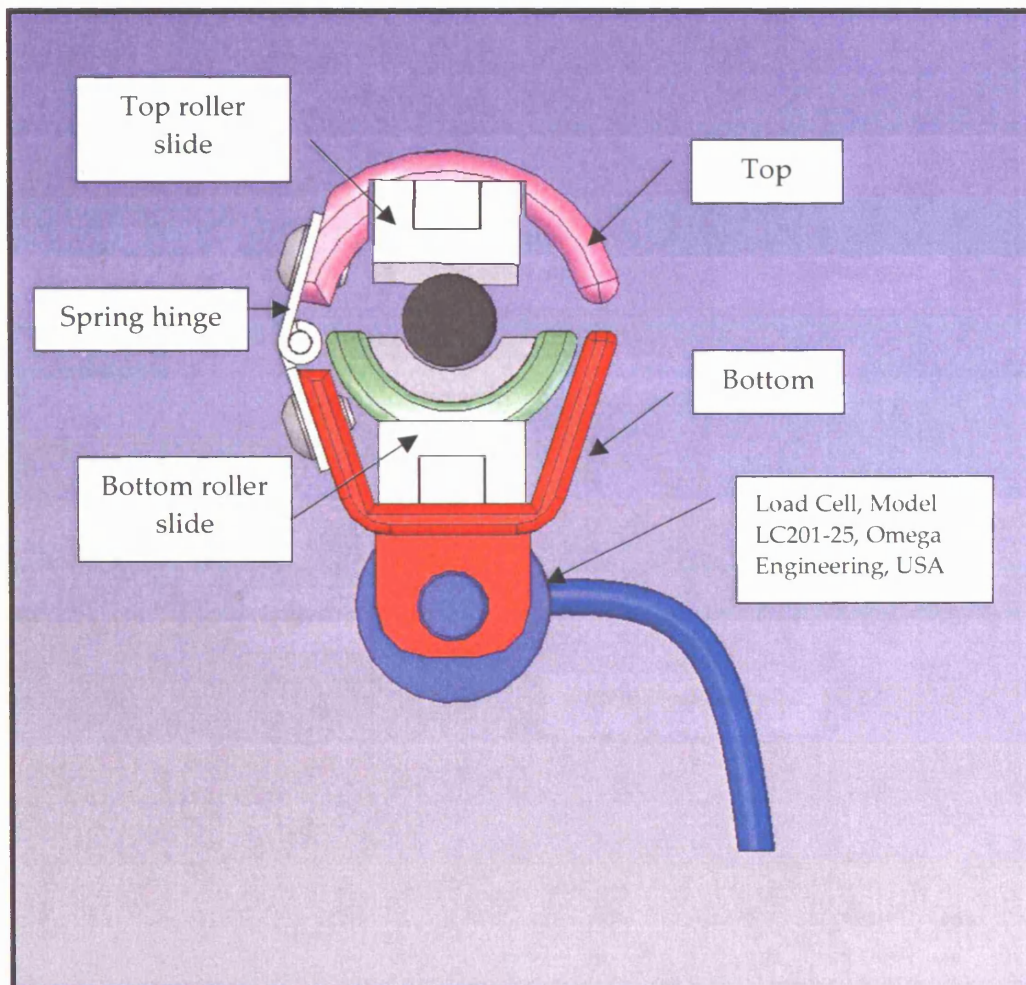


Figure 10-9. End view of the FH-06 force handle.

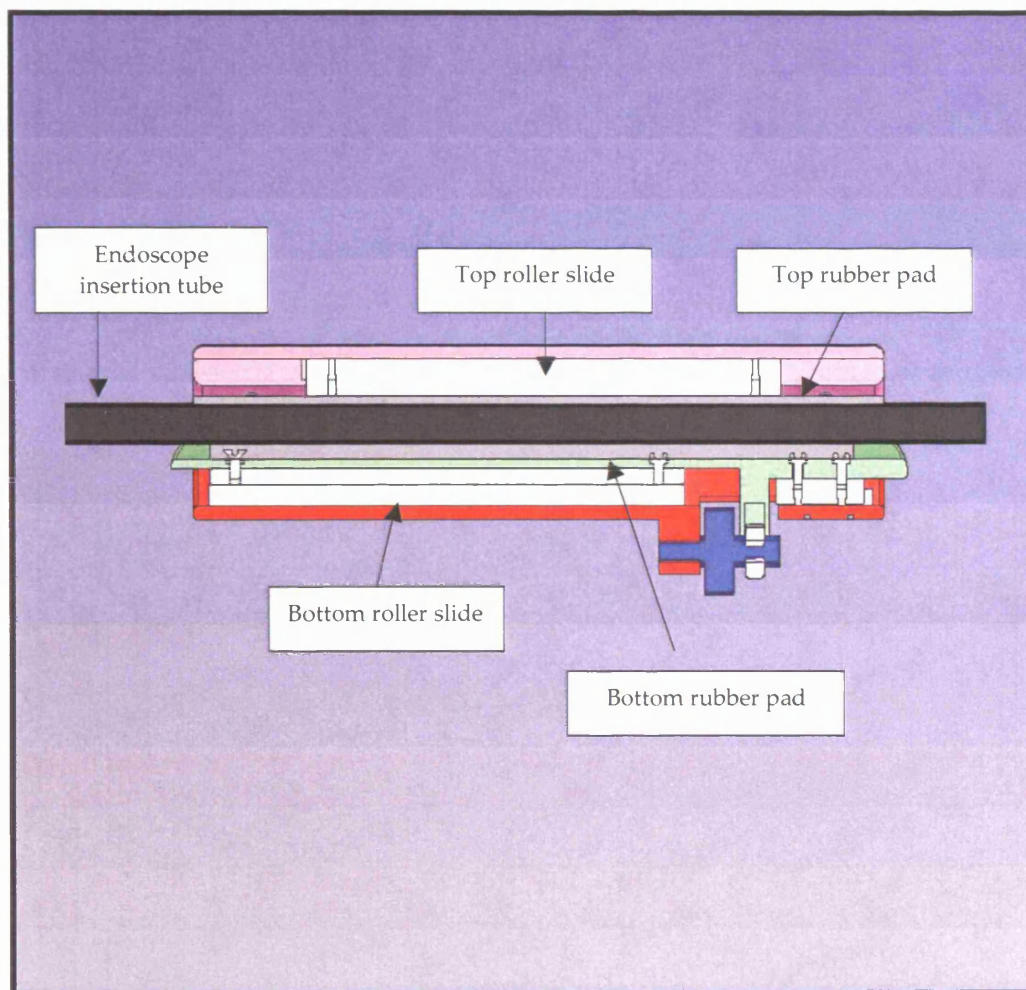


Figure 10-10. Cross section view of the force handle. When the insertion tube is advanced along the colon, the slider transmits the axial force to the load cell.